granular flows and complex flows with *Gerris*

and Basilisk

Pierre-Yves Lagrée,

Lydie Staron, Stéphane Popinet ,

Institut Jean le Rond ∂'Alembert, CNRS, Université Pierre & Marie Curie, 4 place Jussieu, Paris, France

27/10/14

- What is a granular media?
- size > 100µm
- grains of sand, small rocks, glass beads, animal feed pellet, medicines, cereals, wheat, sugar, rice...
- 50 % of the traded products

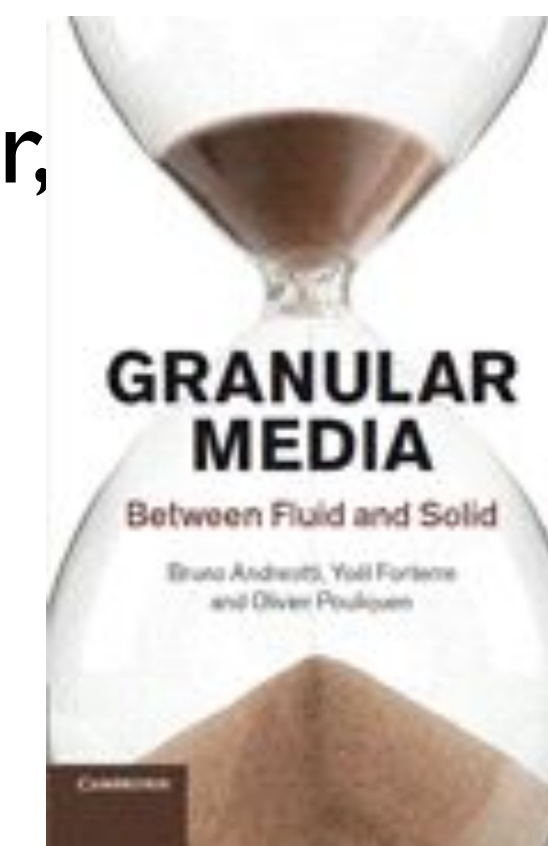

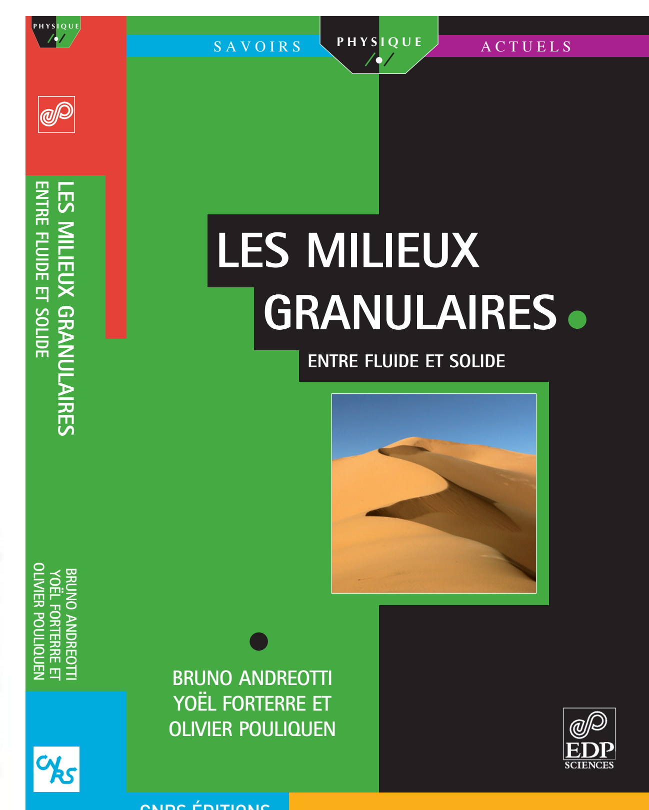


PYL

spoil tip - Australia

spoil tip (boney pile, gob pile, bing or pit heap), «terril» in french


PYL


PYL


Rapide
8
PYL


pyl


PYL

Stromboli

py

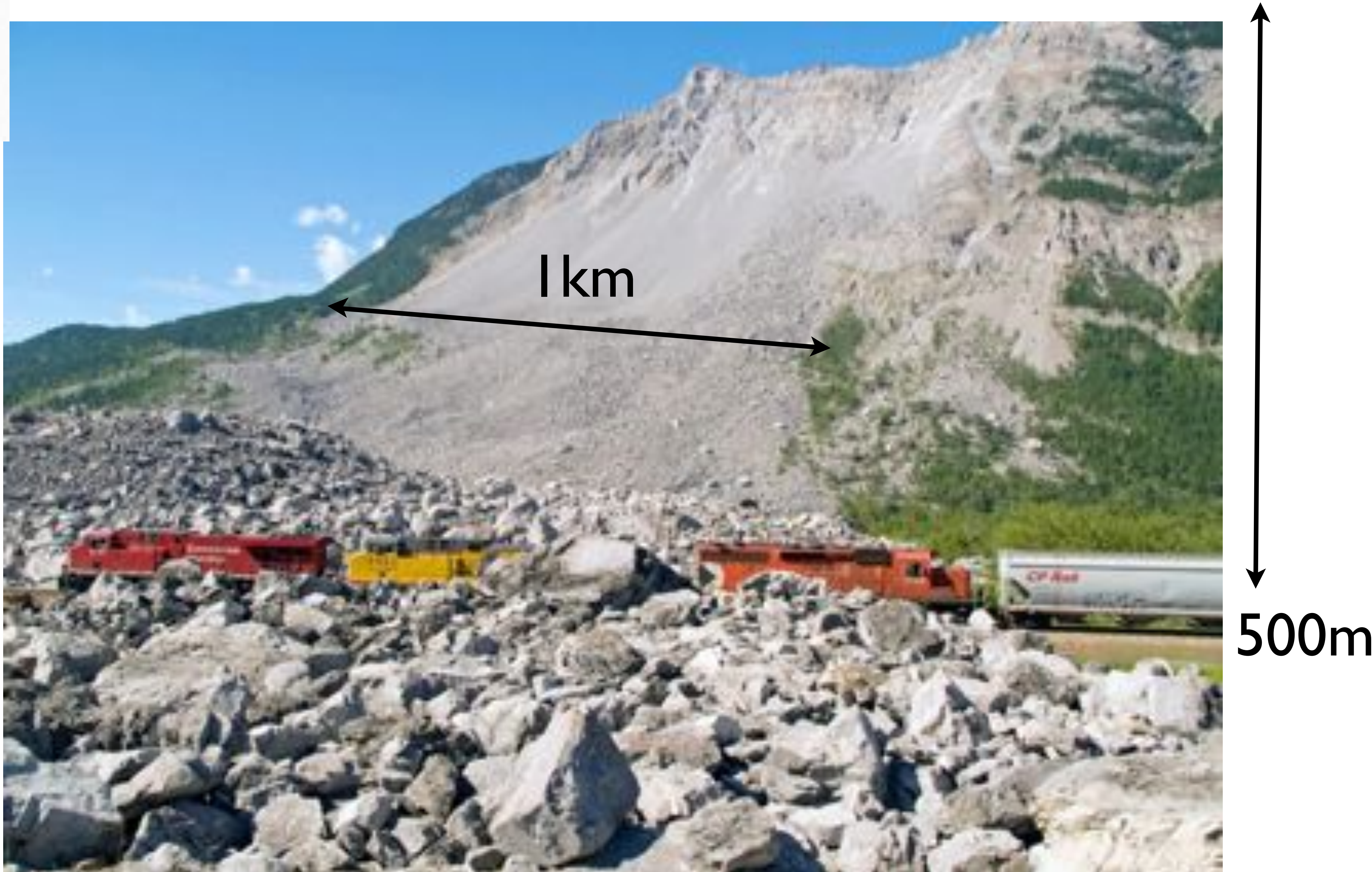

http://www.pbase.com/image/63044602 2006 Gary Hebert

avalanche : le «Frank Slide» 1907

Lofoten Norway

photo PYL

Nasa

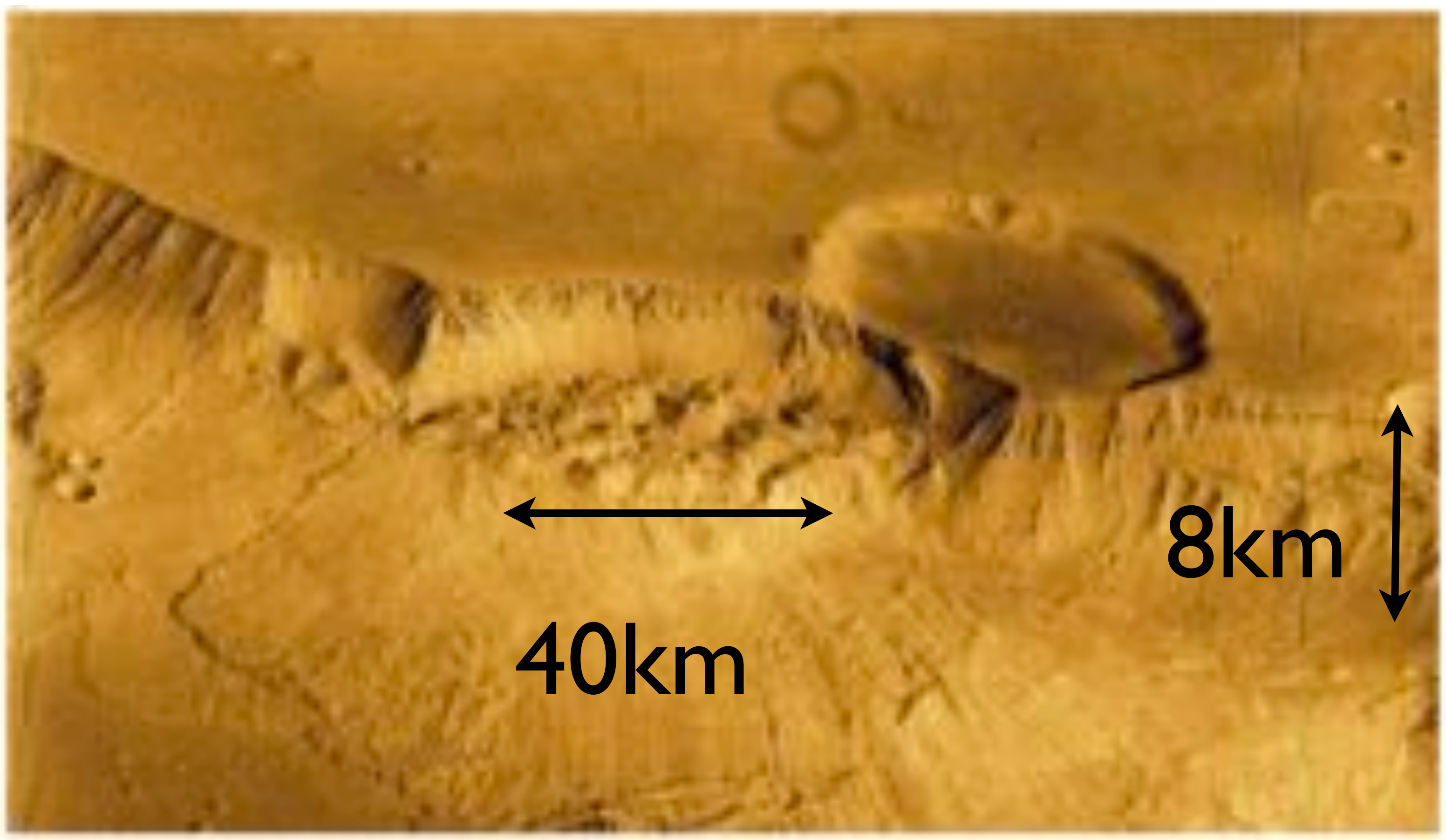

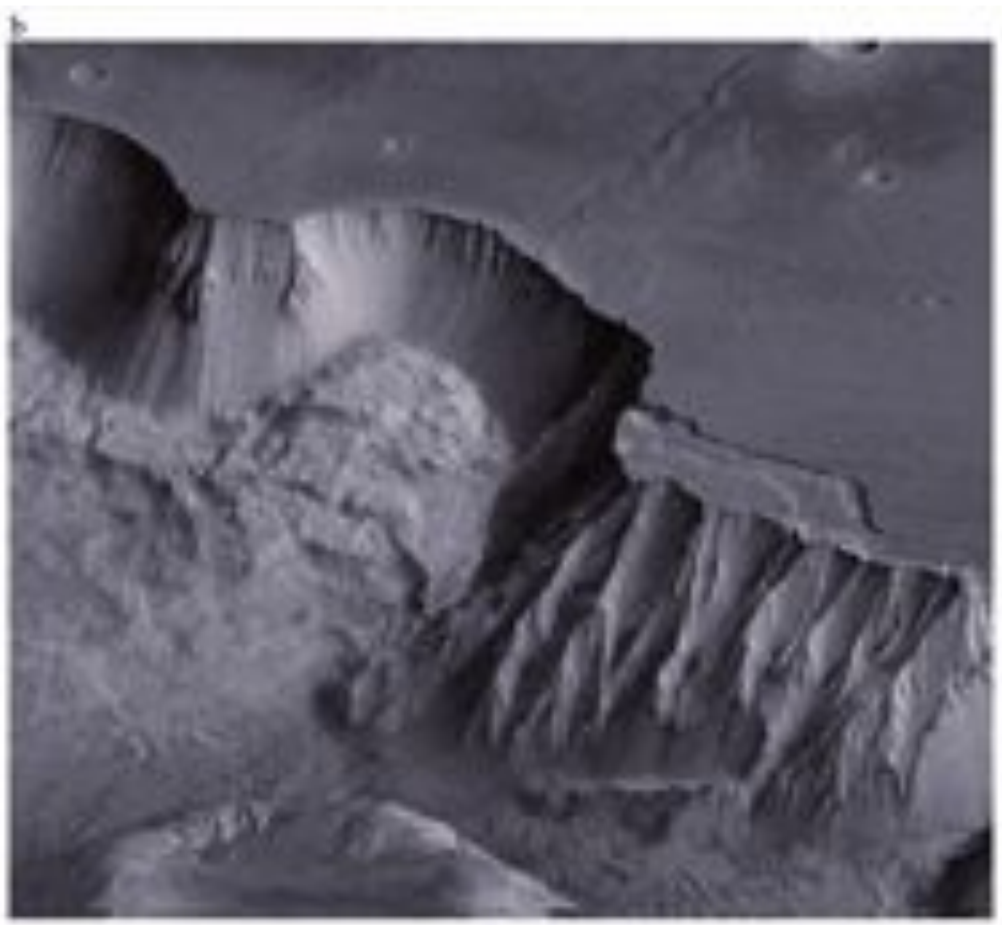

http://books.google.fr/books?id=HY6Z5od4-E4C&pg=PA49&dq=granular+flow&hl=fr&ei=lamtTaa_NYyVOoToldcL&sa=X&oi=book_result&ct=result&resnum=10&ved=0CFkQ6AEwCTgK#v=onepage&q&f=true

http://www.cieletespace.fr/image-du-jour/5126_la-saison-des-avalanches-sur-mars


pyl

Non Newtonian flows

stress tensor $\boxed{\sigma_{ij}} = -p\delta_{ij} + \boxed{\tau_{ij}}$ viscous stress tensor

strain rate $D_{ij} = \frac{1}{2}(\frac{\partial u_j}{\partial x_i} + \frac{\partial u_i}{\partial x_j})$ $\tau_{ij} = 2\eta D_{ij}$

strain rate second invariant $D_2 = \sqrt{D_{ij}D_{ji}}$

Newtonian fluid η constant

generalized Newtonian fluid η function of D_2

power law fluid $\eta(D_2) = \eta_0 D_2^{N-1}$

Non Newtonian flows

strain rate second invariant

$$D_2 = \sqrt{D_{ij}D_{ji}}$$

$$\tau_{ij} = 2\eta D_{ij}$$

τ_y yield stress

Herschel-Bulkley
$$\eta(D_2) = \frac{\tau_y}{2D_2} + \eta_0 D_2^{N-1}$$

Bingham
$$\eta(D_2) = \frac{\tau_y}{2D_2} + \eta_0$$

Drucker Prager
$$\eta(D_2) = \frac{\tau_y}{2D_2}$$

Coulomb yield stress $\tau_y = \mu P$

Non Newtonian flows

Example of Bingham Collapse

Gerris

F. Dufour & G. Pijaudier-Cabot, , Int. J. Numer. Anal. Meth. Geomech. (2005)

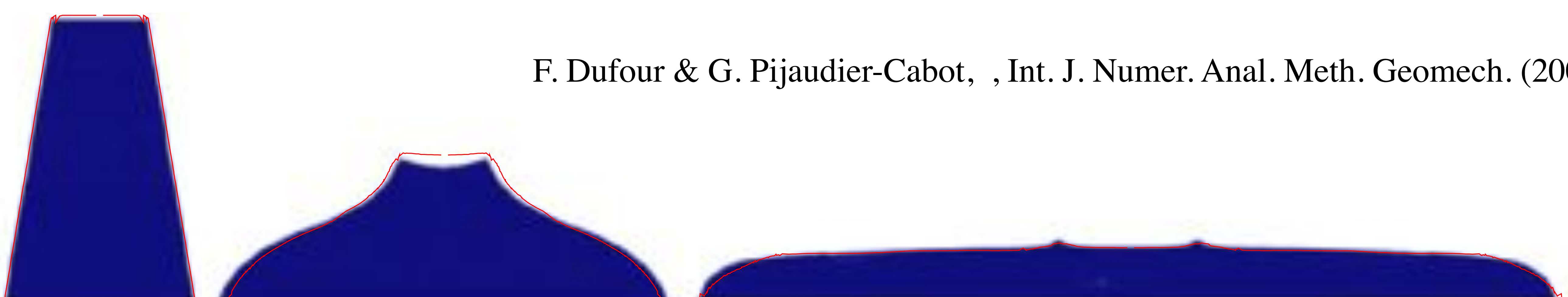

(a) (b) (c)

Non Newtonian flows

Example of Bingham Collapse

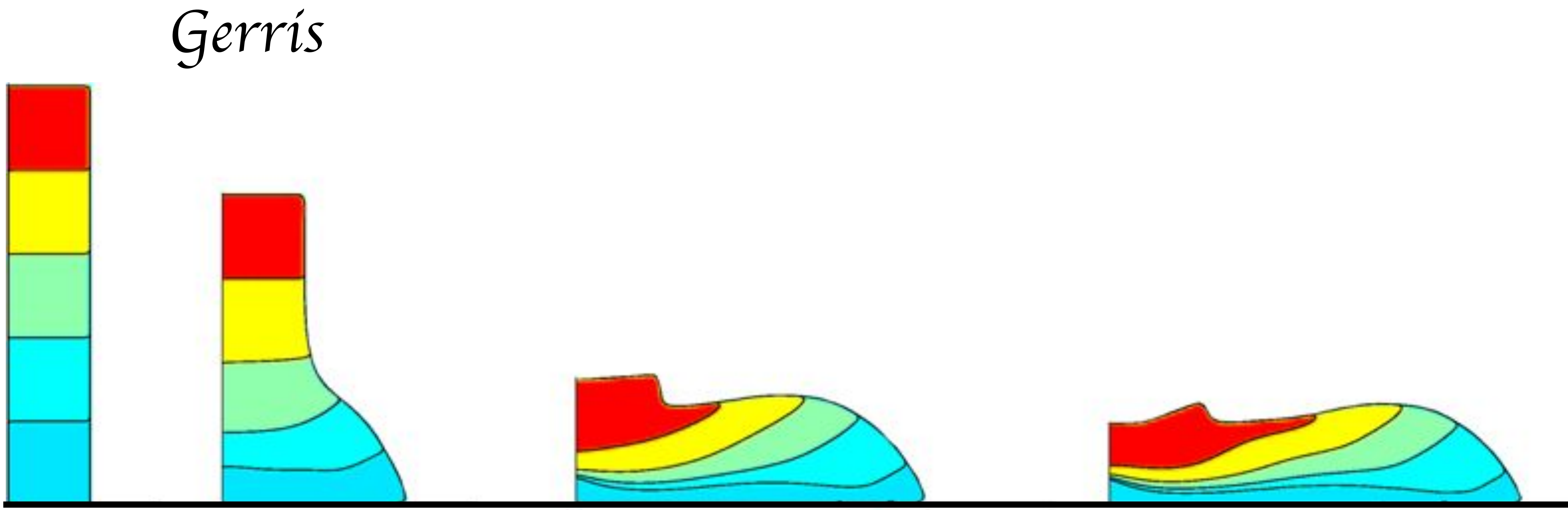

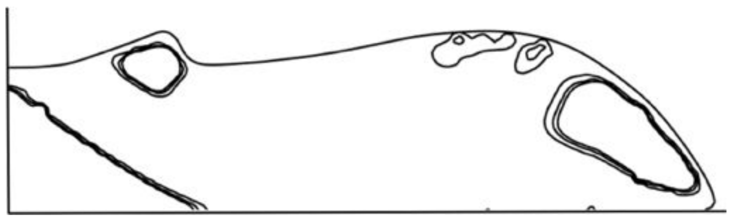

Staron et al J. Rheol 2013

Non Newtonian flows

Example of Bingham Collapse

Basilisk

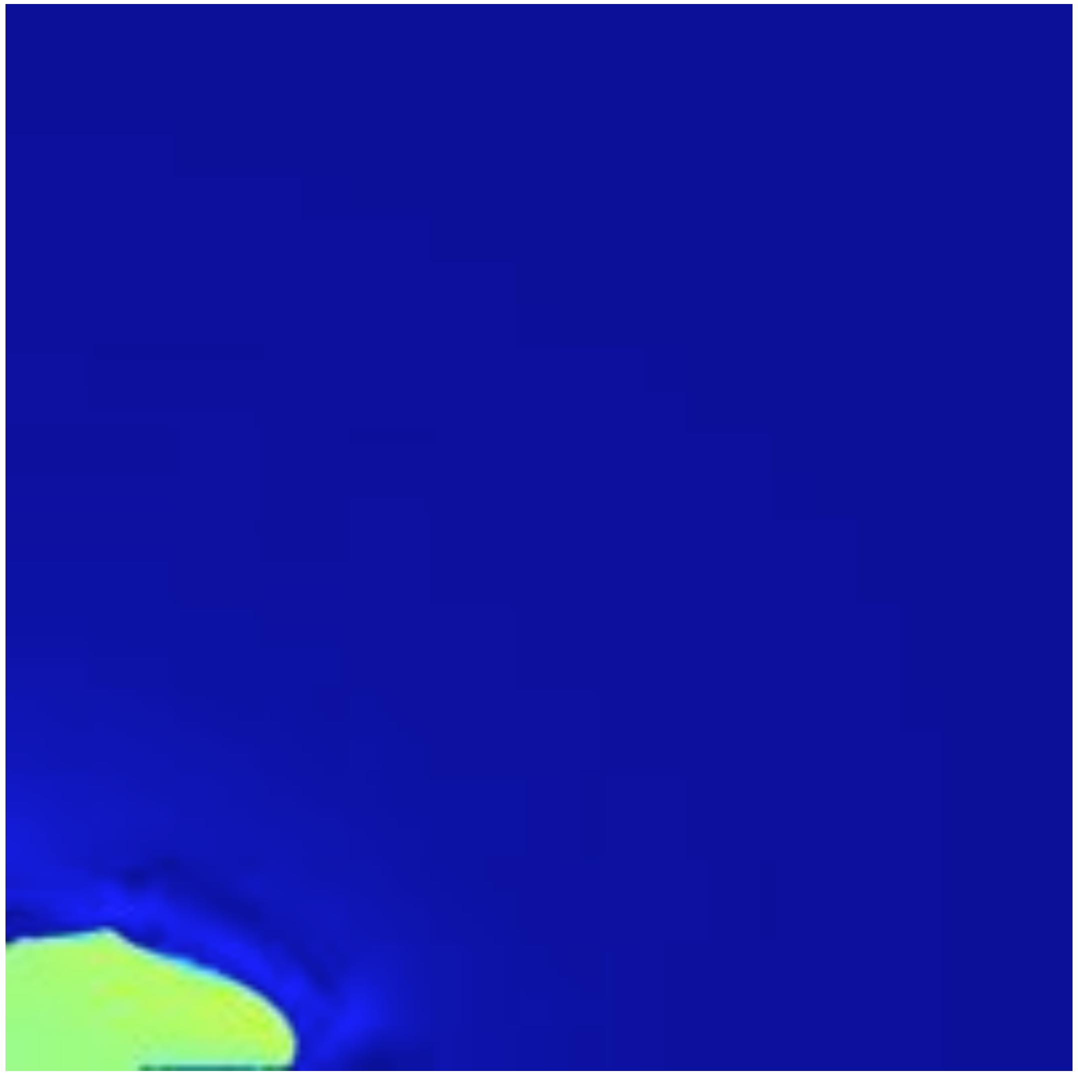

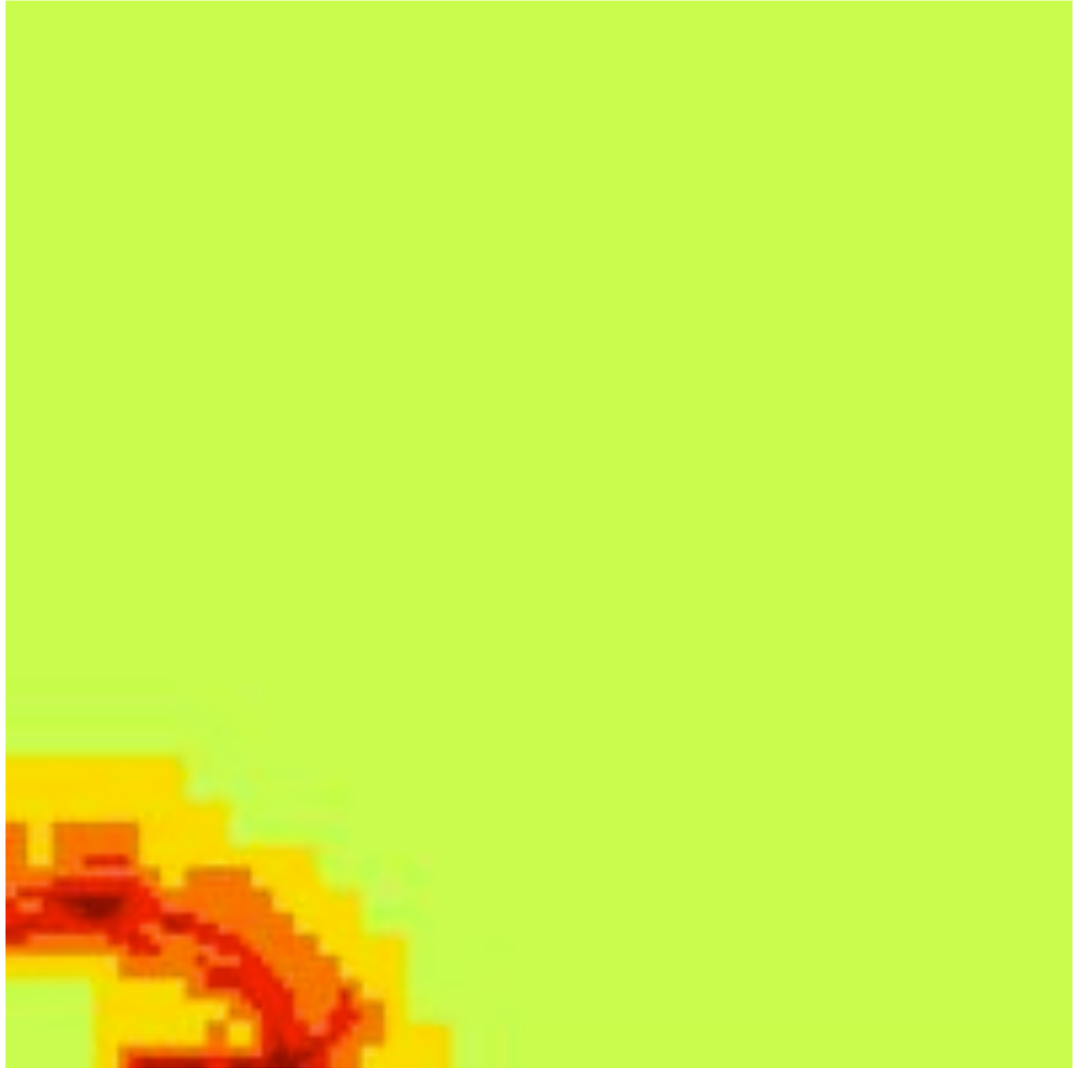

granulars are fluids and solids

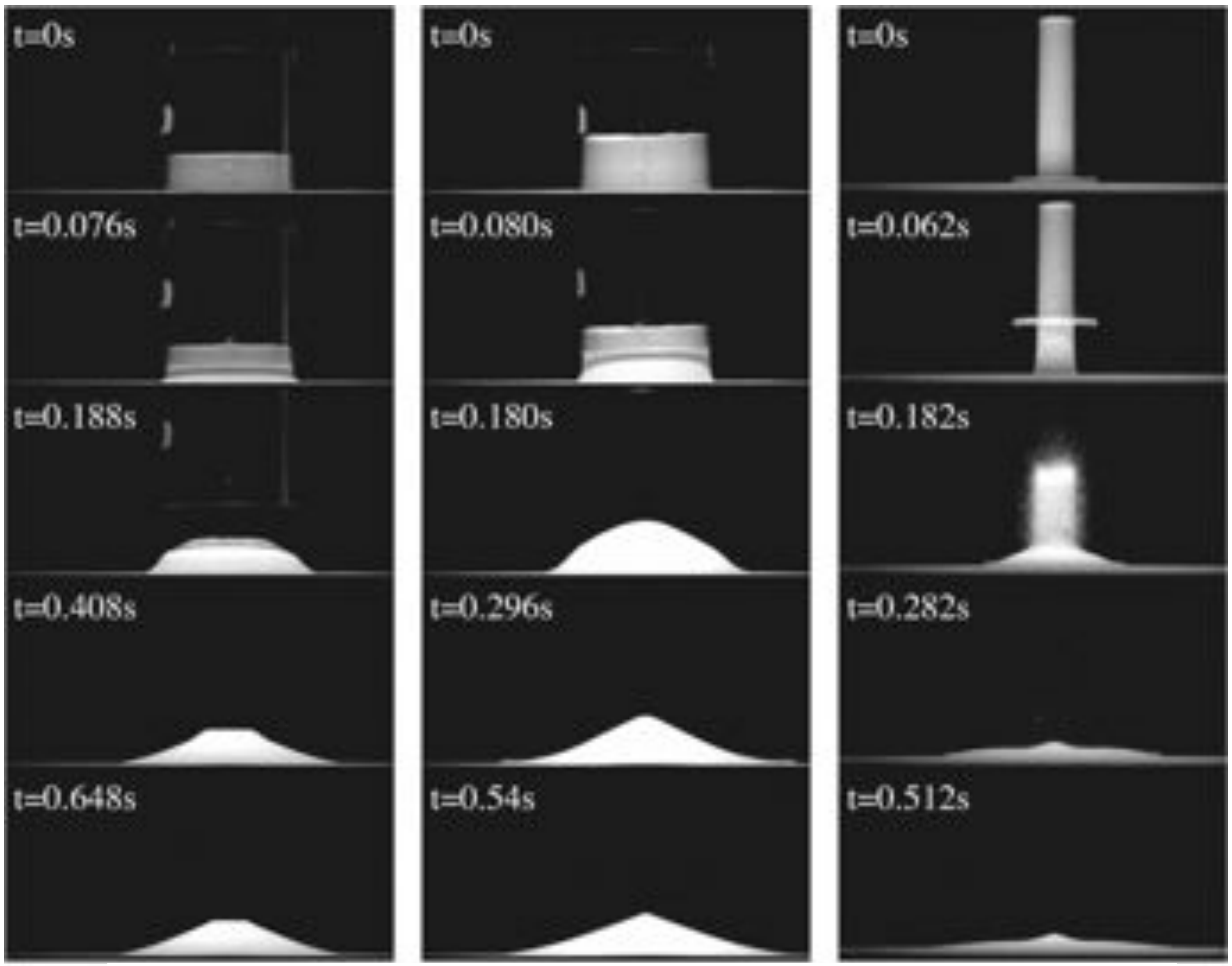

E. Lajeunesse A. Mangeney-Castelnau and J. P. Vilotte PoF 2005

- Looking for a continuum description
- Lot of recent experiments in simple configurations: shear/ inclined plane,

  with model material (glass beads, sand…)
- Simulations with Contact Dynamics

  (disks, polygona, spheres)

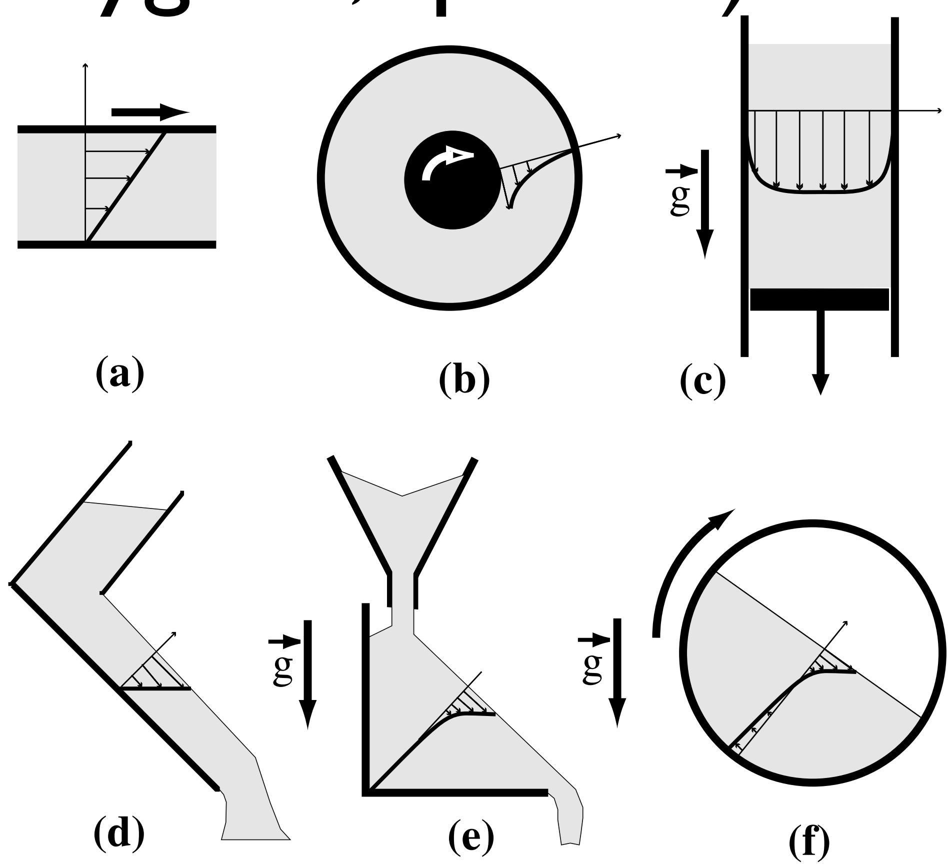

GDR MiDi EPJ E 04

Fig. 1. The six configurations of granular flows: (a) plane shear, (b) annular shear, (c) vertical-chute flows, (d) inclined plane, (e) heap flow, (f) rotating drum.

- Looking for a continuum description
- Lot of recent experiments in simple configurations: shear/ inclined plane,

  with model material (glass beads, sand…)
- Simulations with Contact Dynamics

  (disks, polygona, spheres)

- Defining a «viscosity»
- Implement it in the Navier Stokes solver *Gerris*
- Test on exact «Bagnold» avalanche solution
- Test on granular collapse and hourglass

The μ(I)-rheology

$u(y)$

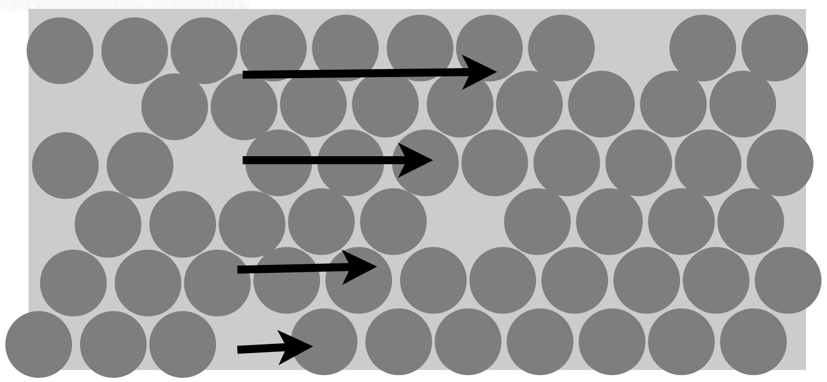

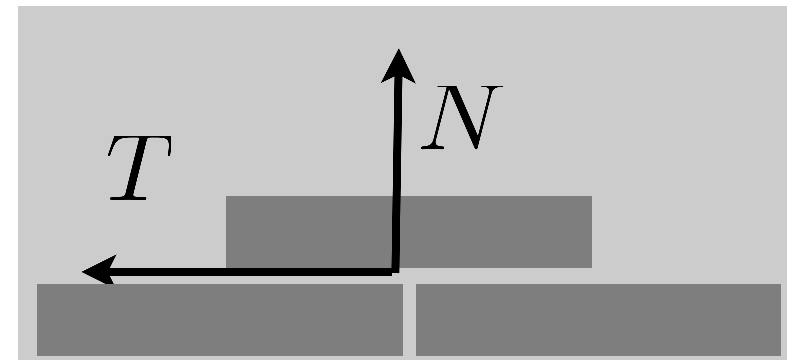

$$T = \mu N$$

constitutive law?

Coulomb dry friction

Coulomb friction law

$$\boxed{\tau = \mu P}$$

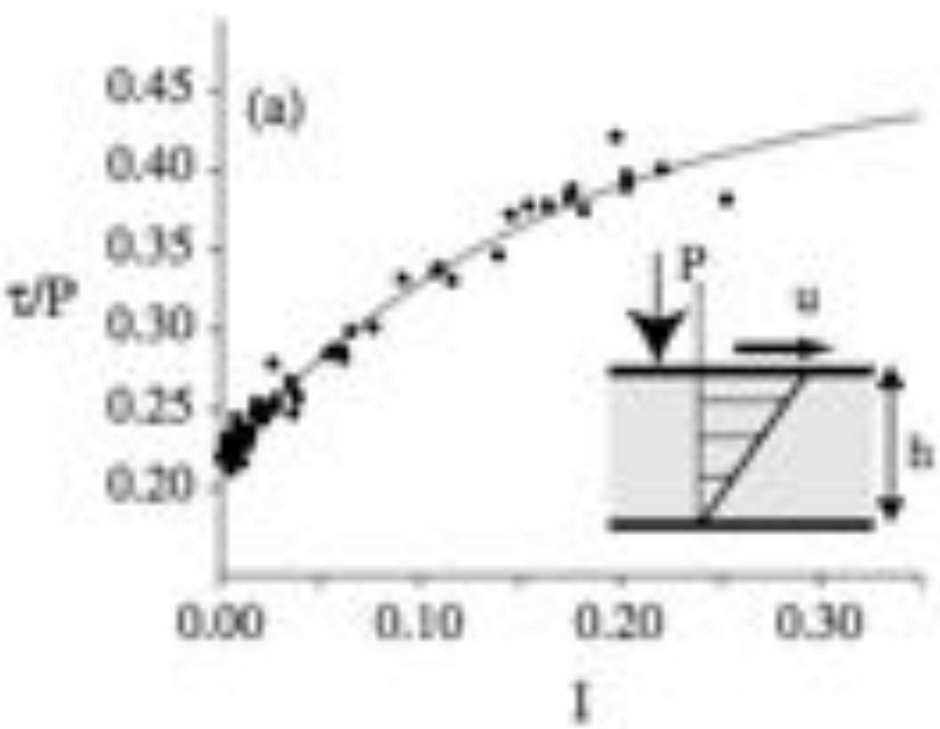

The μ(I)-rheology

$u(y)$

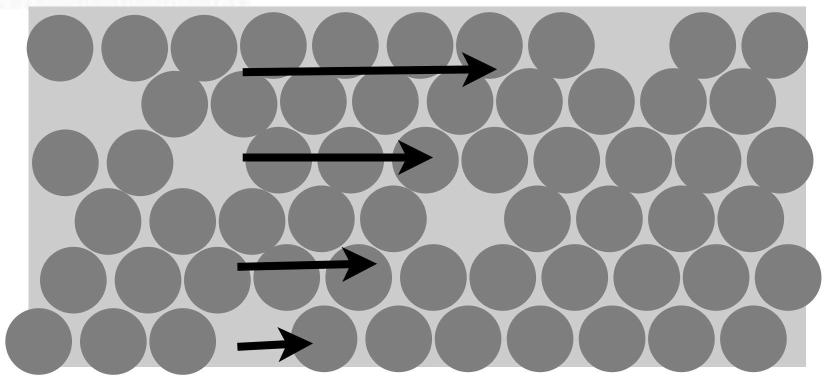

$$I = \frac{d\frac{\partial u}{\partial y}}{\sqrt{P/\rho}}$$

$\dfrac{\text{falling time}}{\text{displacement time}}$

$$\tau = \mu(I)P$$

Coulomb friction law

$$\eta\frac{\partial u}{\partial y} = \mu(I)P$$

local equilibrium

$$\eta = \frac{\mu\left(\frac{d\frac{\partial u}{\partial y}}{\sqrt{P/\rho}}\right)P}{\frac{\partial u}{\partial y}}$$

construction of a viscosity

P. Jop, Y. Forterre, O. Pouliquen, (2006) "A rheology for dense granular flows", Nature 441, pp. 727-730

The μ(I)-rheology

$$D_{ij} = \frac{u_{i,j} + u_{j,i}}{2} \qquad D_2 = \sqrt{D_{ij} D_{ij}}$$

$$u(x, y) \quad v(x, y)$$

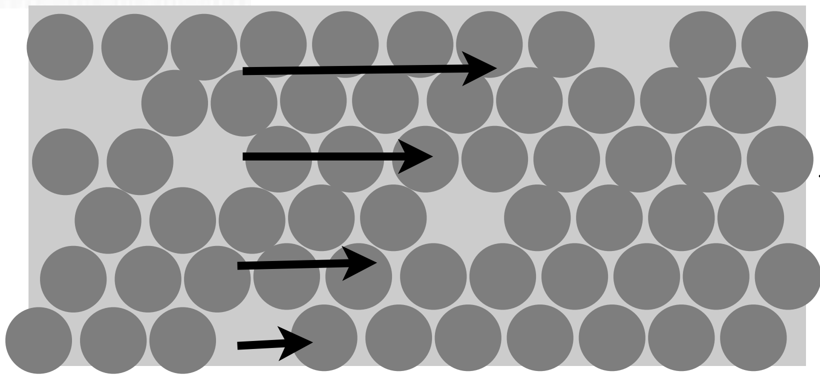

$$I = d\sqrt{2} D_2 / \sqrt{(|p|/\rho)}.$$

$$\frac{\text{falling time}}{\text{displacement time}}$$

$$\tau = \mu(I) P$$

Coulomb friction law

$$\mu(I) = \mu_1 + \frac{\mu_2 - \mu_1}{I_0/I + 1}$$

$$\mu_1 \simeq 0.32 \quad (\mu_2 - \mu_1) \simeq 0.23 \quad I_0 \simeq 0.3$$

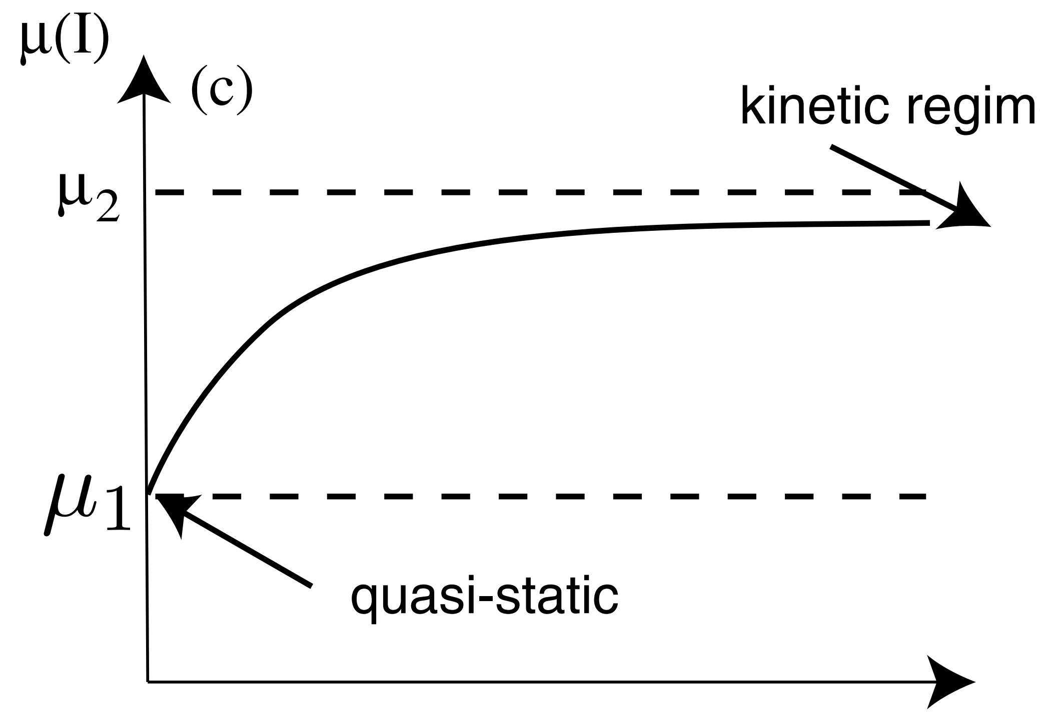

P. Jop, Y. Forterre, O. Pouliquen, (2006) "A rheology for dense granular flows", Nature 441, pp. 727-730

The μ(I)-rheology

$$D_{ij} = \frac{u_{i,j} + u_{j,i}}{2} \qquad D_2 = \sqrt{D_{ij}D_{ij}}$$

$u(x,y) \quad v(x,y)$

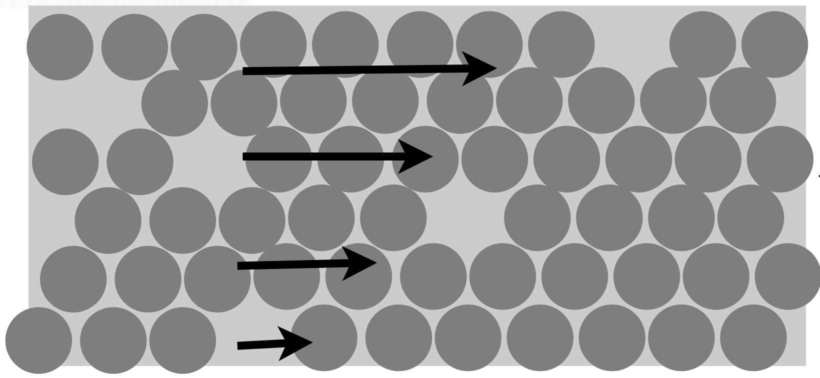

$$I = d\sqrt{2}D_2/\sqrt{(|p|/\rho)}.$$

$$\frac{\text{falling time}}{\text{displacement time}}$$

$$\tau = \mu(I)P$$

Coulomb friction law

construction of a viscosity based on the *D*2 invariant and redefinition of *I*

$$\eta = \left(\frac{\mu(I)}{\sqrt{2}D_2}p\right)$$

construction of a viscosity

P. Jop, Y. Forterre, O. Pouliquen, (2006) "A rheology for dense granular flows", Nature 441, pp. 727-730


ST VENANT

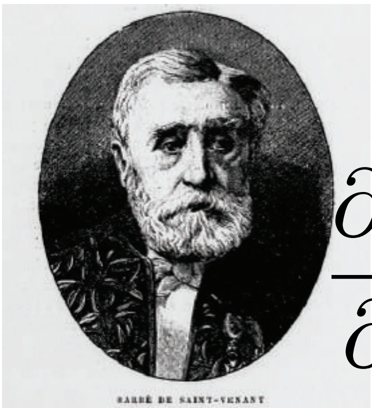

Saint-Venant Savage Hutter *Gerris*

$$\frac{\partial h}{\partial t} + \frac{\partial (Q)}{\partial x} = 0 \quad \frac{\partial Q}{\partial t} + \frac{\partial}{\partial x}\left(\frac{5Q^2}{4h} + \frac{g}{2}(h^2)\right) = -gh\mu(I)\frac{Q}{|Q|}$$

Gerris is a free finite volume code by Stéphane Popinet

one part of the code is a Shallow Water solver

$$\frac{Q^* - Q^n}{\Delta t} + \frac{\partial}{\partial x}\left(\frac{Q^2}{h} + \frac{g}{2}(h^2)\right) = 0 \qquad \frac{Q^{n+1} - Q^*}{\Delta t} = -gh^*\mu(I^*)\frac{Q^{n+1}}{|Q^*|}$$

Audusse et al.

finite volume Rieman Solver + well balanced

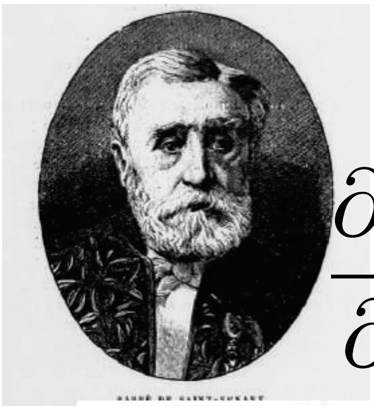

Saint-Venant Savage Hutter

$$\frac{\partial h}{\partial t} + \frac{\partial (Q)}{\partial x} = 0 \qquad \frac{\partial Q}{\partial t} + \frac{\partial}{\partial x}\left(\frac{5Q^2}{4h} + \frac{g}{2}(h^2)\right) = -gh\mu(I)\frac{Q}{|Q|}$$

$$I = d\frac{Q}{h^2\sqrt{P/\rho}}$$

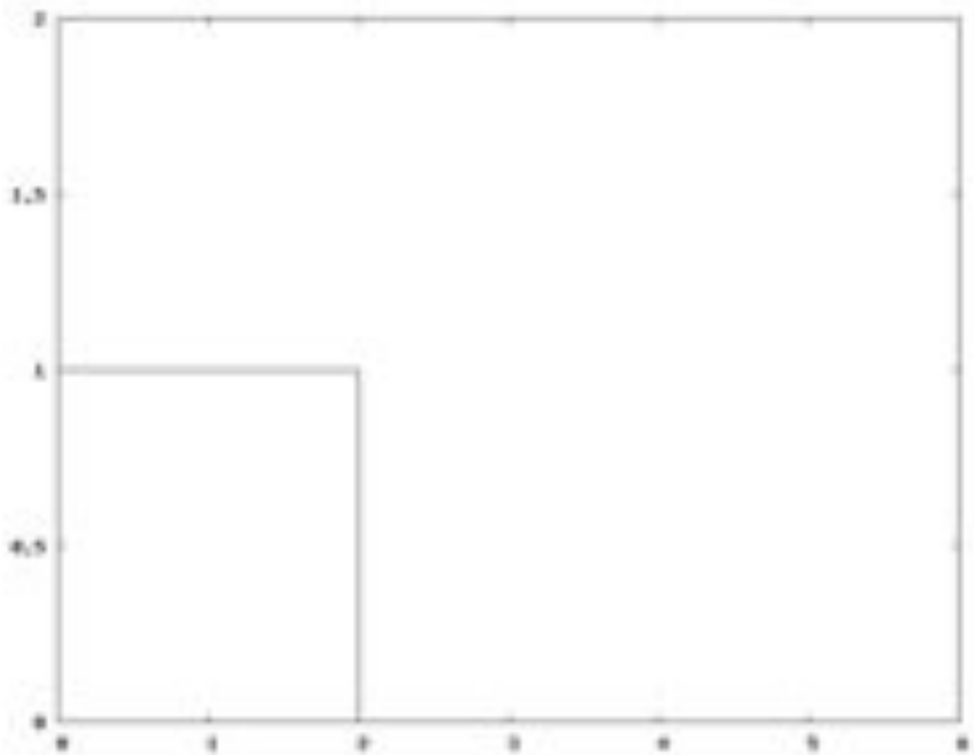

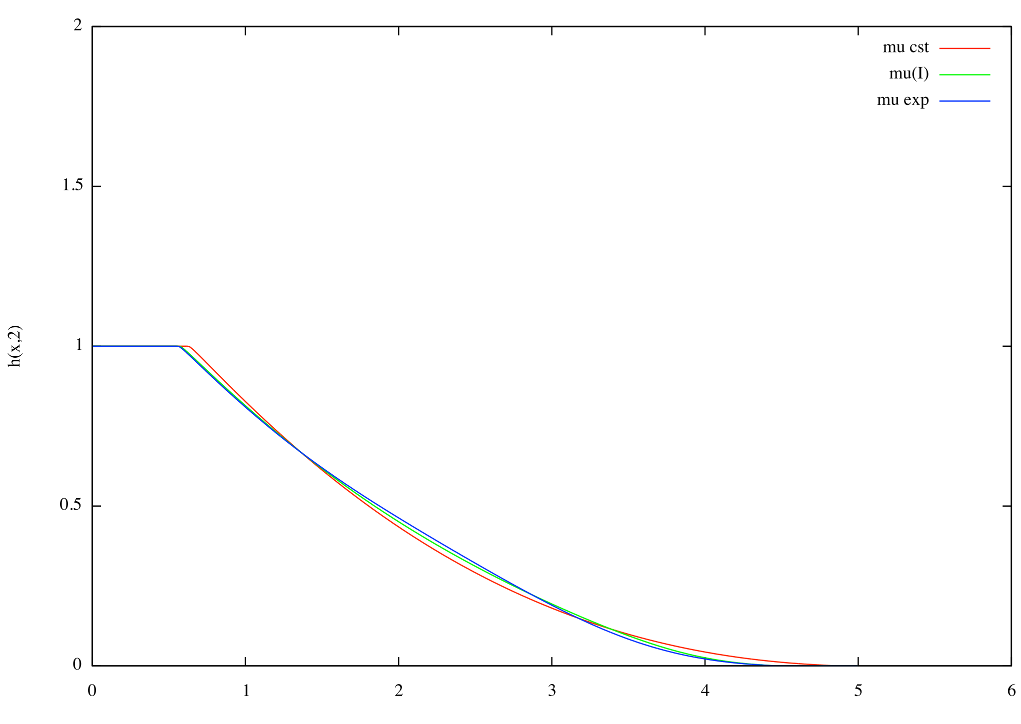

$$\mu(I) = \mu_s$$

$$\mu(I) = \mu_s + \frac{\Delta\mu}{\frac{I_0}{I} + 1}$$

$$\mu(I) = \mu_s + \Delta\mu e^{-\beta/I}$$

mu = 0.45
mu = (0.4 + 0.26/(0.4/In +1))
mu = (0.4 + 0.26*exp(-0.136/In))

Saint-Venant Savage Hutter

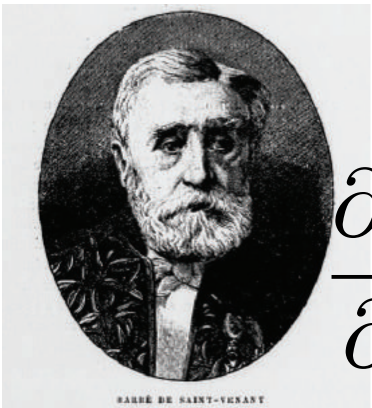

$$\frac{\partial h}{\partial t} + \frac{\partial (Q)}{\partial x} = 0 \quad \frac{\partial Q}{\partial t} + \frac{\partial}{\partial x}\left(\frac{5Q^2}{4h} + \frac{g}{2}(h^2)\right) = -gh\mu(I)\frac{Q}{|Q|}$$

$$I = d\frac{Q}{h^2\sqrt{P/\rho}}$$

Integral over the layer of grains

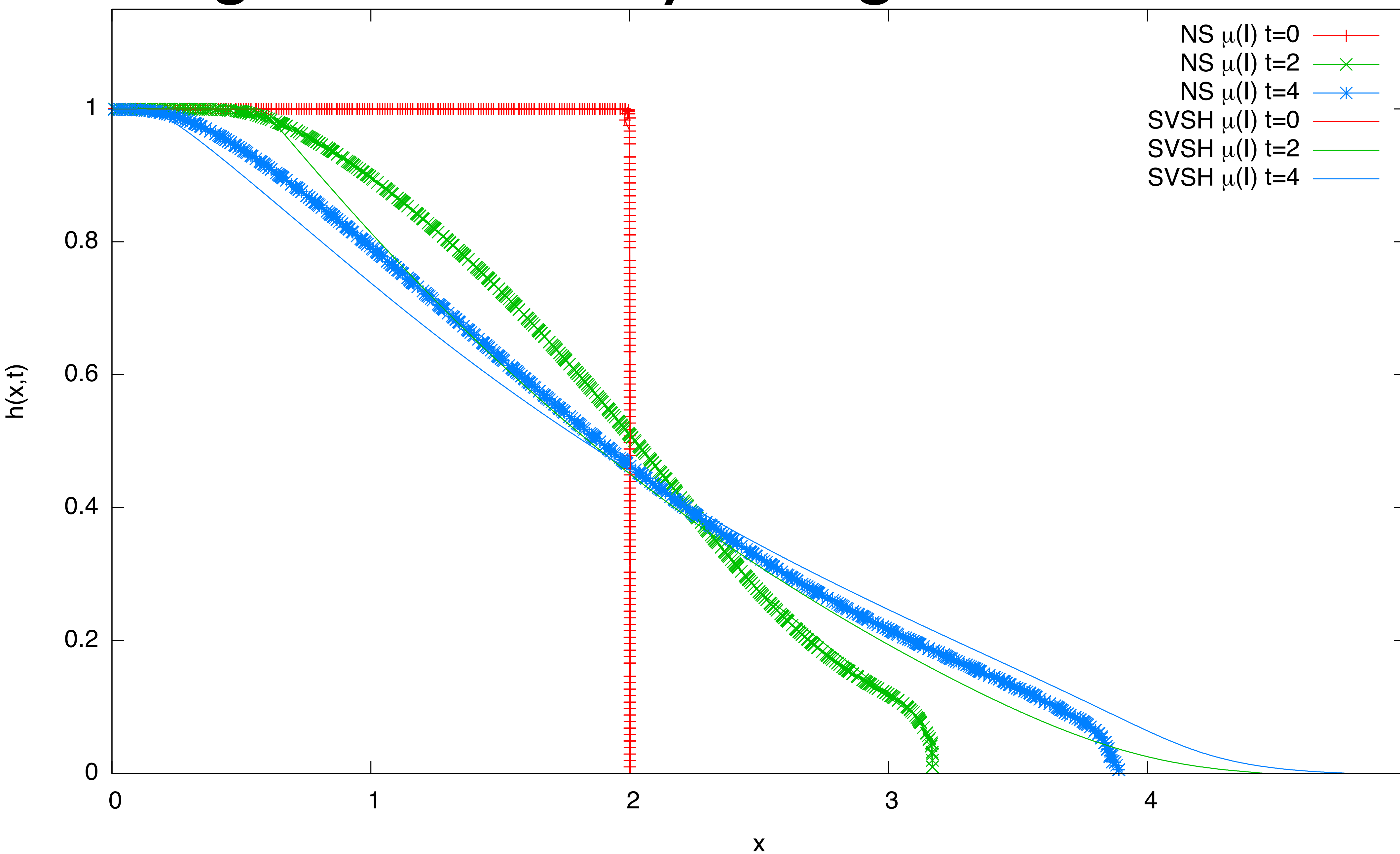

L. Satron, J. Hinch (DAMTP), A. Mangeney (IPGP), E. Larieu (IMFT)

Shallow Water

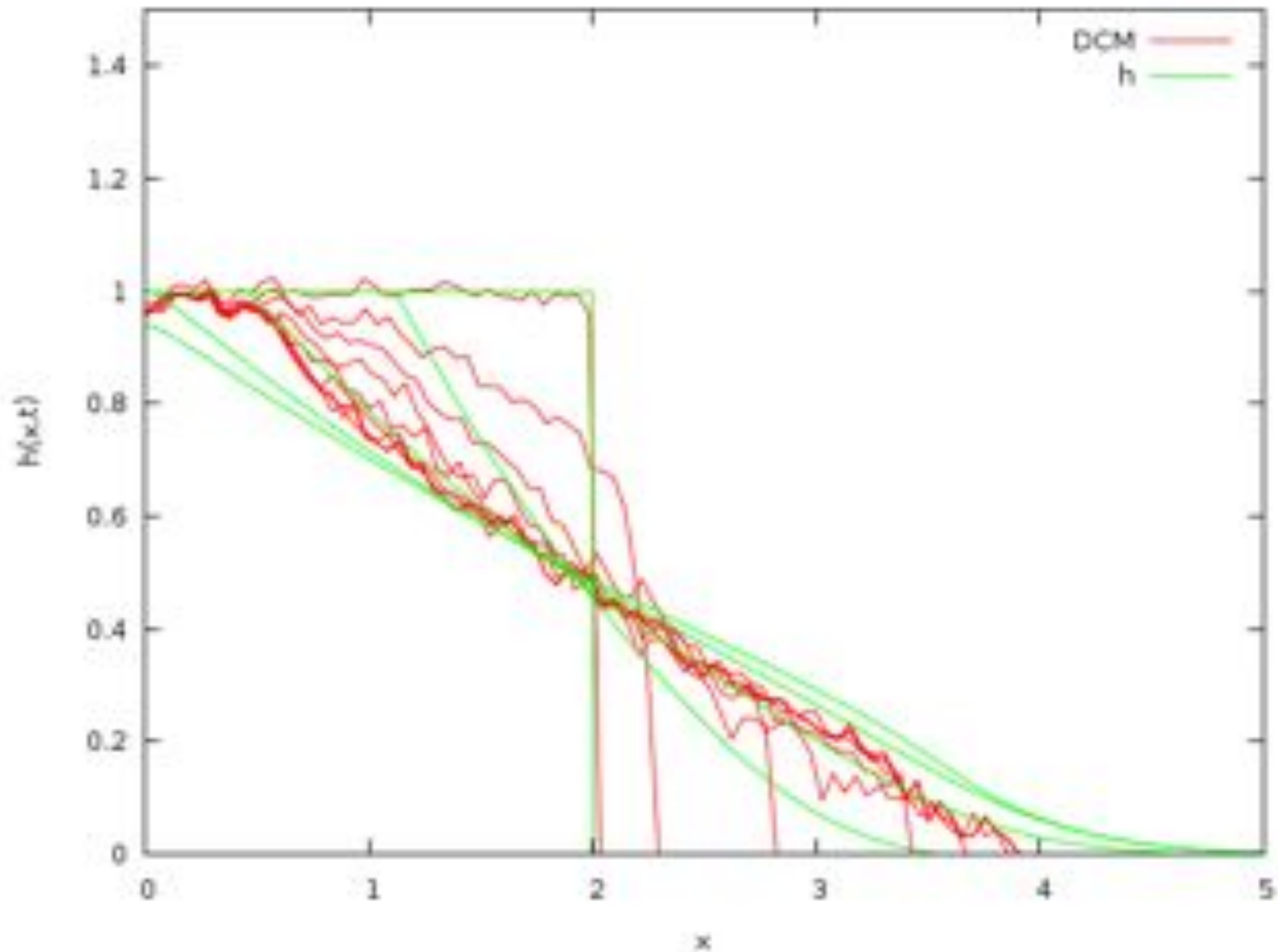

Saint-Venant Savage Hutter *Gerris*

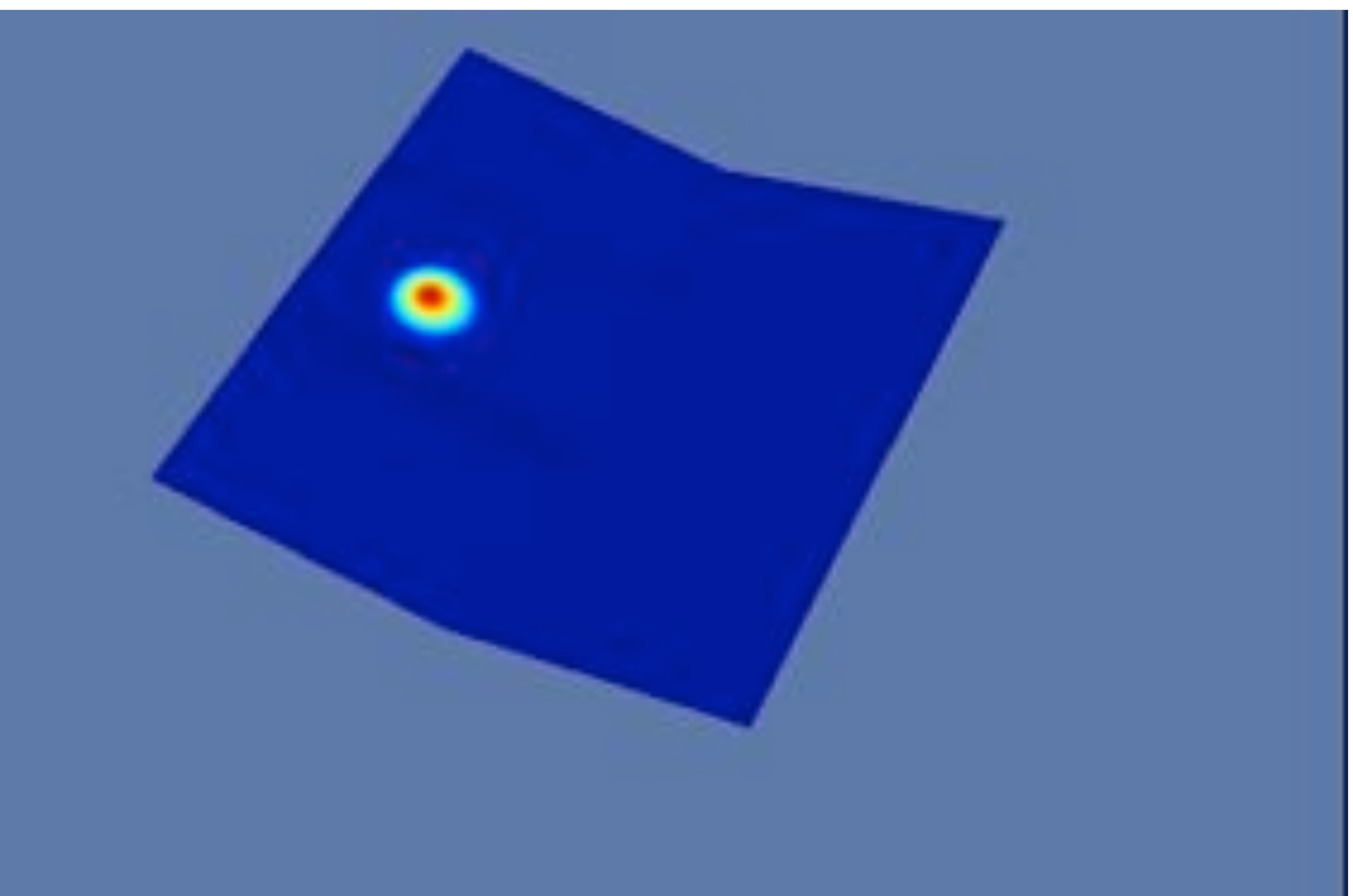

Saint-Venant Savage Hutter *Gerris*

WIELAND, J. M. N. T. GRAY AND K. HUTTER 1999

Marina Pirulli, Marie-Odile Bristeau Anne Mangeney, Claudio Scavia 2006

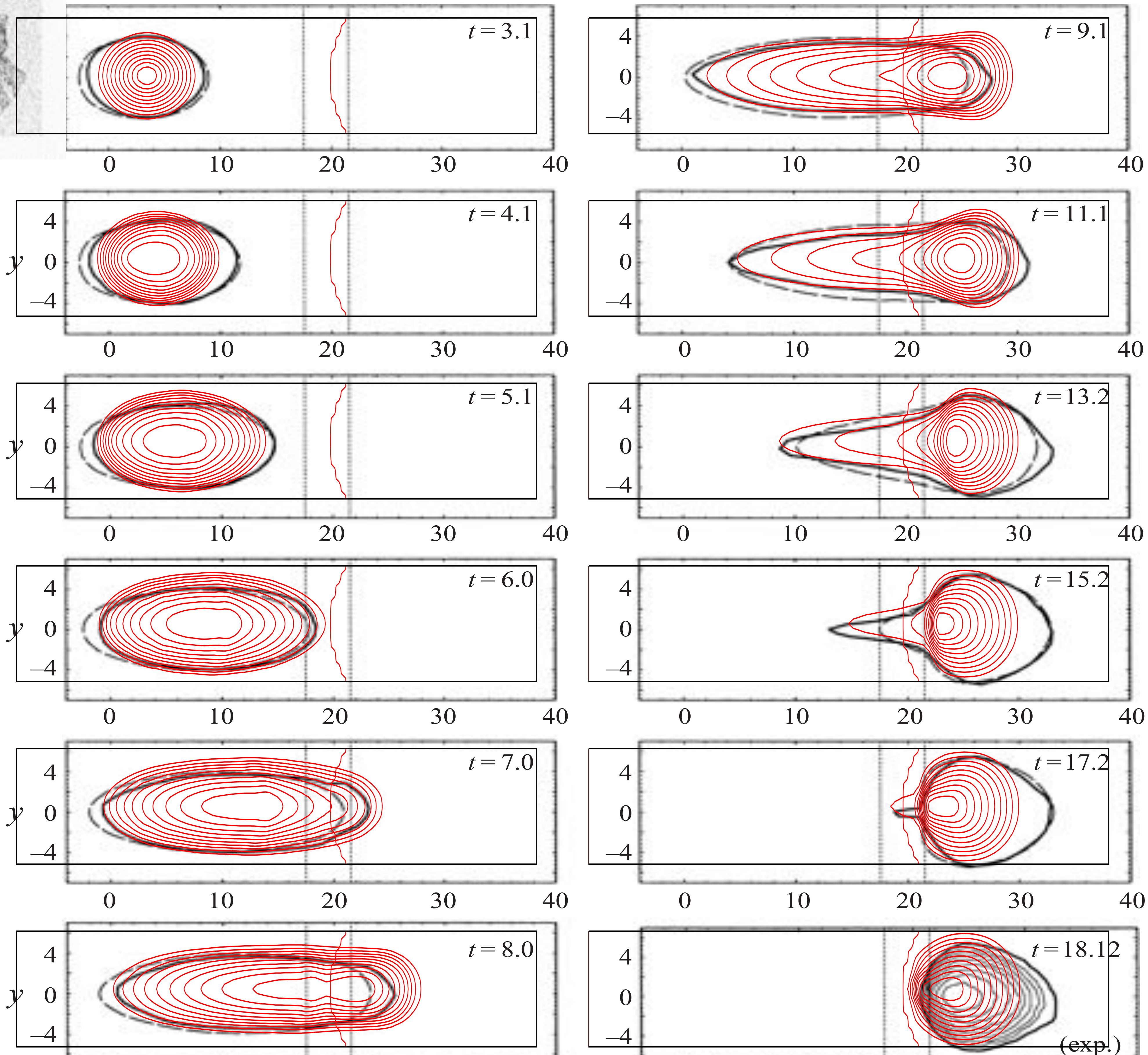

Shallow Water

Full 2D

Basilisk

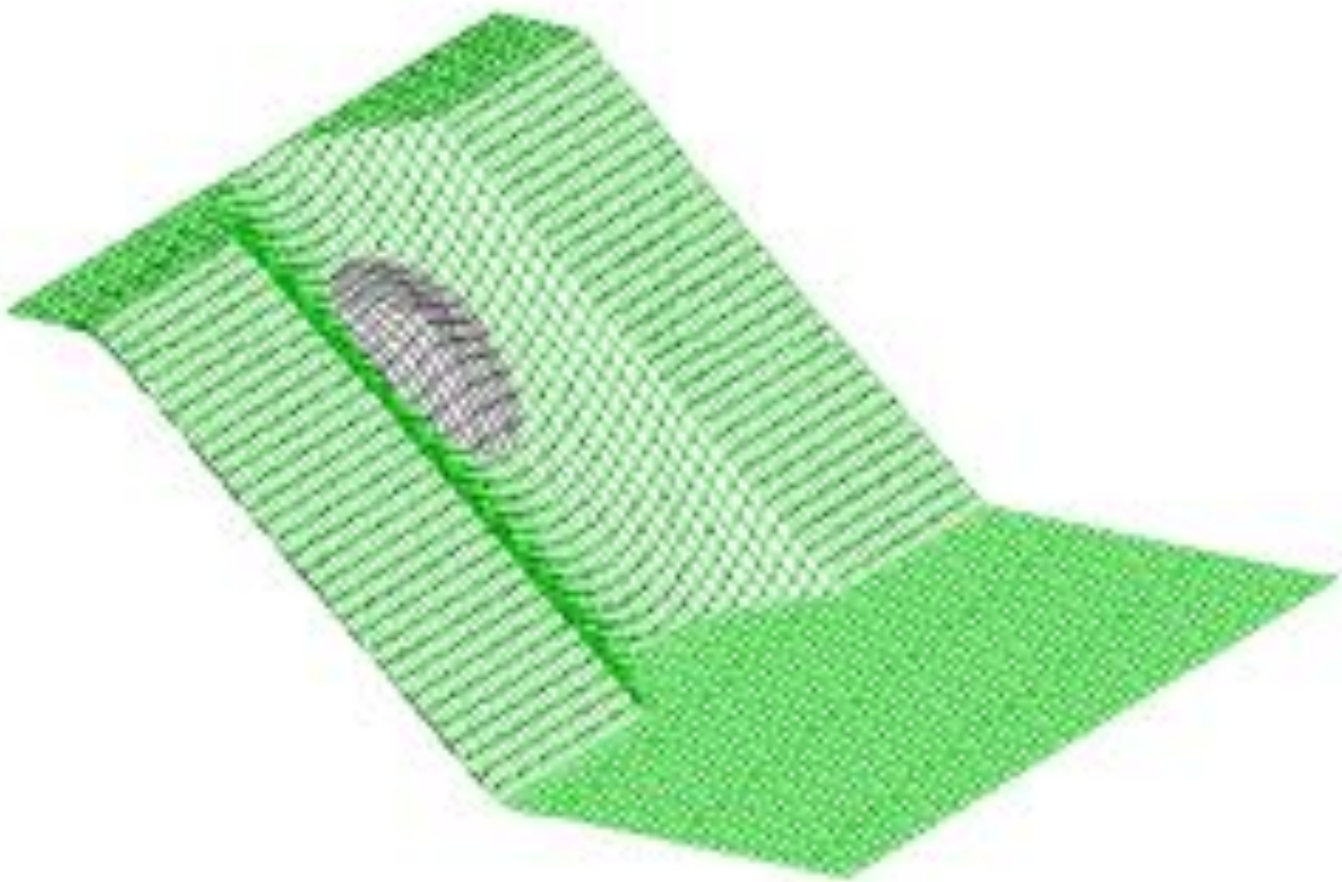

▪

Basiliscus basiliscus is the latin name of the extraordinary Jesus Christ lizard, famous for its ability to run on the surfa of water, a characteristic it shares with another well-known water-walker *Gerris lacustris*.

Shallow water front Pouliquen 99 experiment

Shape of granular fronts down rough inclined planes 1957

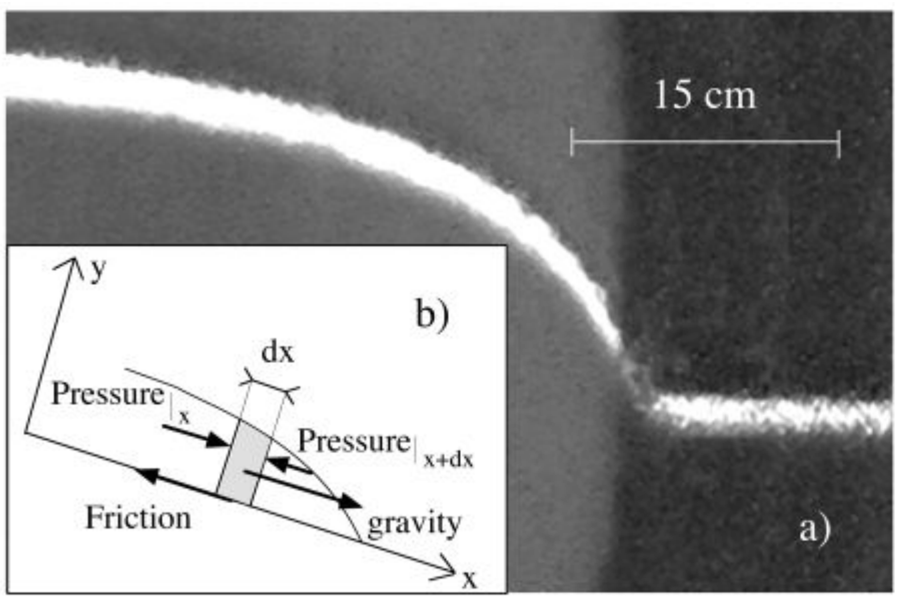

FIG. 2. (a) Picture of the front illuminated by the laser sheet for material 4, $\theta = 21°$, $h_\infty = 9.5$ mm. (b) Forces on an elementary material slice.

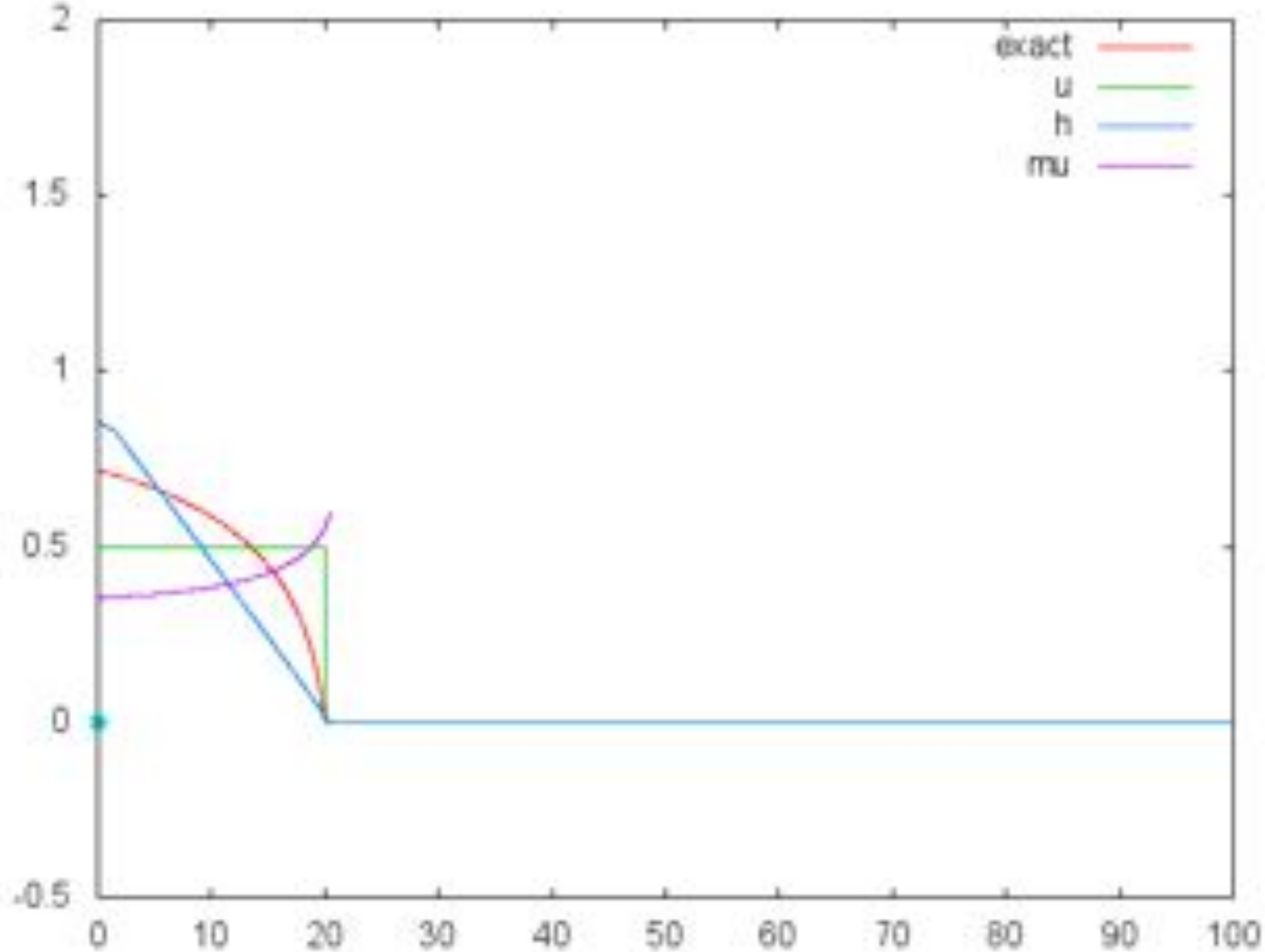

Shallow water front Pouliquen 99 experiment

Edwards Gray 2014

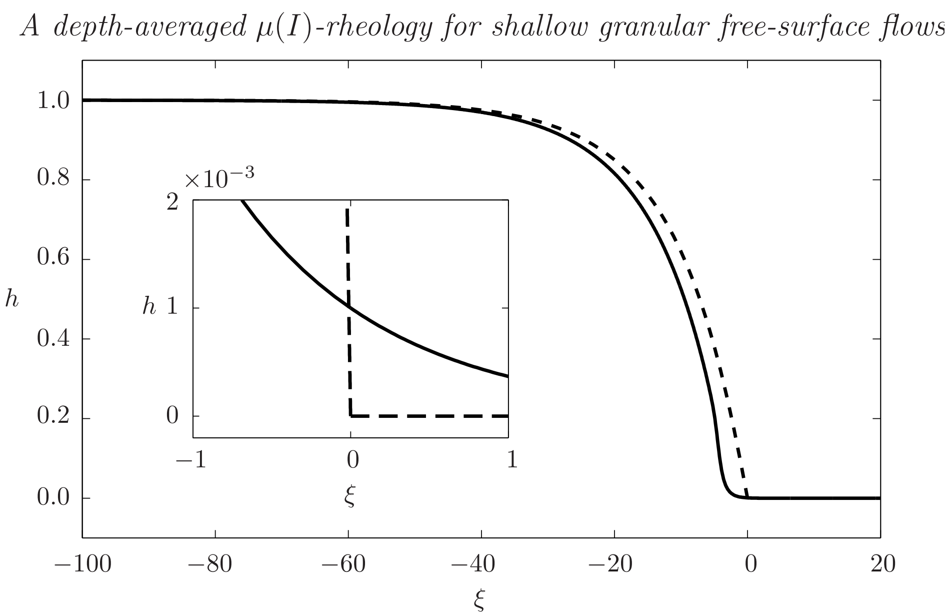

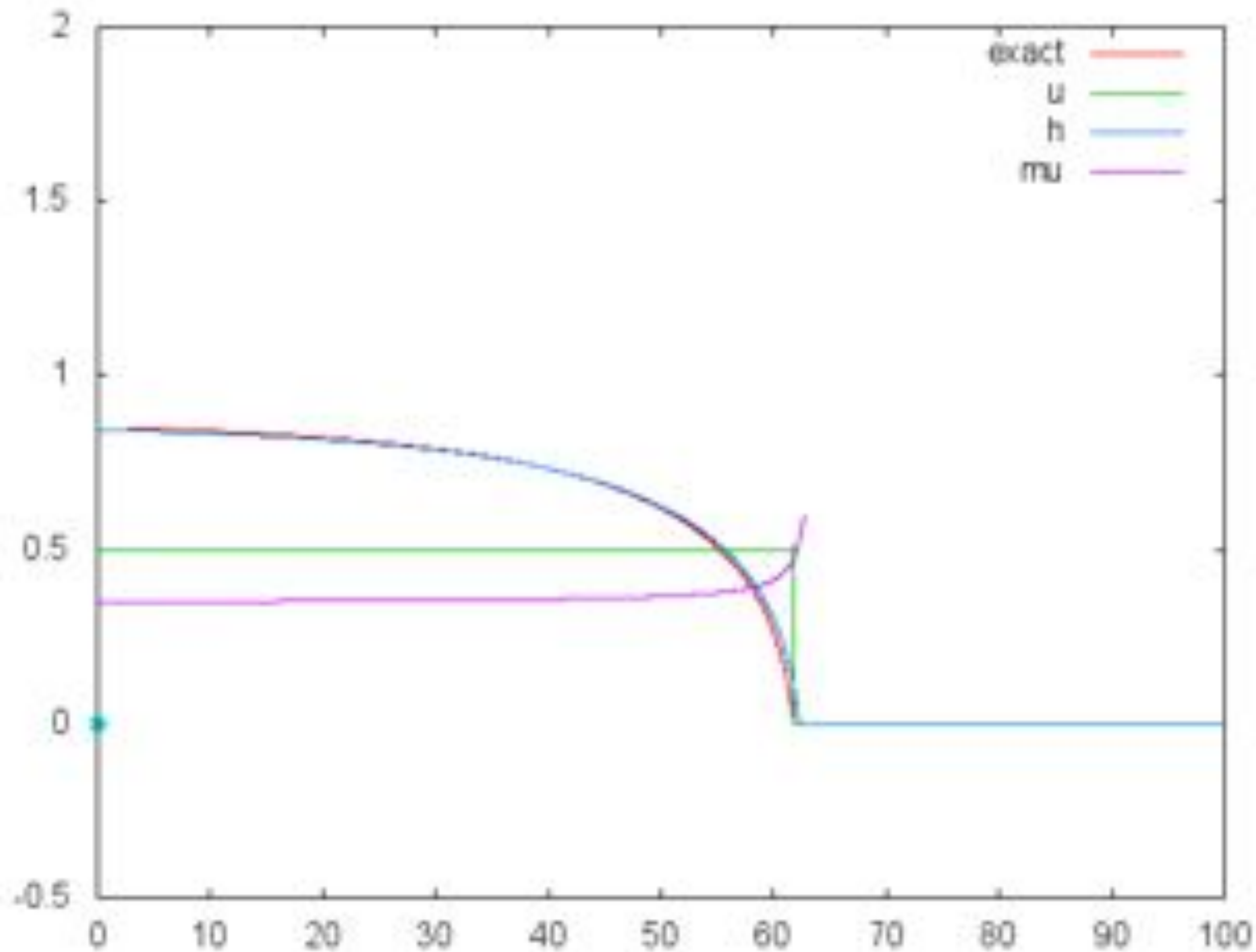

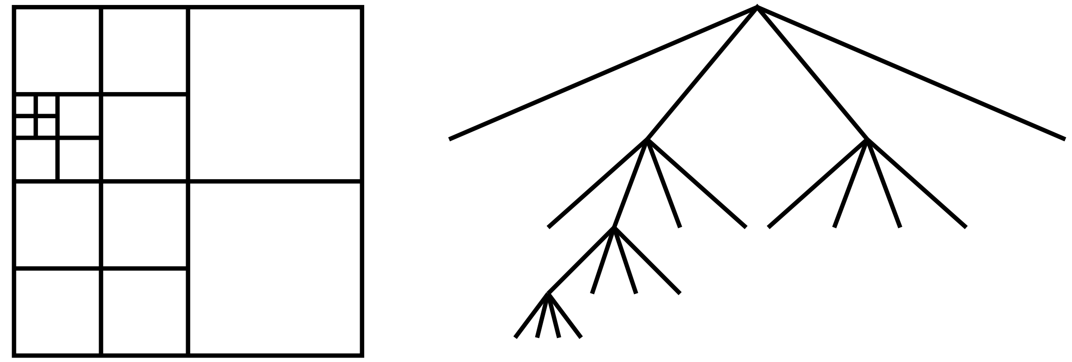

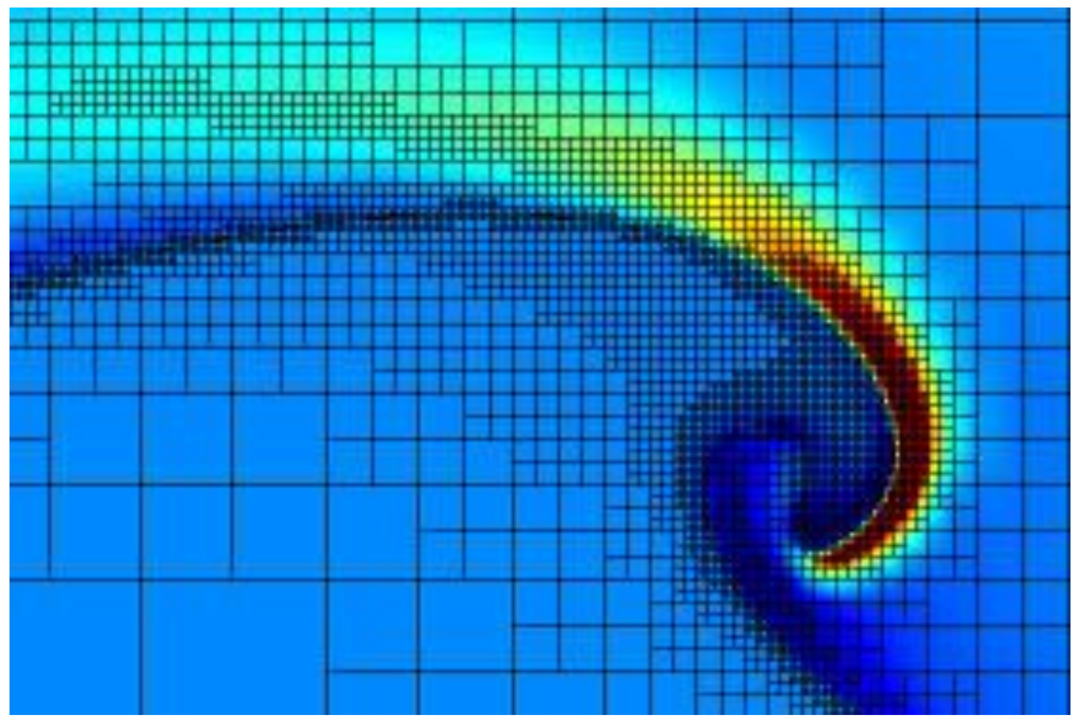

- *Gerris* is a finite volume code by Stéphane Popinet

one part of the code is a Navier Stokes solver

- automatic mesh adaptation
- Volume Of Fluid method for two phase flows
- free on sourceforge

Projection Method

$$\rho_{n+\frac{1}{2}}\left(\frac{\mathbf{u}_*-\mathbf{u}_n}{\Delta t}+\mathbf{u}_{n+\frac{1}{2}}\cdot\boldsymbol{\nabla}\mathbf{u}_{n+\frac{1}{2}}\right)=\boldsymbol{\nabla}\cdot(\eta_{n+\frac{1}{2}}\mathbf{D}_*)-\boldsymbol{\nabla}p_{n-\frac{1}{2}},$$

$$\mathbf{u}_{n+1}=\mathbf{u}_*-\frac{\Delta t}{\rho_{n+\frac{1}{2}}}(\boldsymbol{\nabla}p_{n+\frac{1}{2}}-\boldsymbol{\nabla}p_{n-\frac{1}{2}}),$$

$$\boldsymbol{\nabla}\cdot\mathbf{u}_{n+1}=0.$$

multigrid solver for Laplacien of pressure

$$\boldsymbol{\nabla}\cdot\left(\frac{\Delta t}{\rho_{n+\frac{1}{2}}}\boldsymbol{\nabla}p_{n+\frac{1}{2}}\right)=\boldsymbol{\nabla}\cdot\left(\mathbf{u}_*+\frac{\Delta t}{\rho_{n+\frac{1}{2}}}\boldsymbol{\nabla}p_{n-\frac{1}{2}}\right)$$

implicit for u*

$$\frac{\rho_{n+\frac{1}{2}}}{\Delta t}\mathbf{u}_\star-\frac{1}{2}\nabla\cdot(\eta_{n+\frac{1}{2}}\nabla\mathbf{u}_\star) = \rho_{n+\frac{1}{2}}\left[\frac{\mathbf{u}_n}{\Delta t}-\mathbf{u}_{n+\frac{1}{2}}\cdot\nabla\mathbf{u}_{n+\frac{1}{2}}\right]-\nabla p_{n-\frac{1}{2}}+\frac{1}{2}\nabla\mathbf{u}_n^T\nabla\eta_{n+\frac{1}{2}}.$$

VOF reconstruction

$$\frac{c_{n+\frac{1}{2}}-c_{n-\frac{1}{2}}}{\Delta t}+\nabla\cdot(c_n\mathbf{u}_n)=0$$

implementation in *Gerris* flow solver?

$$\mu(I) = \mu_1 + \frac{\mu_2 - \mu_1}{I_0/I + 1}$$

$$D_2 = \sqrt{D_{ij} D_{ij}} \qquad D_{ij} = \frac{u_{i,j} + u_{j,i}}{2}$$

construction of a viscosity based on the D_2 invariant and redefinition of *I*

$$\eta = \min(\eta_{max}, \max\left(\frac{\mu(I)}{\sqrt{2}D_2} p\ ,\ 0\right)) \qquad I = d\sqrt{2}D_2/\sqrt{(|p|/\rho)}.$$

- the «min» limits viscosity to a large value
- always flow, even slow

Boundary Conditions: no slip and *P=0* at the interface

implementation in *Gerris* flow solver?

$$\mu(I) = \mu_1 + \frac{\mu_2 - \mu_1}{I_0/I + 1}$$

$$D_2 = \sqrt{D_{ij} D_{ij}} \qquad D_{ij} = \frac{u_{i,j} + u_{j,i}}{2}$$

construction of a viscosity based on the *D*2 invariant and redefinition of *I*

$$\eta = \min(\eta_{max}, \max\left(\frac{\mu(I)}{\sqrt{2}D_2} p \ , \ 0\right)) \qquad I = d\sqrt{2}D_2/\sqrt{(|p|/\rho)}.$$

$$\nabla \cdot \mathbf{u} = 0, \ \ \rho\left(\frac{\partial \mathbf{u}}{\partial t} + \mathbf{u} \cdot \nabla \mathbf{u}\right) = -\nabla p + \nabla \cdot (2\eta \mathbf{D}) + \rho g,$$

Boundary Conditions: no slip and *P=0* at the interface

implementation in *Gerris* flow solver?

$$\mu(I) = \mu_1 + \frac{\mu_2 - \mu_1}{I_0/I + 1}$$

$$D_2 = \sqrt{D_{ij}D_{ij}} \qquad D_{ij} = \frac{u_{i,j} + u_{j,i}}{2}$$

construction of a viscosity based on the *D*2 invariant and redefinition of *I*

$$\eta = \min(\eta_{max}, \max\left(\frac{\mu(I)}{\sqrt{2}D_2}p\ ,\ 0\right)) \qquad I = d\sqrt{2}D_2/\sqrt{(|p|/\rho)}.$$

$$\nabla \cdot \mathbf{u} = 0, \ \ \rho\left(\frac{\partial \mathbf{u}}{\partial t} + \mathbf{u}\cdot\nabla\mathbf{u}\right) = -\nabla p + \nabla\cdot(2\eta\mathbf{D}) + \rho g,$$

$$\frac{\partial c}{\partial t} + \nabla\cdot(c\mathbf{u}) = 0, \ \ \rho = c\rho_1 + (1-c)\rho_2, \ \ \eta = c\eta_1 + (1-c)\eta_2$$

The granular fluid is covered by a passive light fluid (it allows for a zero pressure boundary condition at the surface, bypassing an up to now difficulty which was to impose this condition on a unknown moving boundary).

Boundary Conditions: no slip and *P=0* at the top

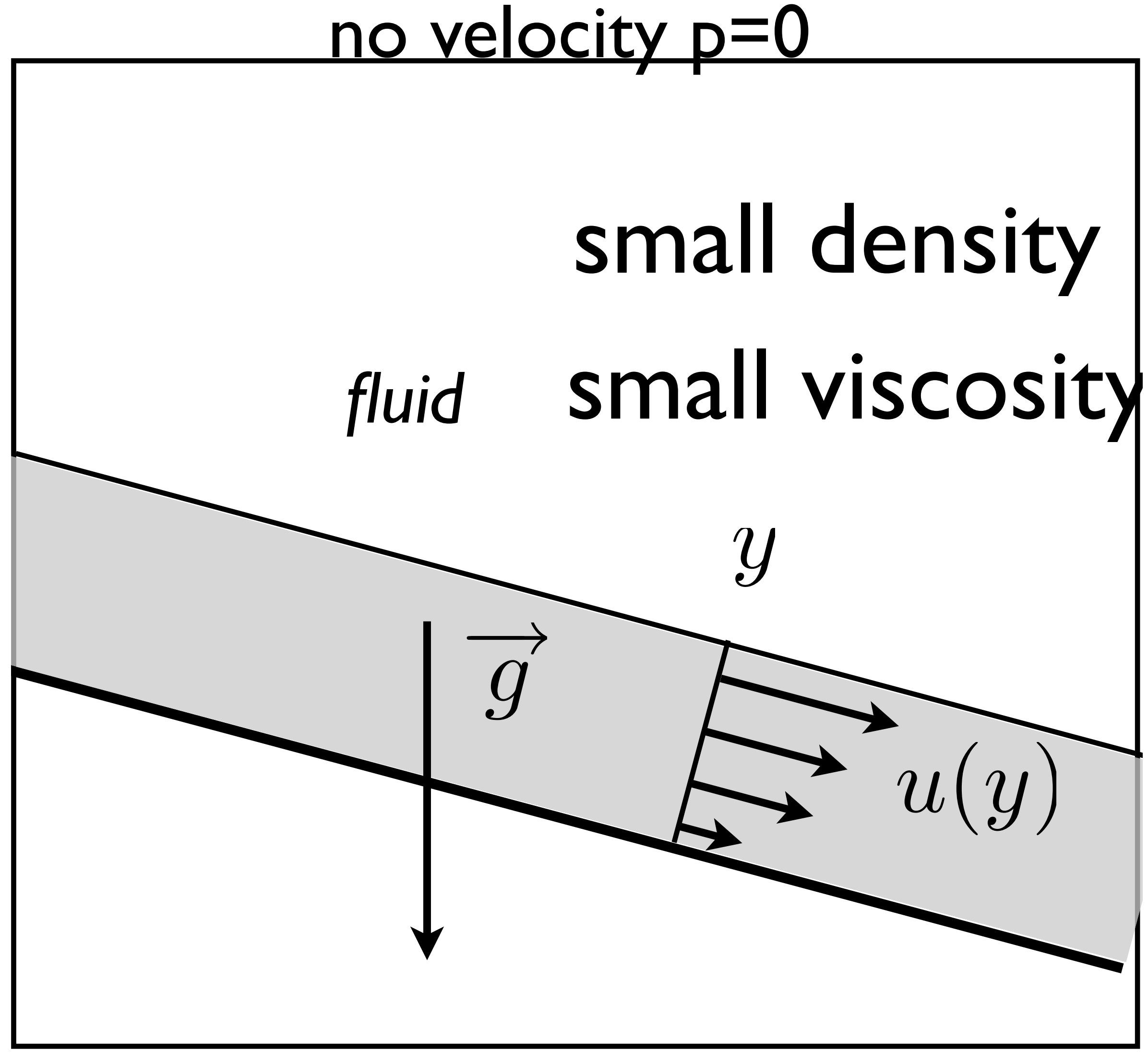

$$\frac{\partial c}{\partial t} + \nabla \cdot (c\mathbf{u}) = 0, \quad \rho = c\rho_1 + (1-c)\rho_2, \quad \eta = c\eta_1 + (1-c)\eta_2$$

The granular fluid is covered by a passive light fluid (it allows for a zero pressure boundary condition at the surface, bypassing an up to now difficulty which was to impose this condition on a unknown moving boundary).

Boundary Conditions: no slip and *P=0* at the top

Test of the code: «Bagnold» avalanche

kind of Nusselt film solution
"Half Poiseuille"

Contact Dynamic simulation Lydie Staron

Test of the code: «Bagnold» avalanche

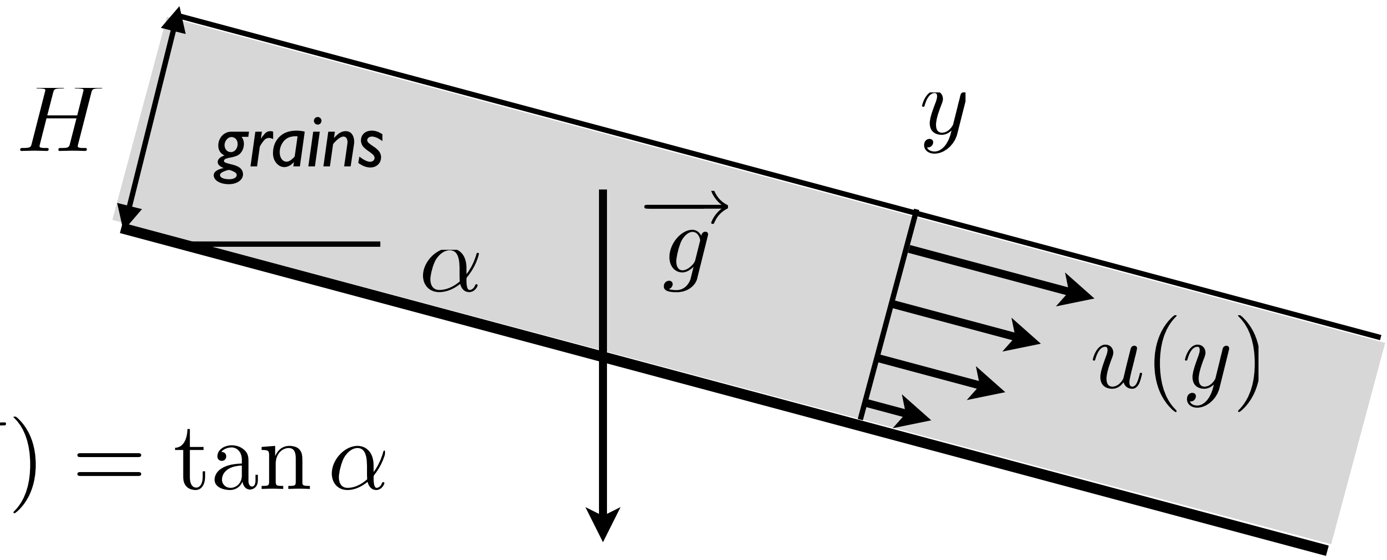

$$\mu(I) = \tan\alpha$$

$$u = \frac{2}{3} I_\alpha \sqrt{g d \cos\alpha \frac{H^3}{d^3}} \left(1 - \left(1 - \frac{y}{H}\right)^{3/2}\right),$$

$$v = 0, \;\; p = \rho g H \left(1 - \frac{y}{H}\right) \cos\alpha.$$

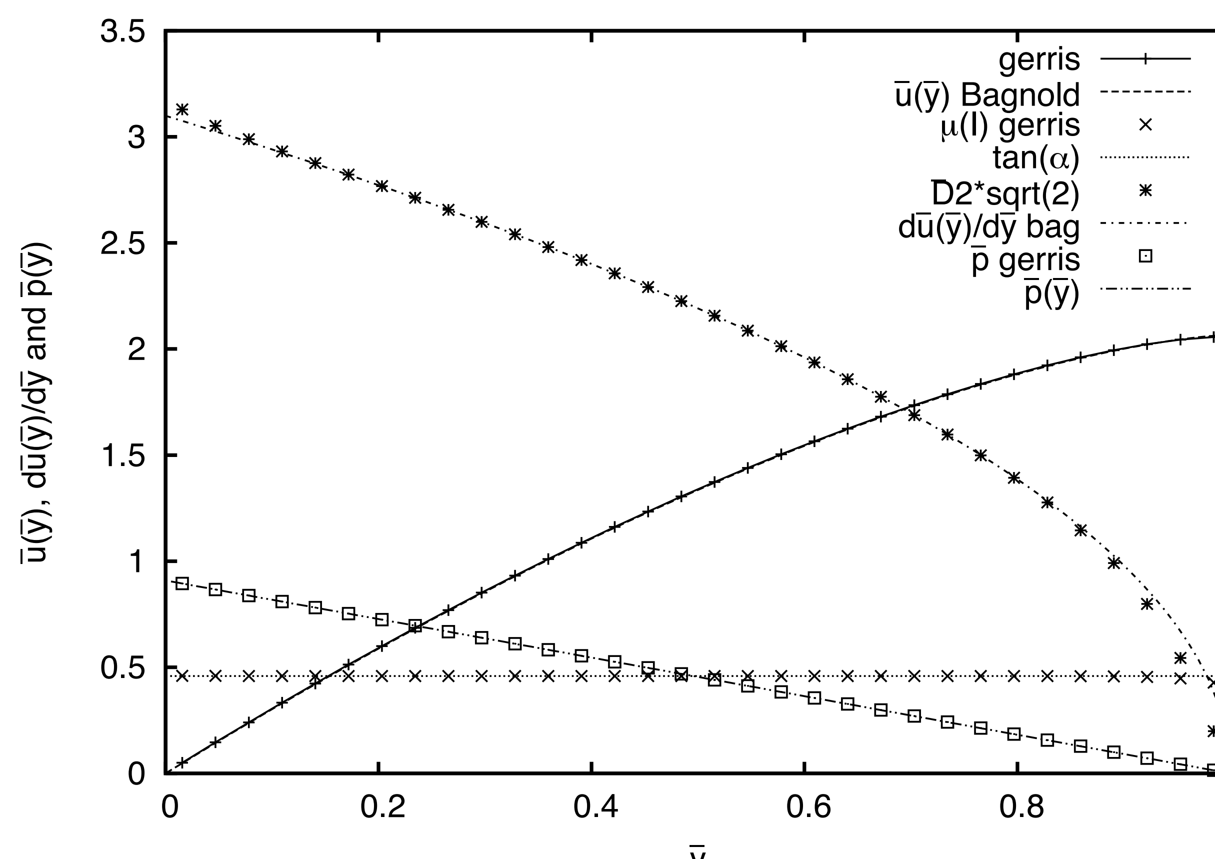

Test of the code: «Bagnold» avalanche

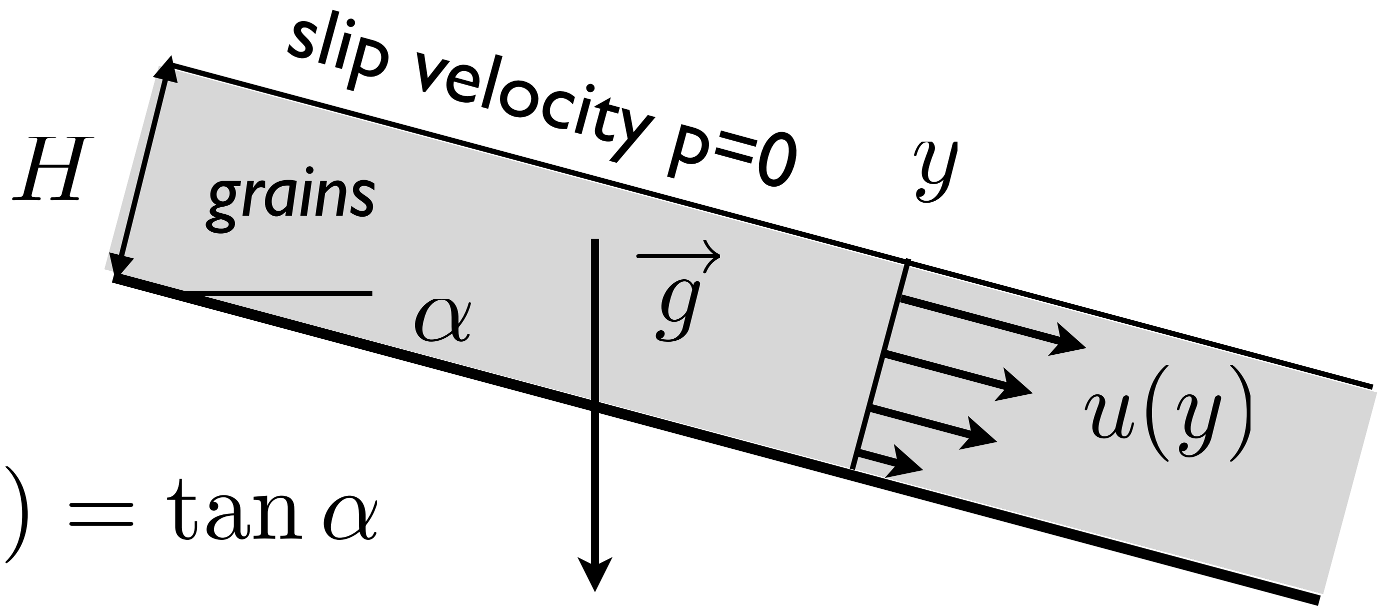

$$\mu(I) = \tan\alpha$$

$$u = \frac{2}{3} I_\alpha \sqrt{gd\cos\alpha \frac{H^3}{d^3}} \left(1 - \left(1 - \frac{y}{H}\right)^{3/2}\right),$$

$$v = 0, \quad p = \rho g H \left(1 - \frac{y}{H}\right) \cos\alpha.$$

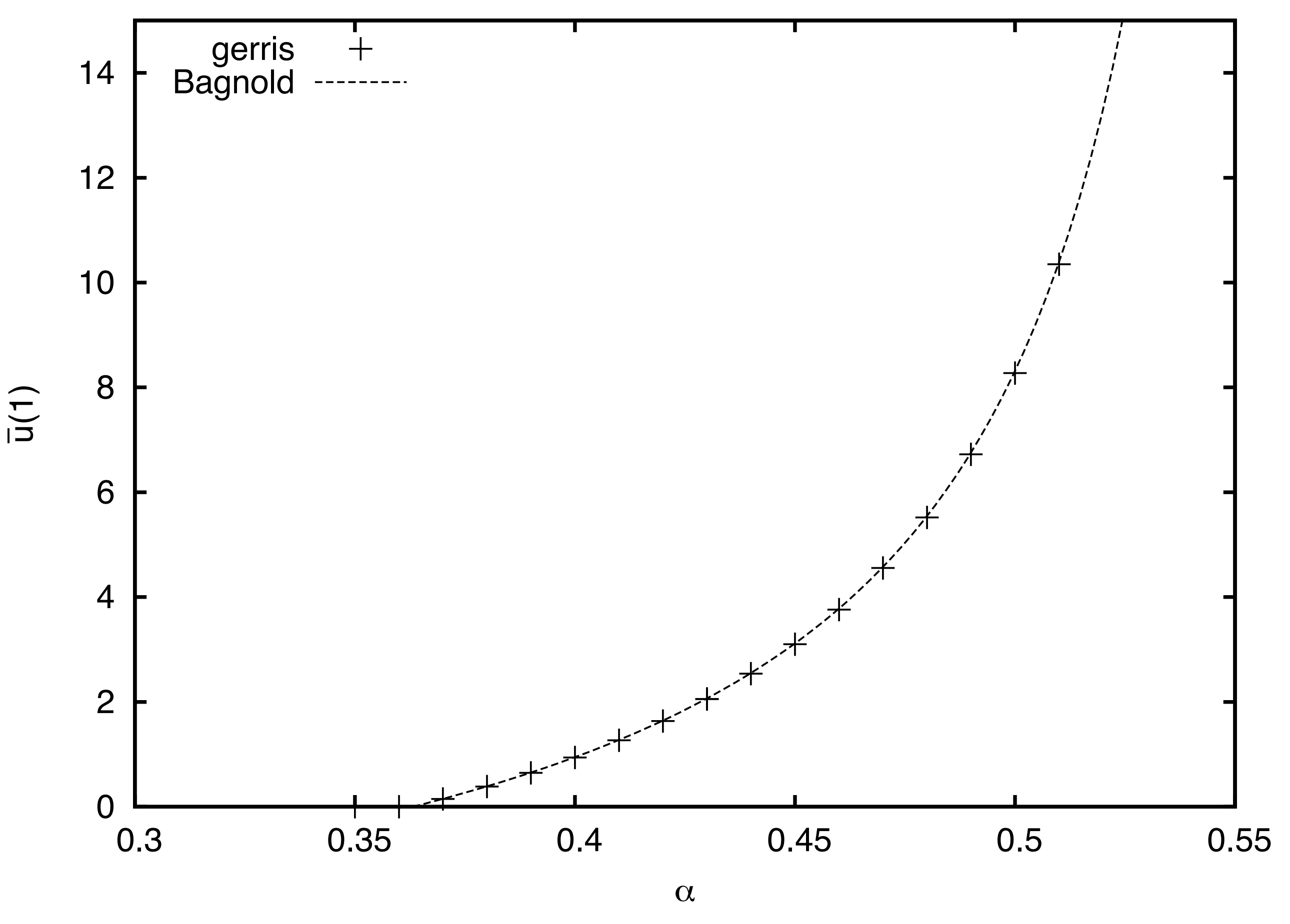

The sand pit problem: quickly remove the bucket of sand

http://www.mylot.com/w/photokeywords/pail.asp

Granular Column Collapse

E. Lajeunesse A. Mangeney-Castelnau and J. P. Vilotte PoF 204

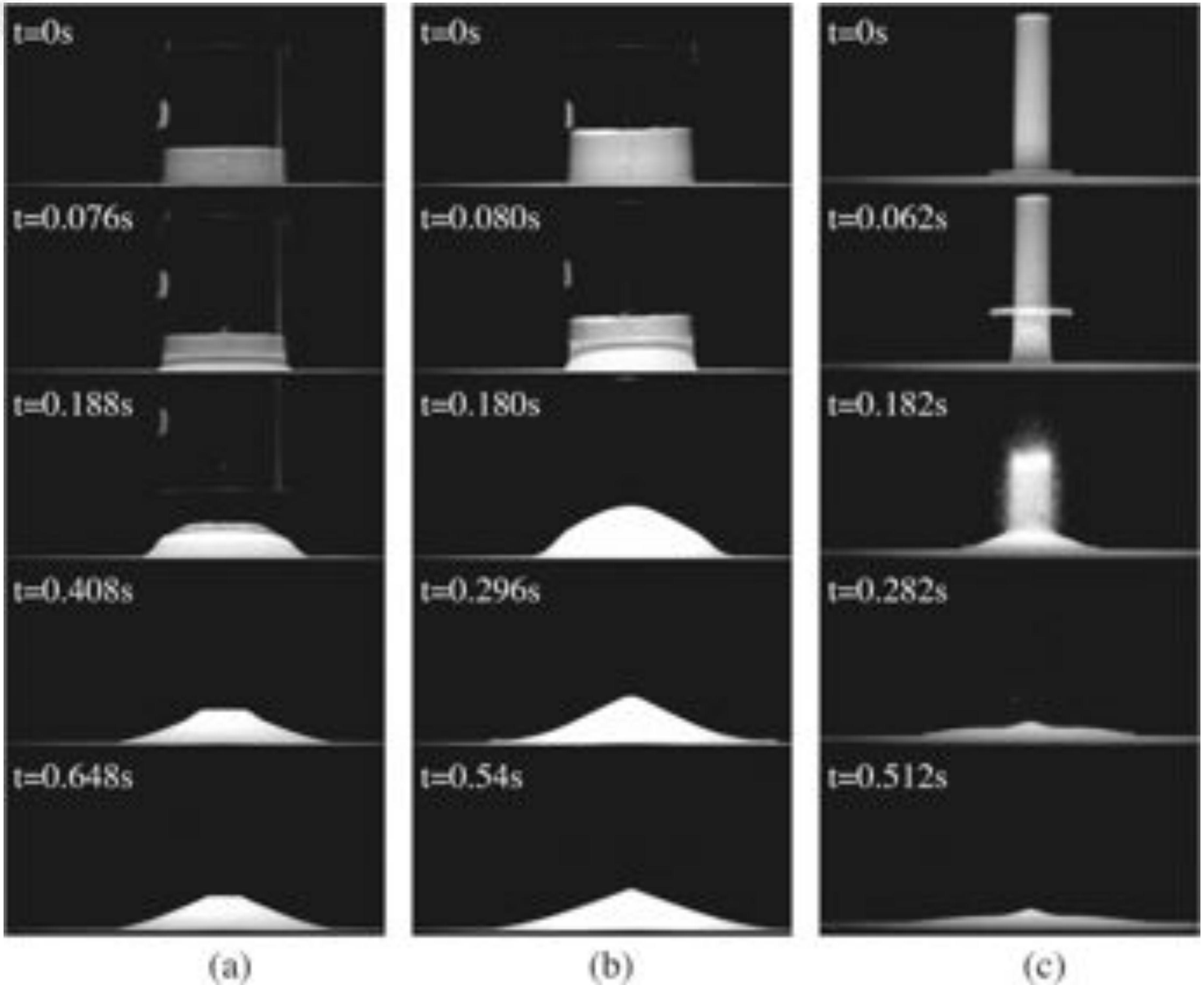

The sand pit problem: quickly remove the bucket of sand

http://www.mylot.com/w/photokeywords/pail.asp

Granular Column Collapse

aspect ratio $a = H_0/R_0 = H_0/L_0$

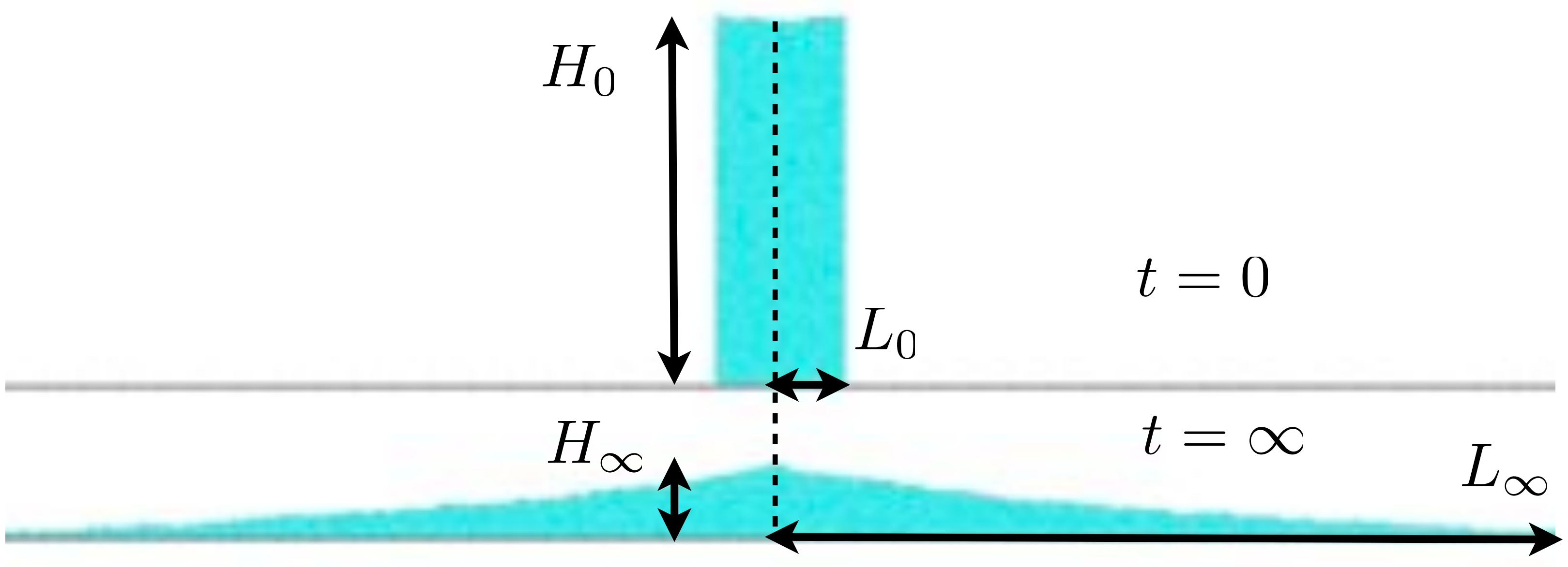

The sand pit problem: quickly remove the bucket of sand

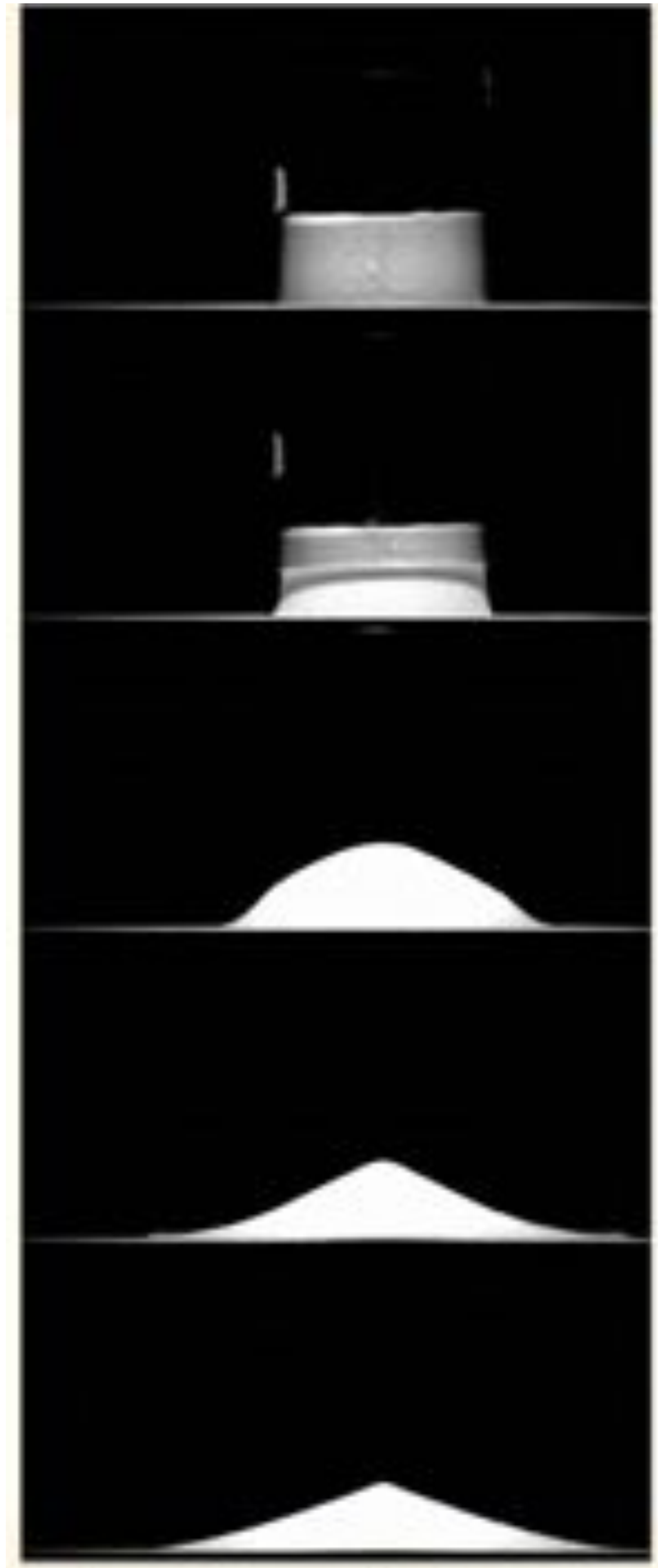

Lajeunesse et al., 2004

Collapse of columns

a=0.37

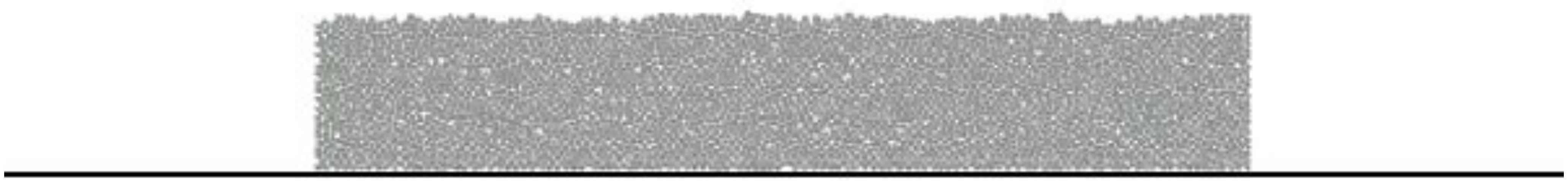

Contact Dynamic simulation Lydie Staron

Collapse of columns

a=0.90

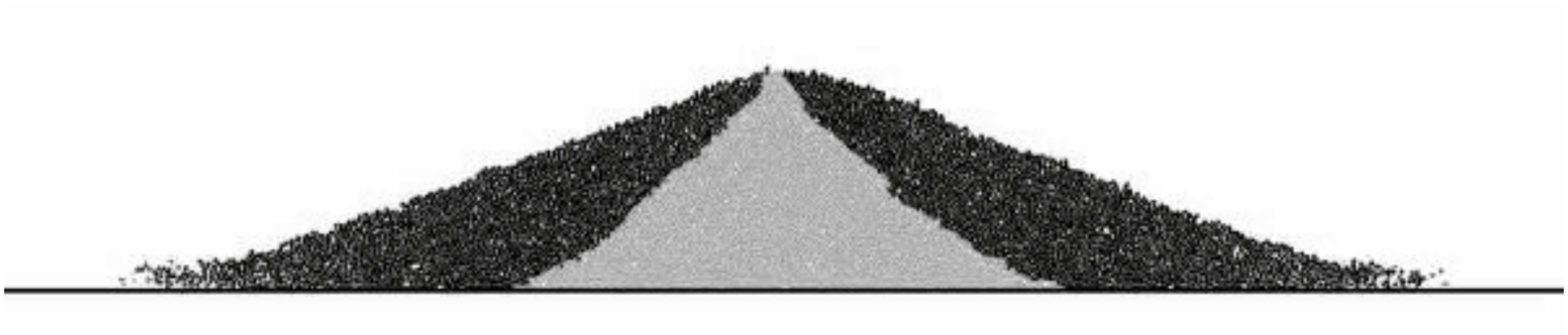

Contact Dynamic simulation Lydie Staron

Collapse of columns simulation *Gerris* $\mu(I)$

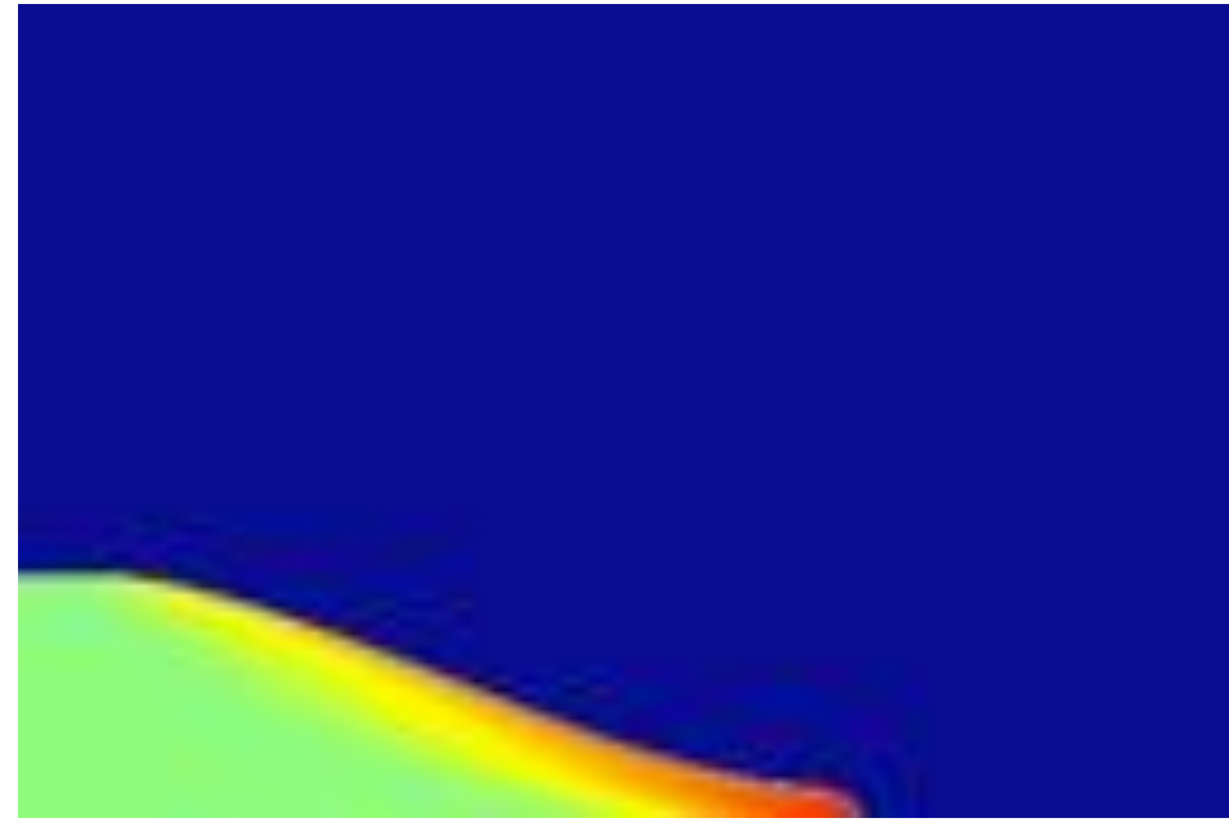

Collapse of columns of aspect ratio 0.5 comparison of Discrete Simulation Contact Method and Navier Stokes gerris, shape at time 0, 1, 2, 3, 4 and position of the front of the avalanche as function of time (time measured with $\sqrt{H_0/g}$ and space with aH_0)

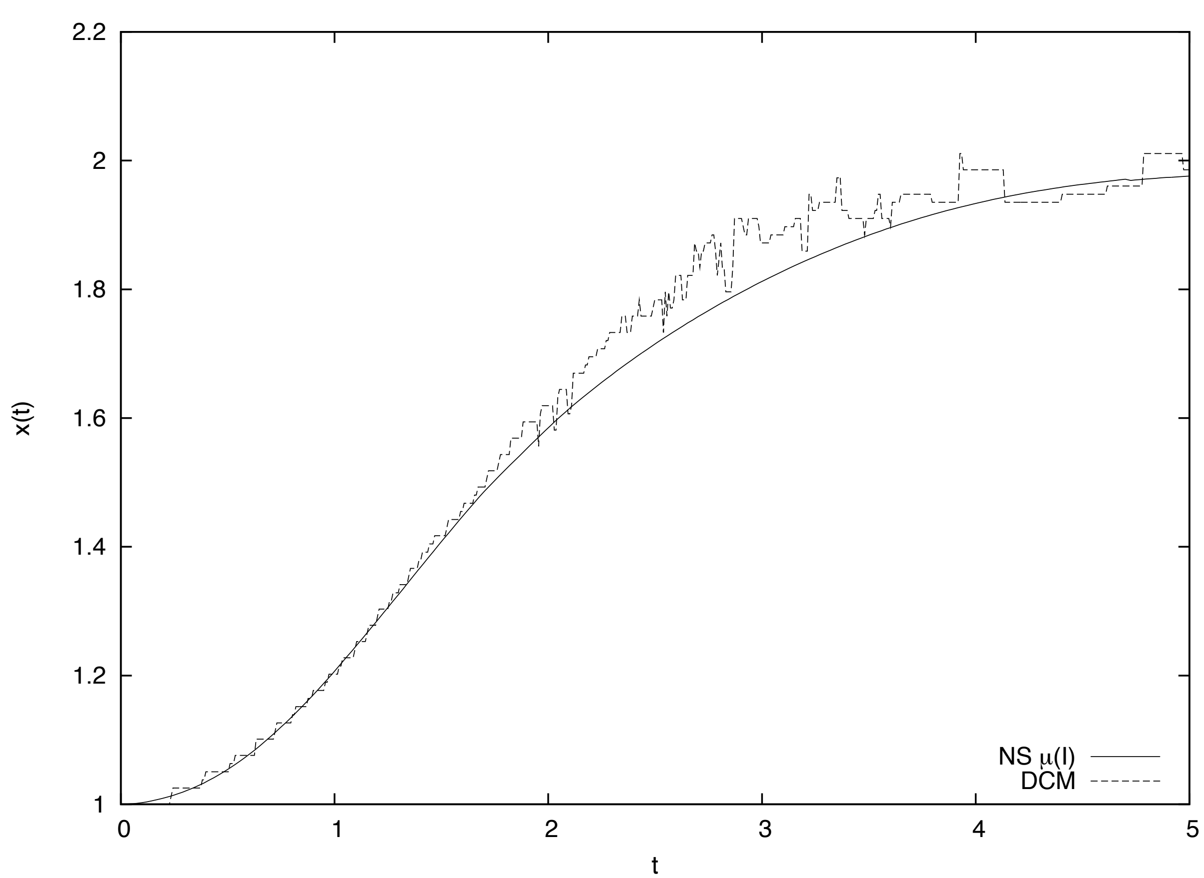

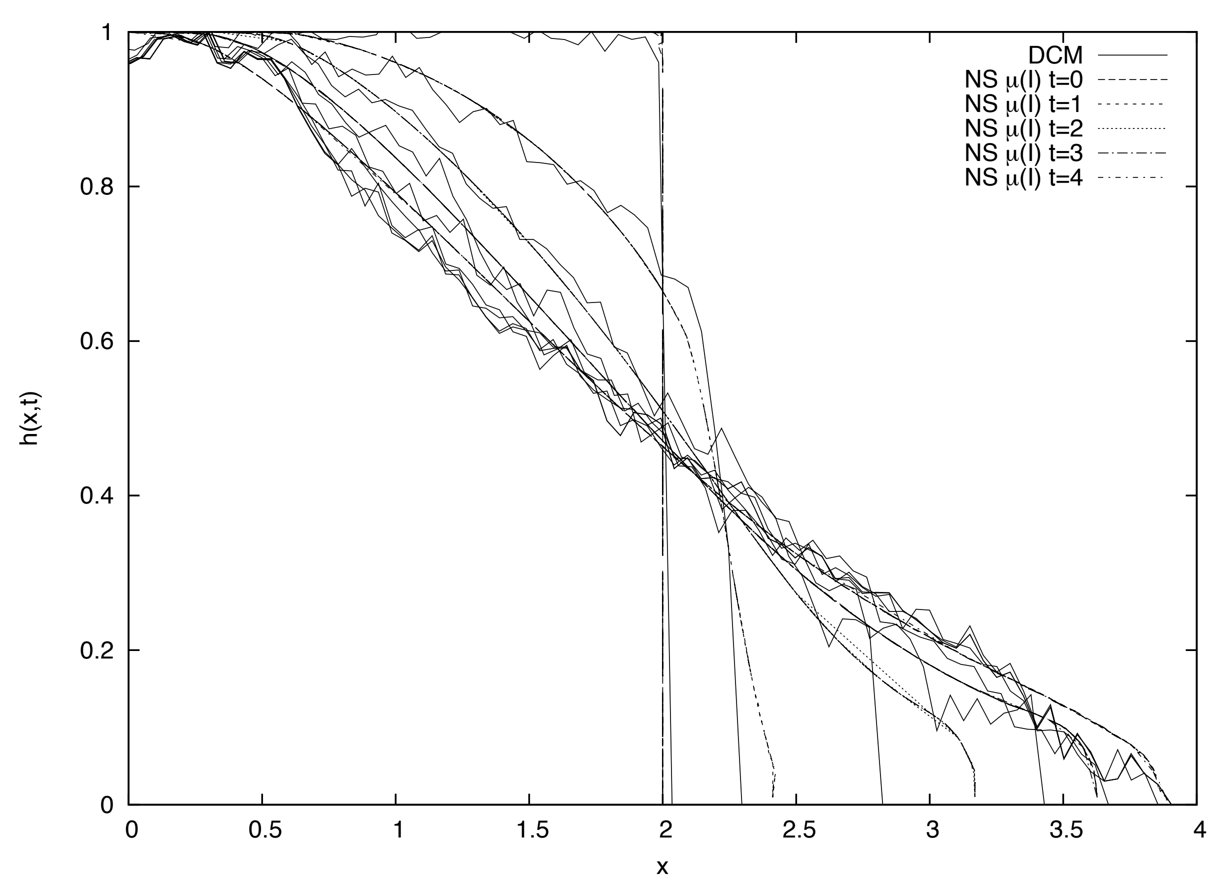

Collapse of columns simulation *Gerris μ(I)*

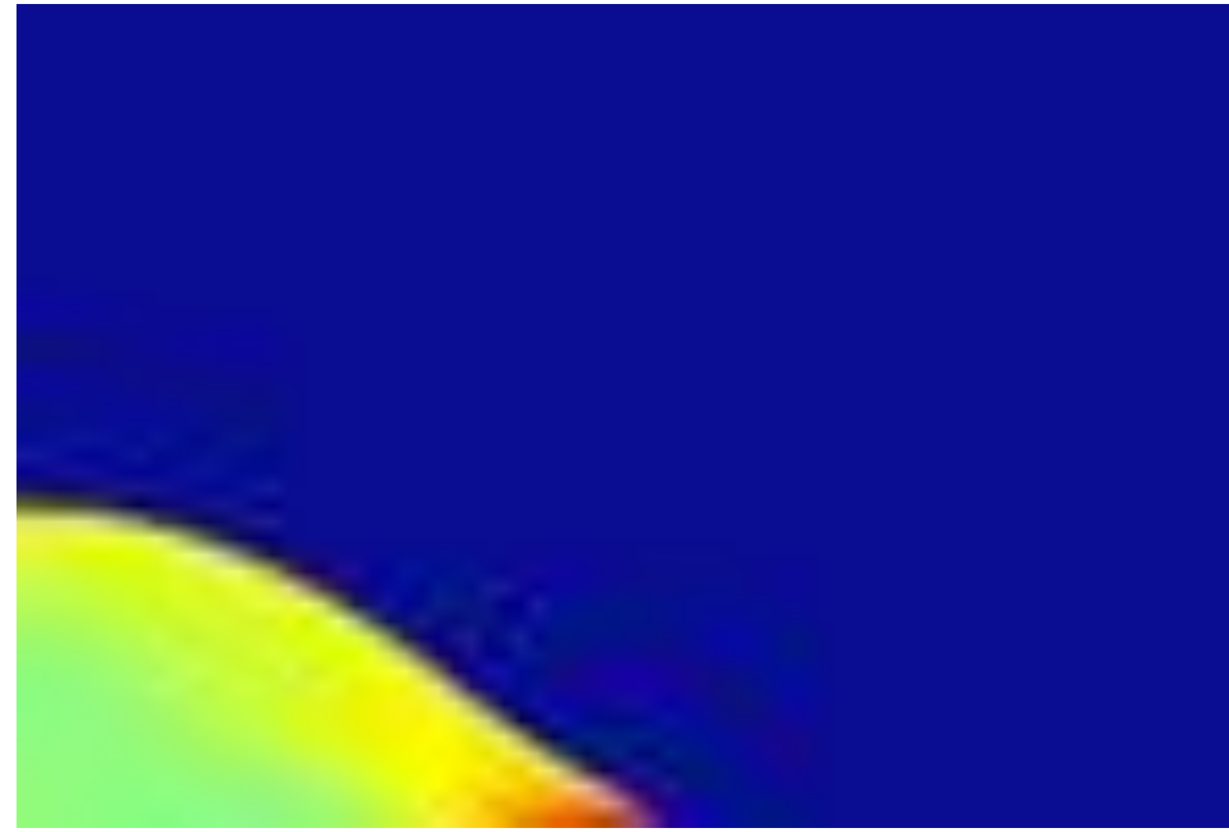

Collapse of columns of aspect ratio 1.42 comparison of Discrete Simulation Contact Method and Navier Stokes gerris, shape at time 0, 1, 2, 3, 4 and position of the front of the avalanche as function of time (time measured with $\sqrt{H_0/g}$ and space with aH_0)

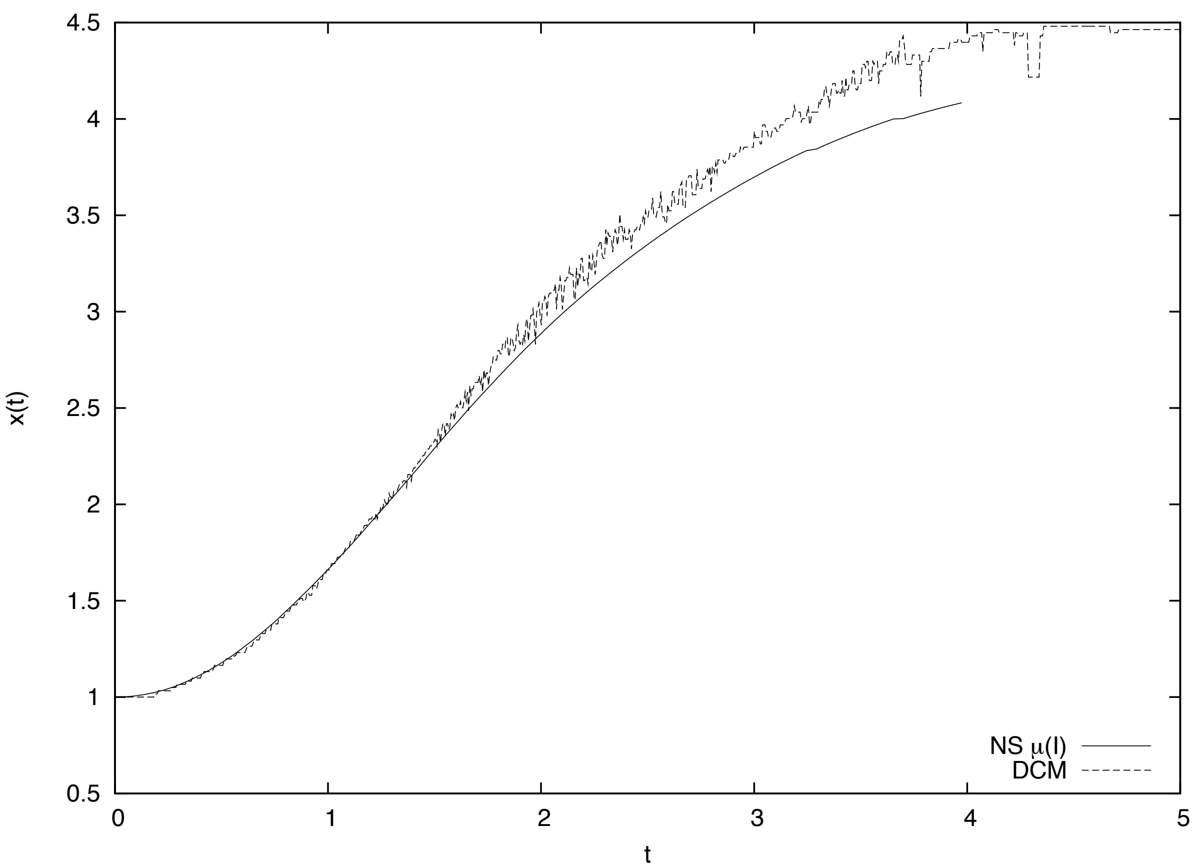

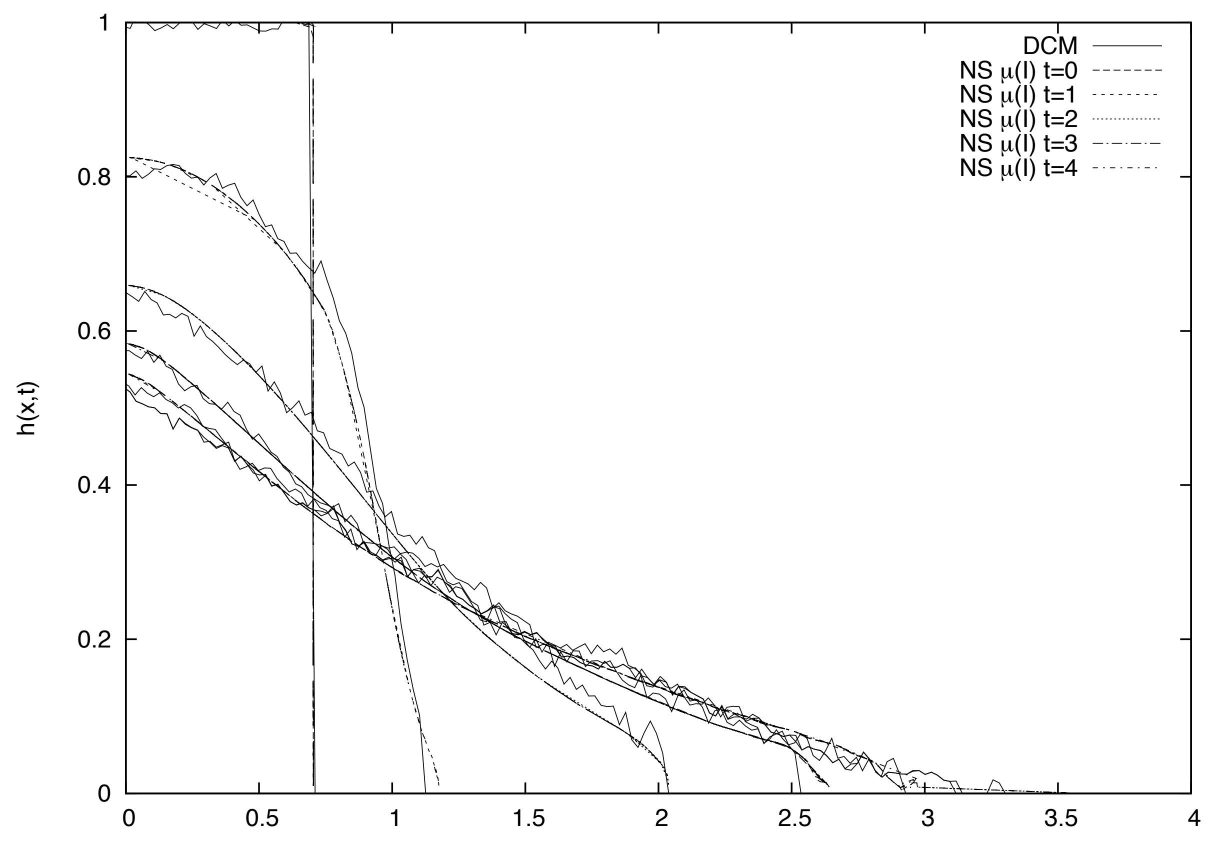

Collapse of columns simulation *Gerris* $\mu(I)$

Collapse of columns of aspect ratio 6.26 comparison of Discrete Simulation Contact Method and Navier Stokes gerris, shape at time 0, 1, 2, 3, 4 and position of the front of the avalanche as function of time (time measured with $\sqrt{H_0/g}$ and space with aH_0)

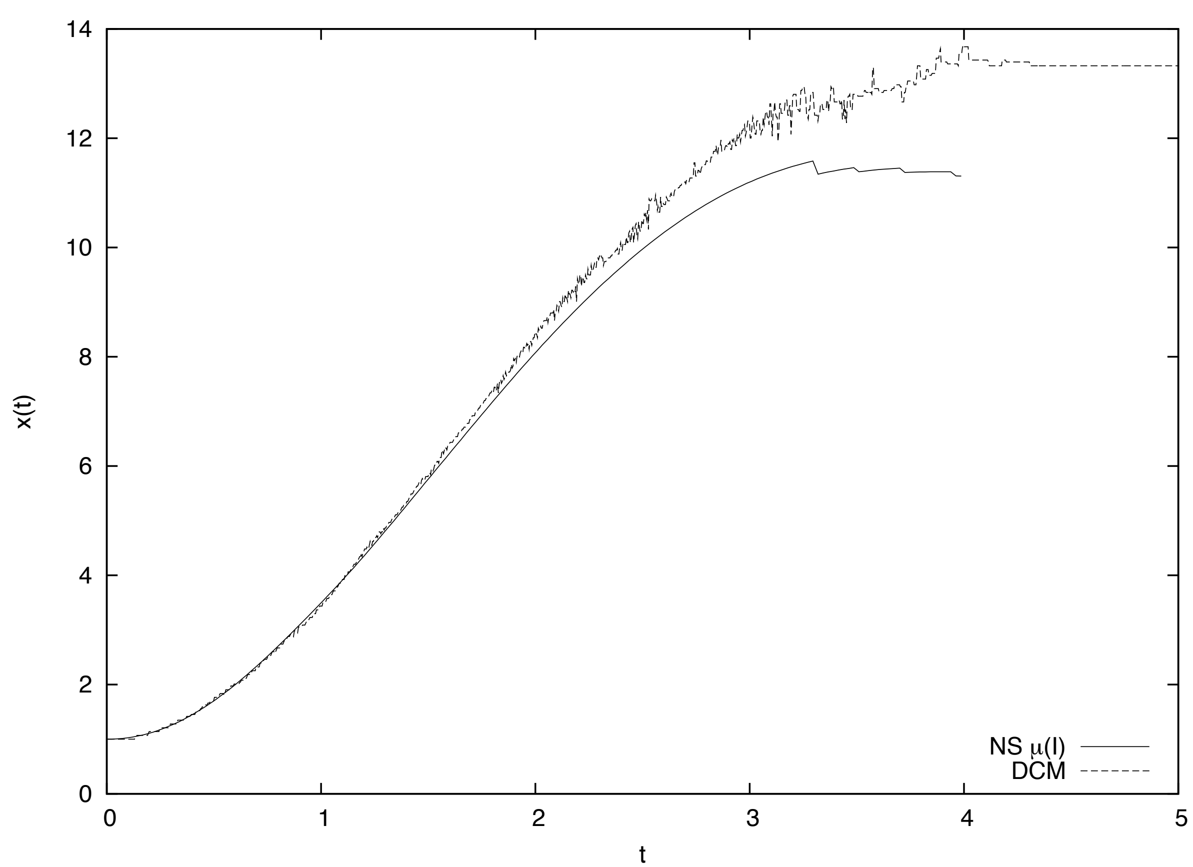

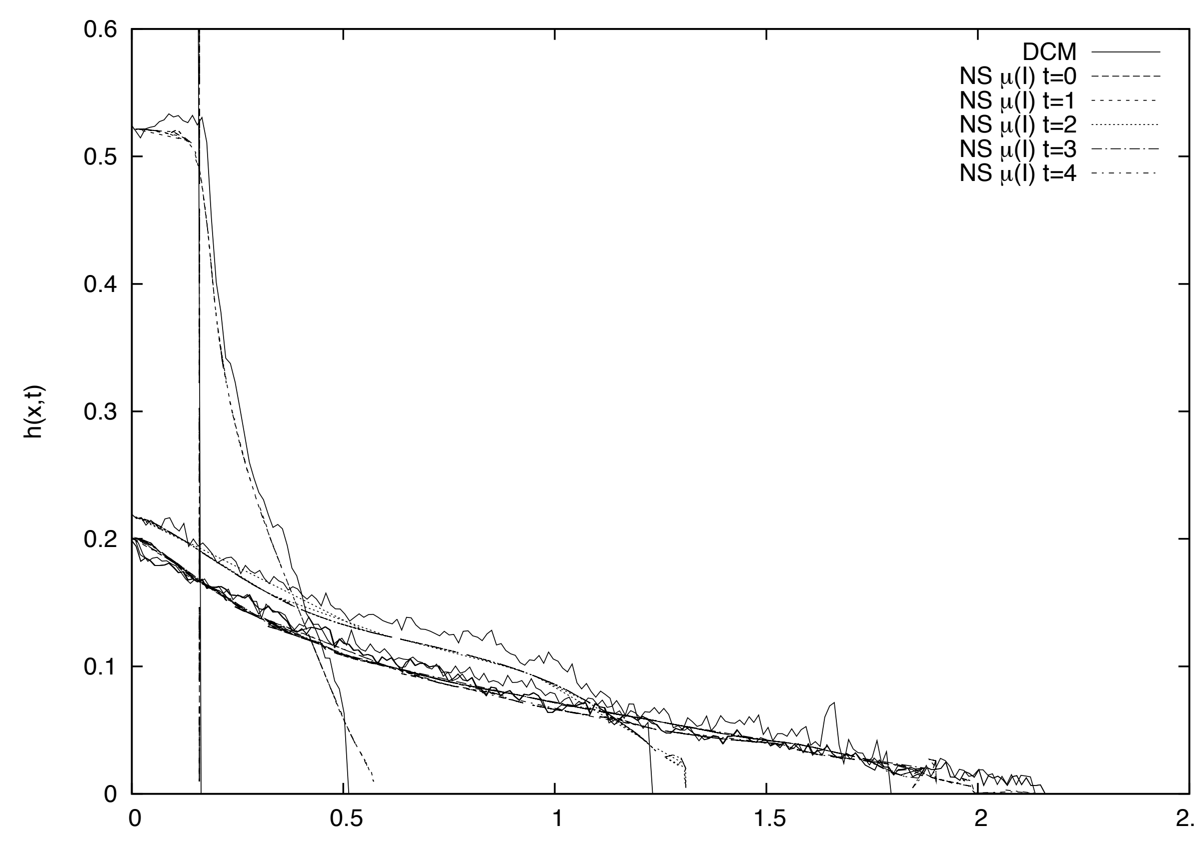

Collapse of columns simulation *Gerris* μ(I)

$a = 0.5$ DCM vs *Gerris* μ(I)

Collapse of columns simulation *Gerris* $\mu(I)$

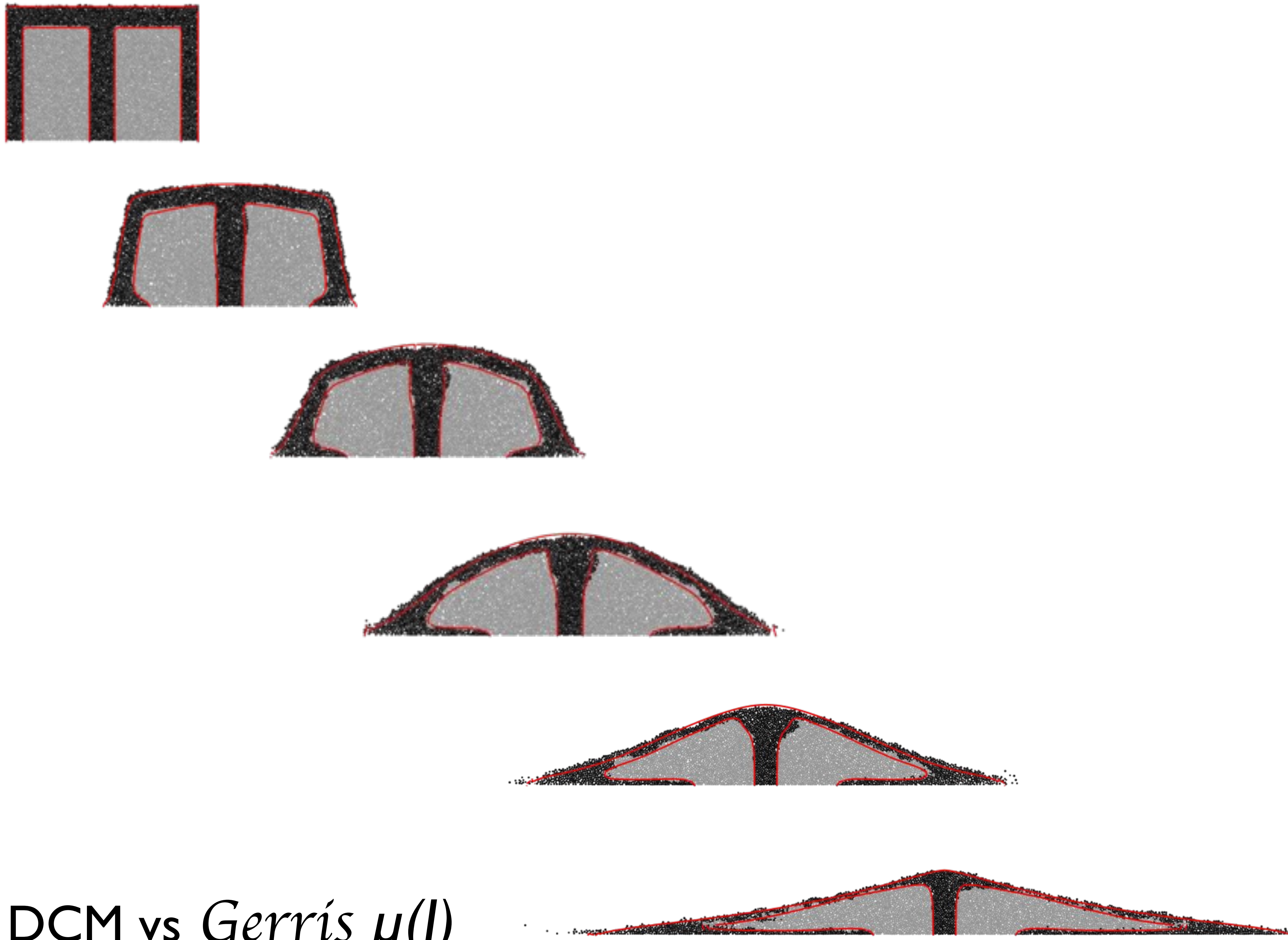

$a = 1.42$ DCM vs *Gerris* $\mu(I)$

Collapse of columns simulation *Gerris* $\mu(I)$

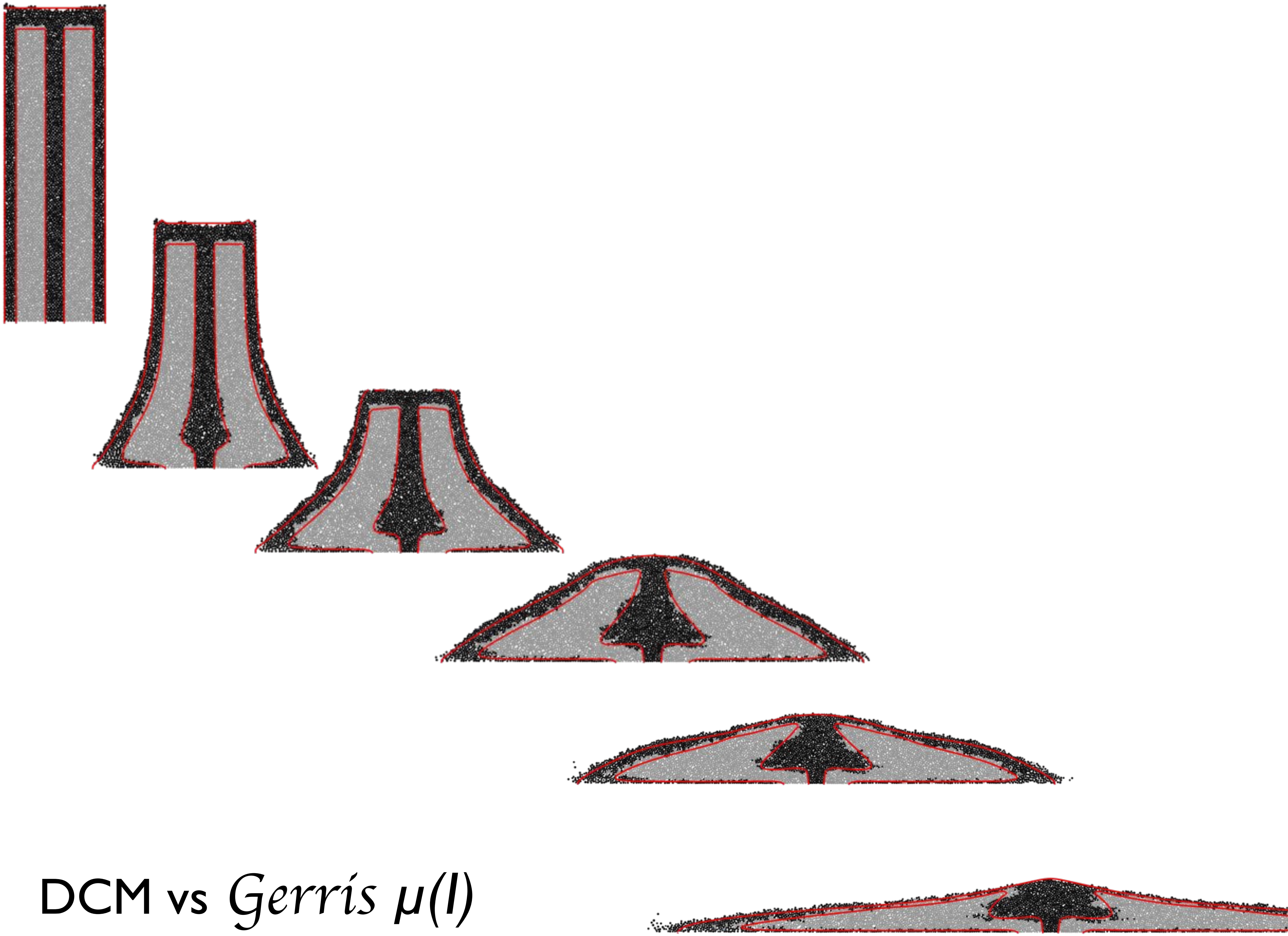

$a = 6.6$ DCM vs *Gerris* $\mu(I)$

Basilisk

Full 2D

Basiliscus basiliscus is the latin name of the extraordinary Jesus Christ lizard, famous for its ability to run on the surface of water, a characteristic it shares with another well-known water-walker *Gerris lacustris*.

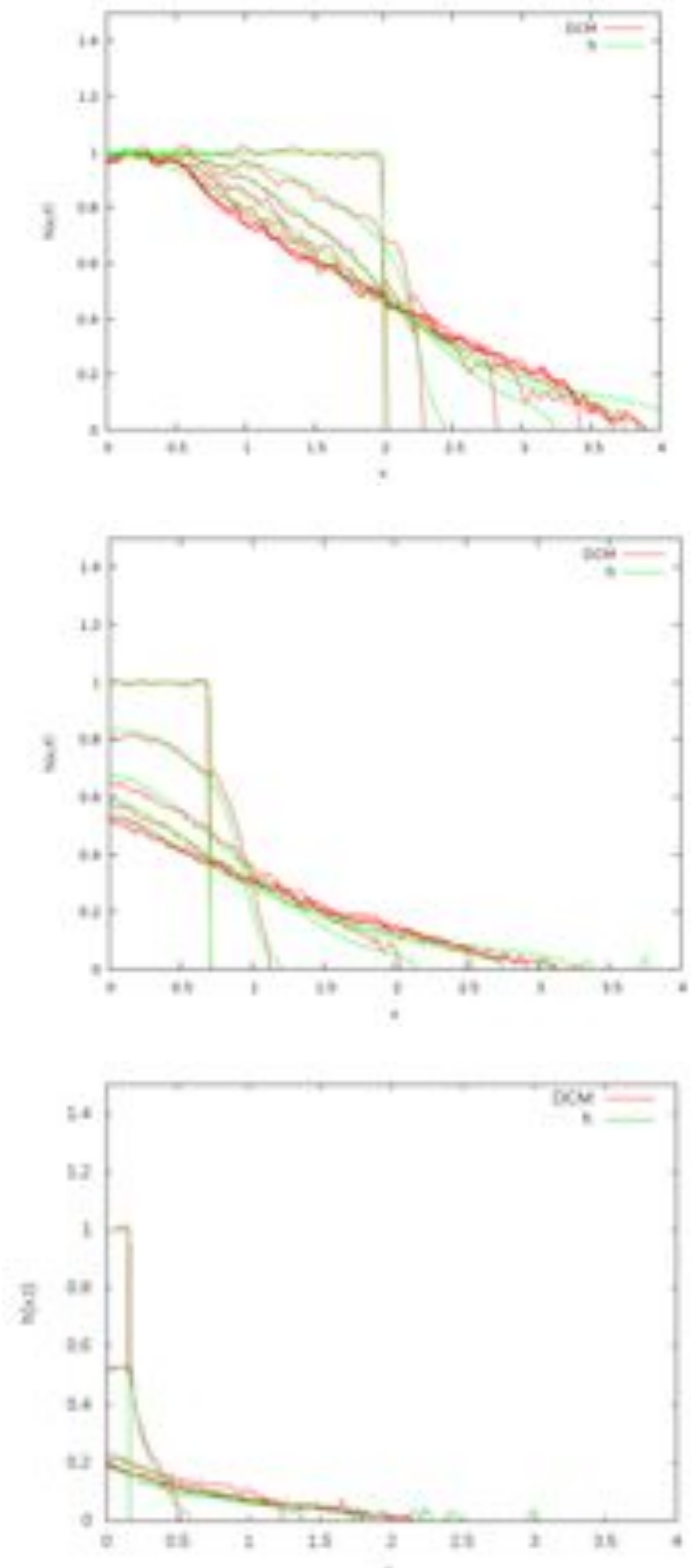

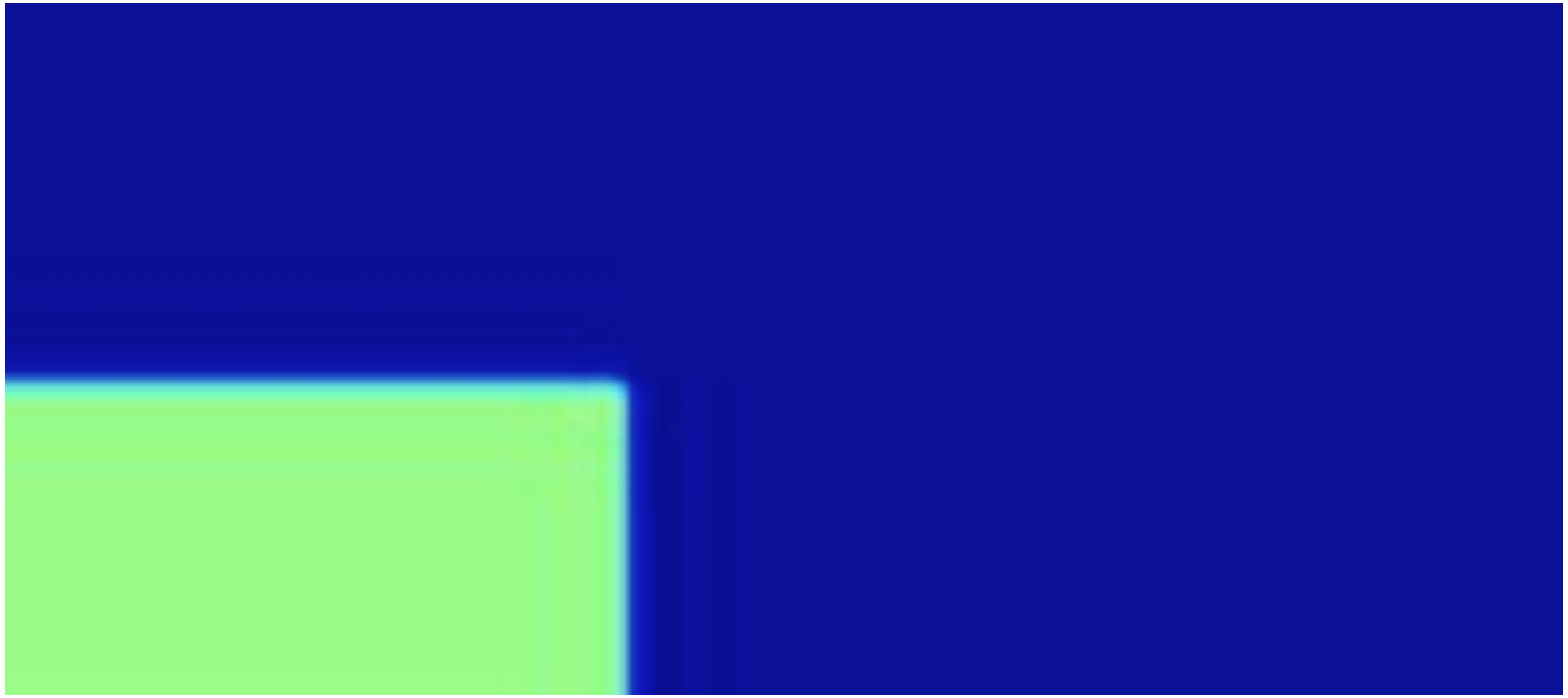

Collapse of columns simulation *Gerris* $\mu(I)$

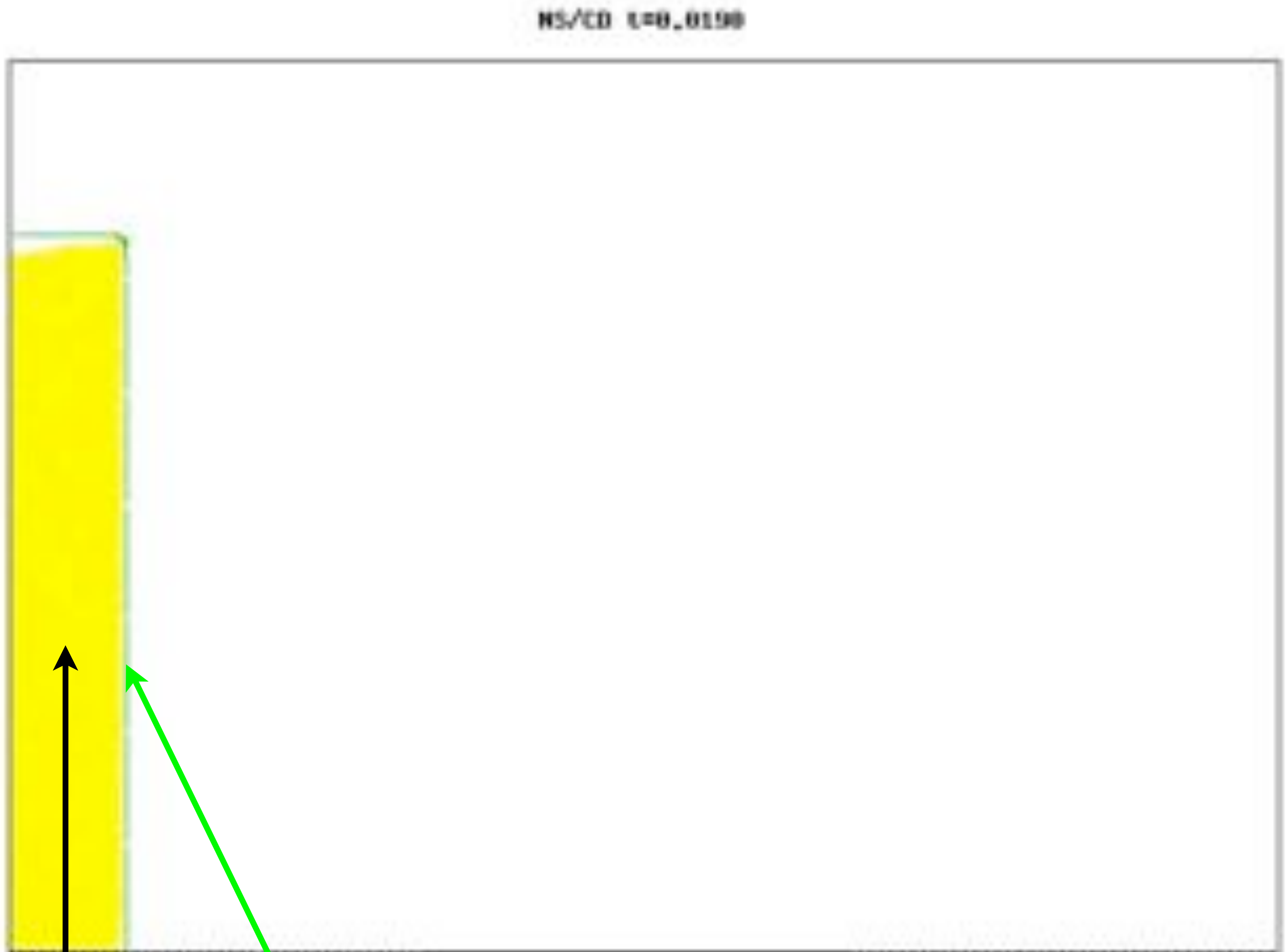

DCM vs *Gerris* $\mu(I)$

Collapse of columns   simulation *Gerris* $\mu(I)$

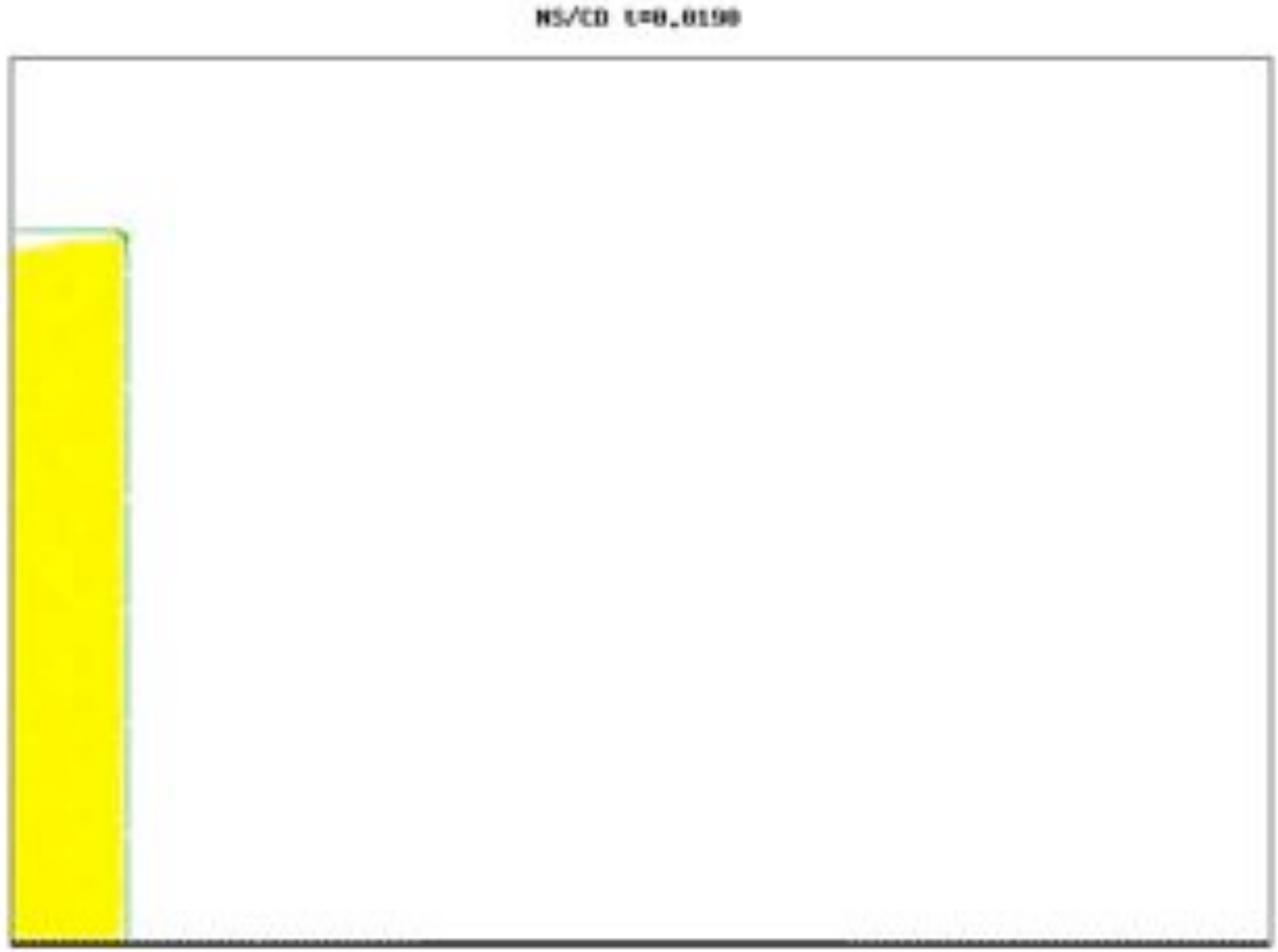

DCM vs *Gerris* $\mu(I)$

Collapse of columns simulation *Gerris* $\mu(I)$

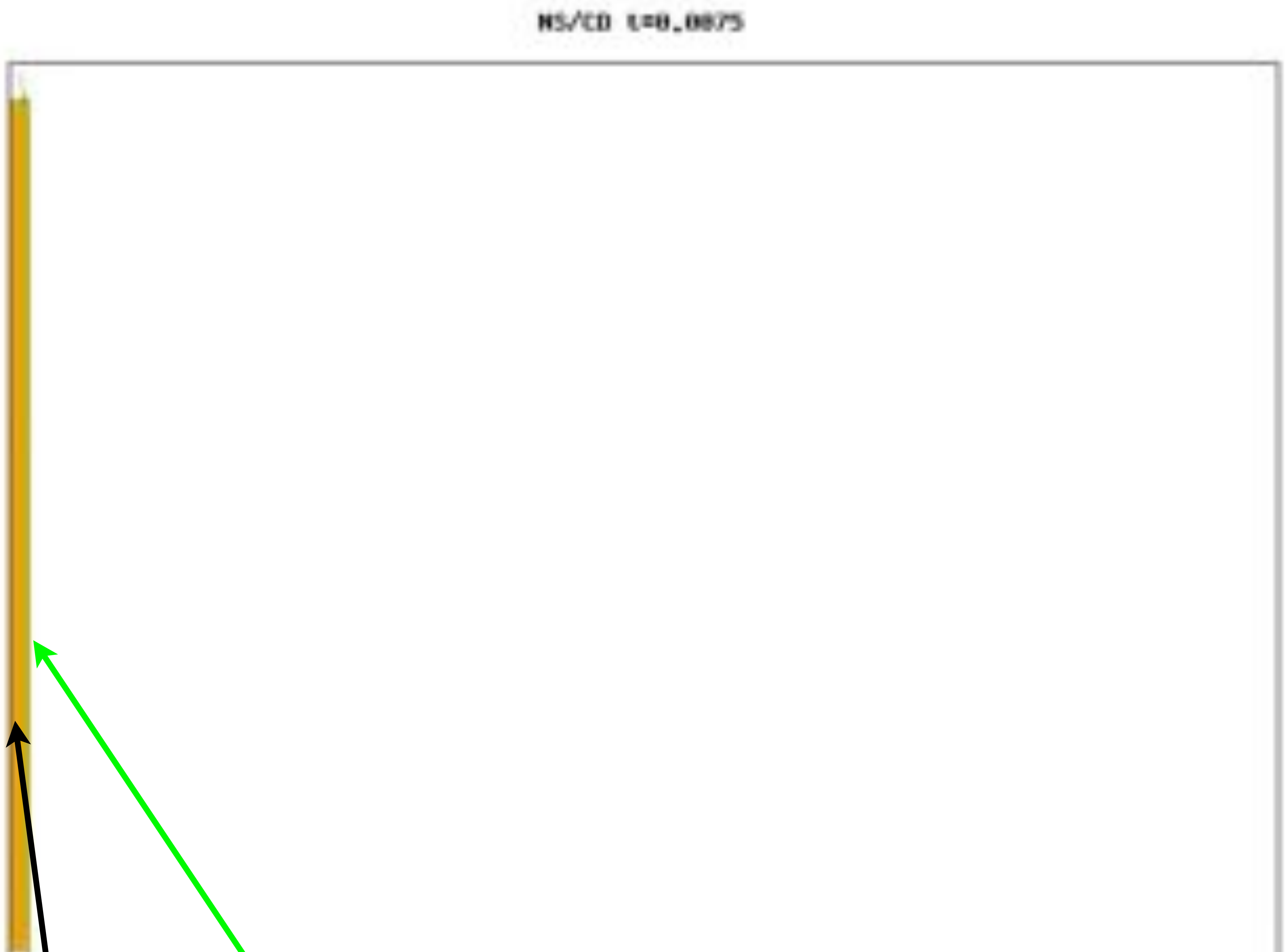

DCM vs *Gerris* $\mu(I)$

Collapse of columns simulation *Gerris* $\mu(I)$

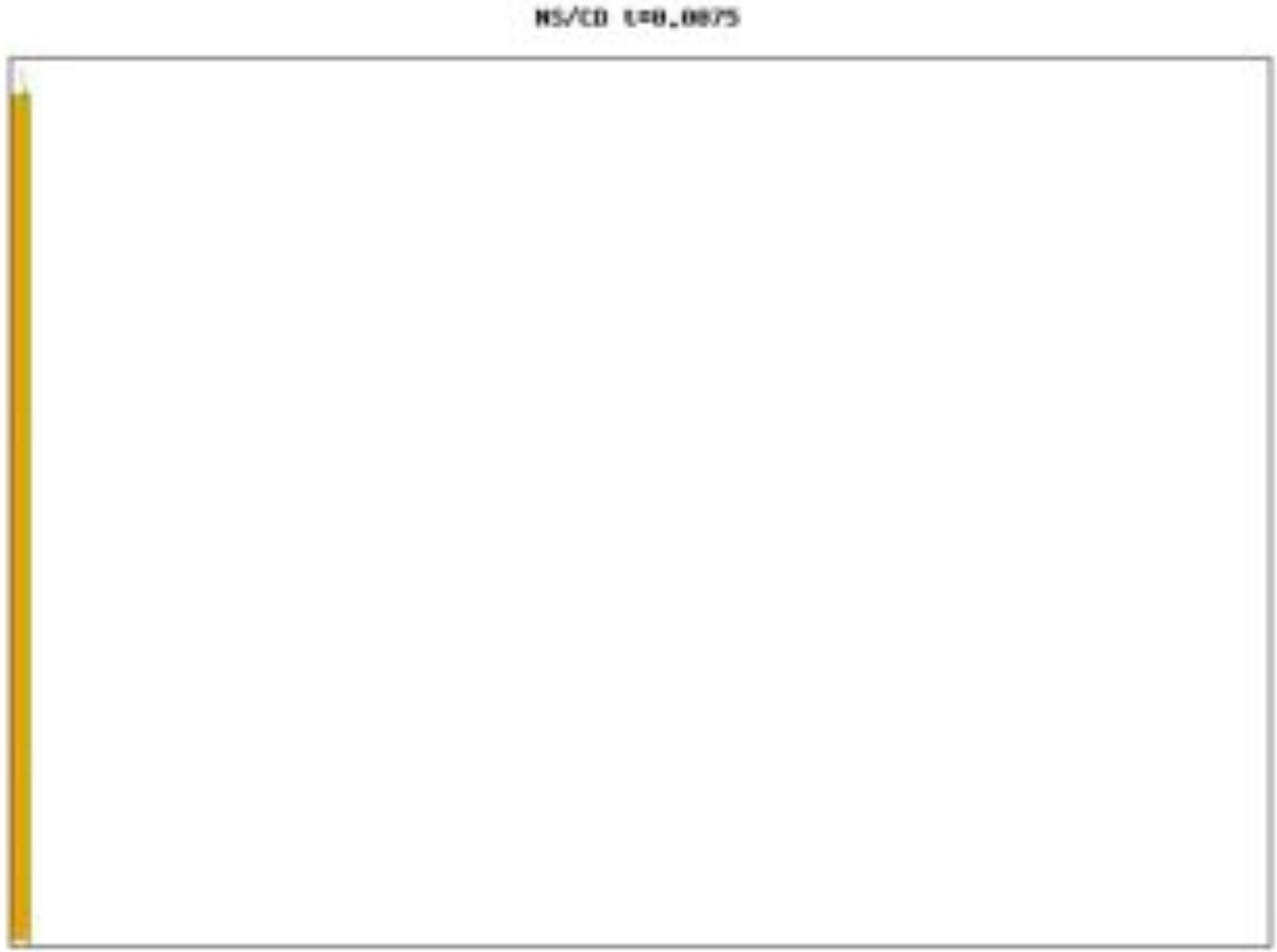

DCM vs *Gerris* $\mu(I)$

Collapse of columns   simulation *Gerris* $\mu(I)$

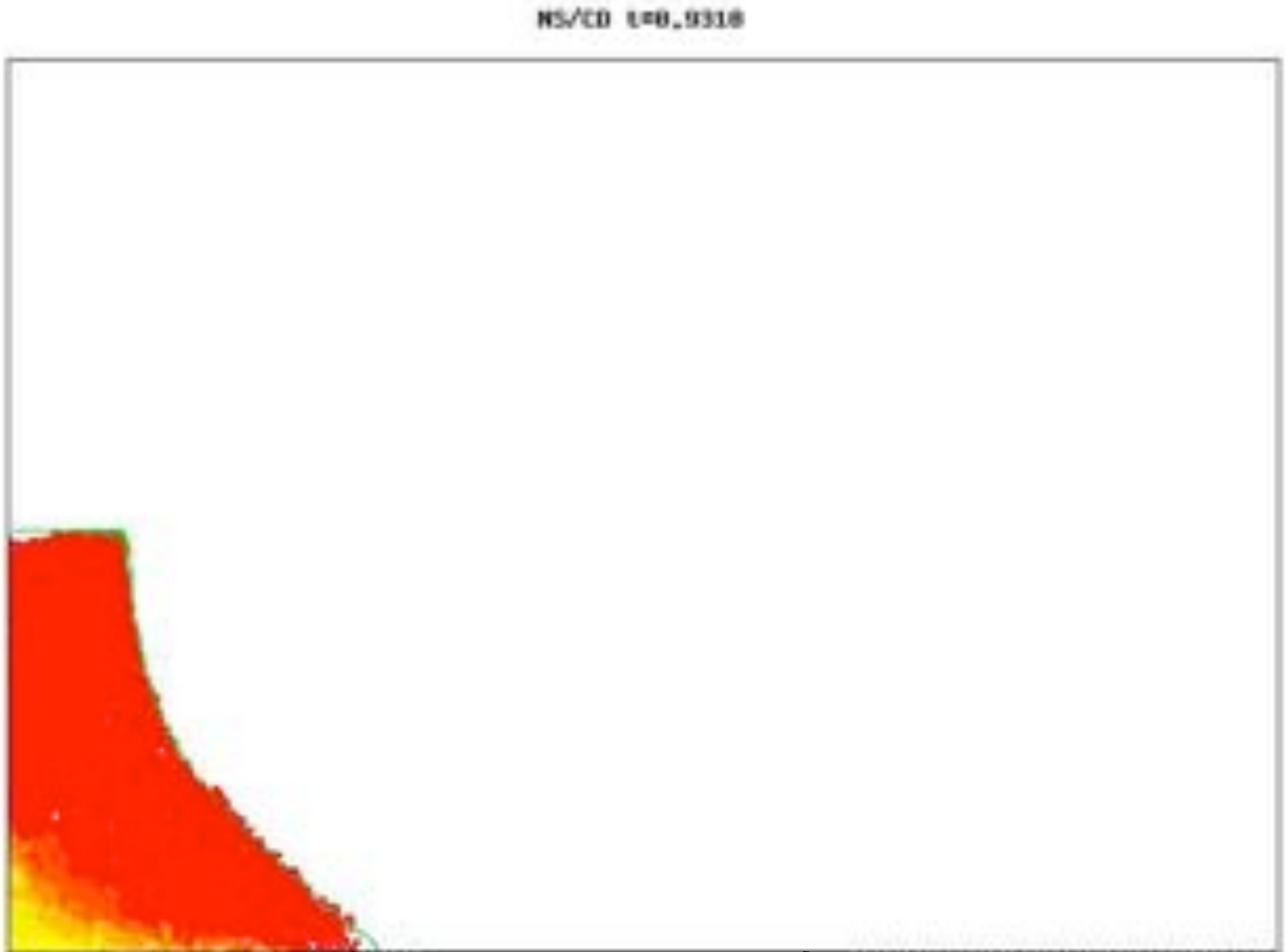

at the tip, a=6.6 t=1.33 2 2.66

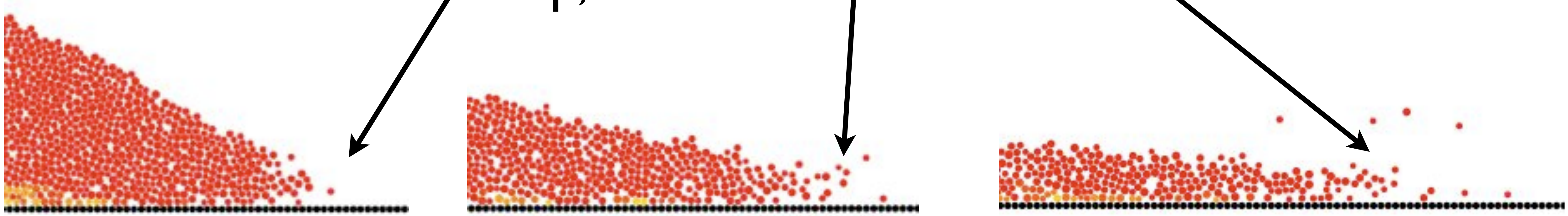

DCM vs *Gerris* $\mu(I)$

Collapse of columns simulation *Gerris μ(I)*

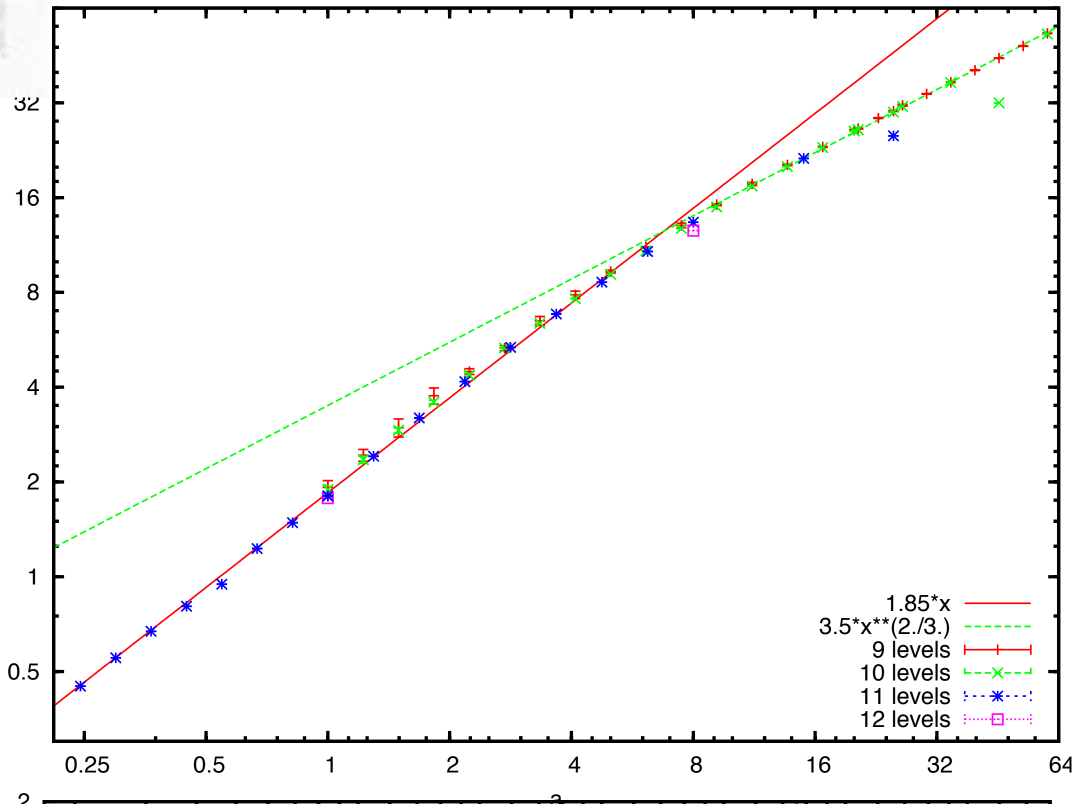

Normalised final deposit extent as a function of aspect ratio *a*.
Well-defined power law dependencies with exponents of 1 and 2/3 respectively.

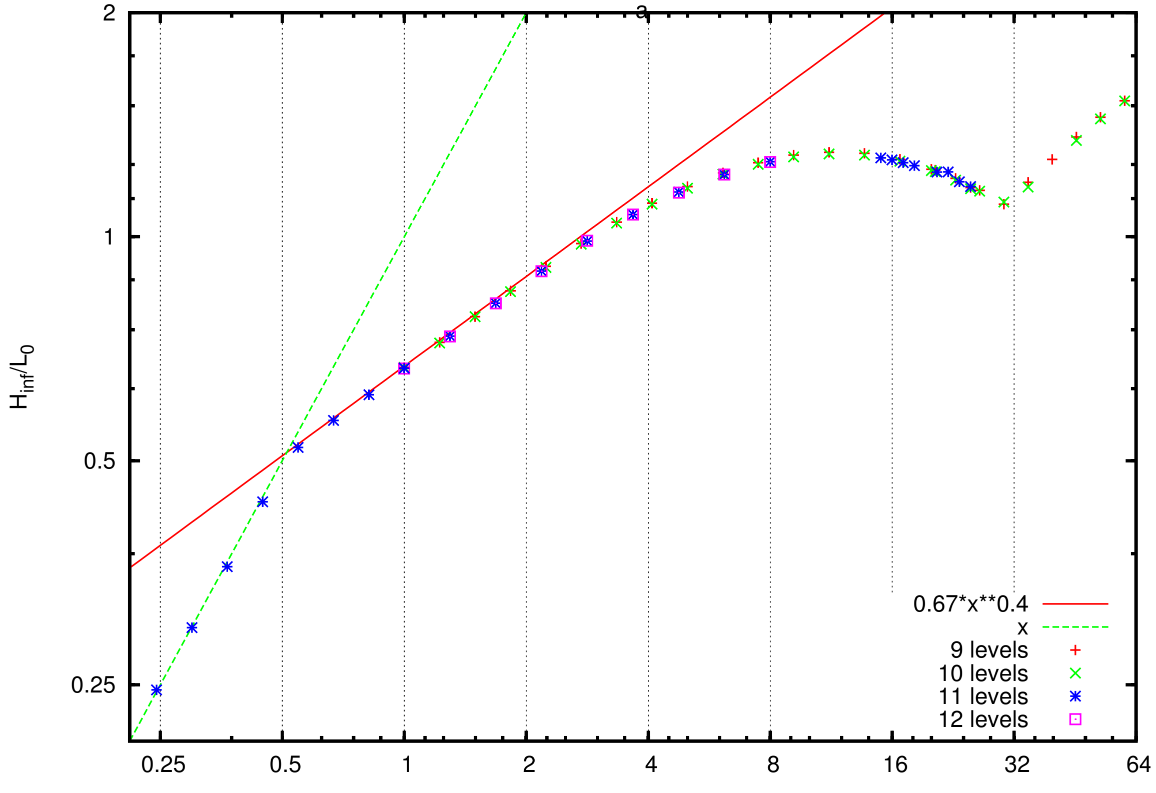

We recover the experimental scaling [Lajeunesse et al. 04] and [Staron et al. 05]. Differences between the values of the prefactors are due to the difficulties to obtain the run out length: friction in the Navier Stokes code tends to underestimate it, whereas direct simulation shows that the tip is very gazeous, it can no longer explained by a continuum mechanic description.

E Lajeunesse J. B. Monnier and G. M. Homsy PoF 05

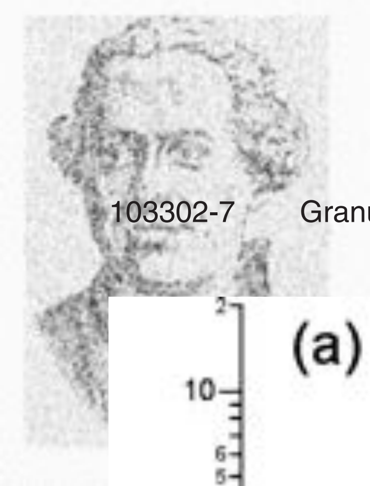

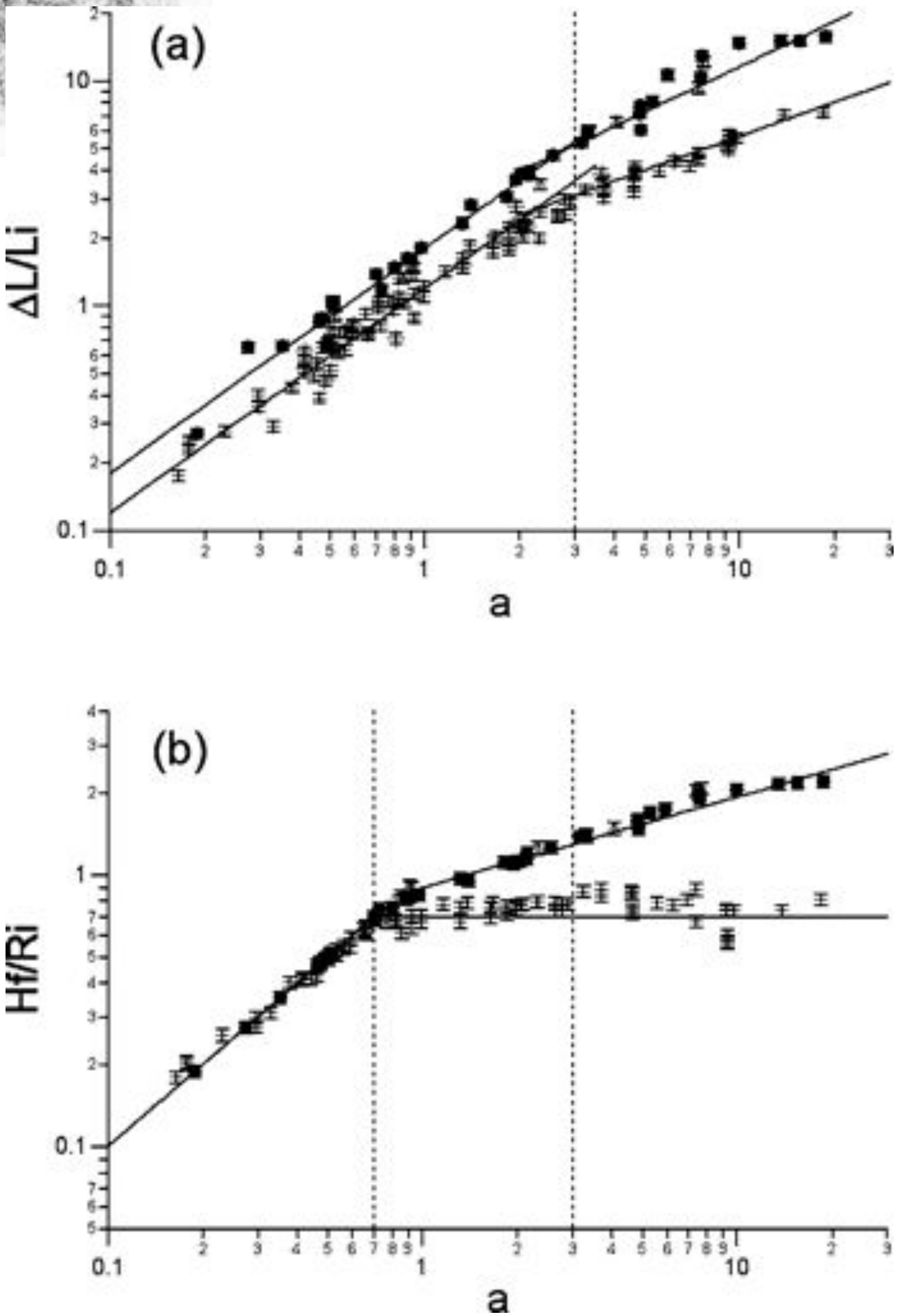

- In the axisymmetric geometry

$$\frac{H_f}{L_i} = \begin{cases} a & a \lesssim 0.74, \\ 0.74 & a \gtrsim 0.74, \end{cases}$$

$$\frac{\Delta L}{L_i} \propto \begin{cases} a & a \lesssim 3, \\ a^{1/2} & a \gtrsim 3. \end{cases}$$

- In the rectangular channel:

$$\frac{H_f}{L_i} \propto \begin{cases} a & a \lesssim 0.7, \\ a^{1/3} & a \gtrsim 0.7, \end{cases}$$

$$\frac{\Delta L}{L_i} \propto \begin{cases} a & a \lesssim 3, \\ a^{2/3} & a \gtrsim 3. \end{cases}$$

FIG. 6. Scaled runout $\Delta L/L_i$ (a) and scaled deposit height H_f/L_i (b) as functions of a. Circles and triangles correspond to experiments performed in the 2D channel working respectively with glass beads of diameter $d = 1.15$ mm or $d=3$ mm. Crosses correspond to the data set of axisymmetric collapses from Lajeunesse *et al.* (Ref. 10).

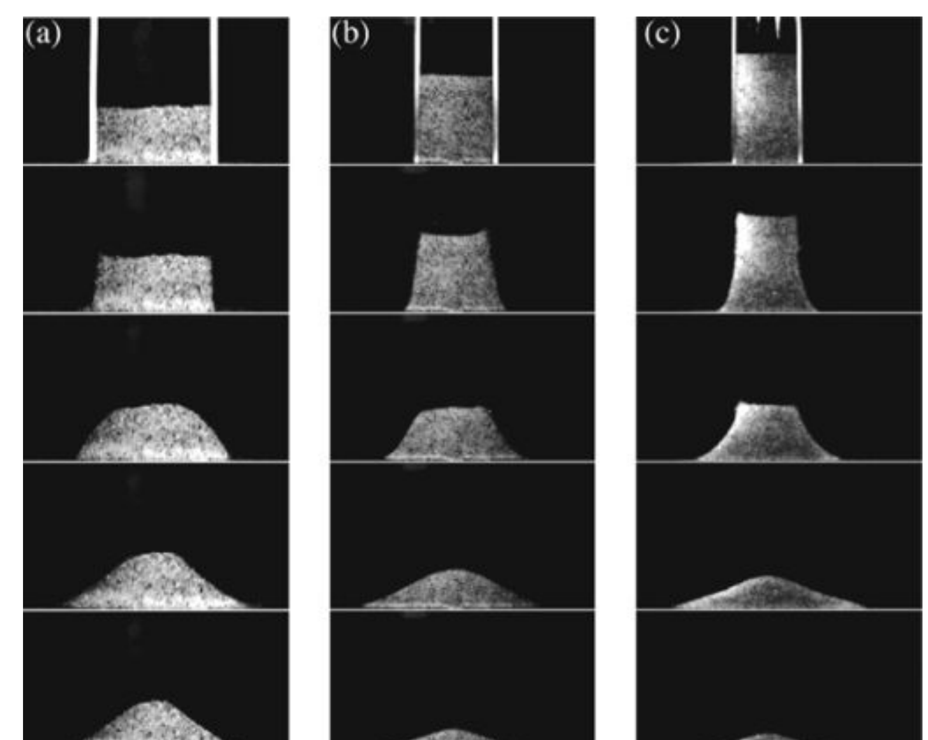

- good quantitative behaviour
- test another case?

- A well know experimental result:
  Hagen Beverloo constant discharge law
- Tool:

  contact dynamics for *discrete* simulation

  and *continuum* «μ(I) rheology»
- the Hour Glass: discrete *versus* continuum simulations

XVIII century

SABLIER DE DEMI-HEURE
Reconstitution d'un modèle du XVIII^e siècle
Verre et bois. Haut. 14 cm ; larg. 5 cm
Nationaal Scheepvaartmuseum, Anvers
Inv. n° AS 53 23 1

Le sablier d'une demi-heure représentait les 1/8^e d'une garde. L'instrument devait être tourné chaque demi-heure au moment où on sonnait le glas.

Les sabliers sont de très anciens instruments de mesure du temps. Dès les premières expéditions maritimes, ils figurent à bord. Les sabliers de demi-heure étaient appelés «horloges», ou «horloges à sablon». Ils étaient tournés à partir de midi, à chaque demi-heure. Huit renversements signifiaient le changement de quart de l'équipage. Leur précision était toute relative. Les types de sabliers étaient différents, ainsi que leur durée (quart d'heure, une heure, etc).

L'usage des sabliers à bord des navires se prolongea jusqu'au XIX^e siècle.

watchkeeping

The Hour Glass

catalogue de l'exposition à la Conquête des Mers, Hospice Comtesse Lille 1983

The Hour Glass

2D model computed with DCM
~ 90x90 grains

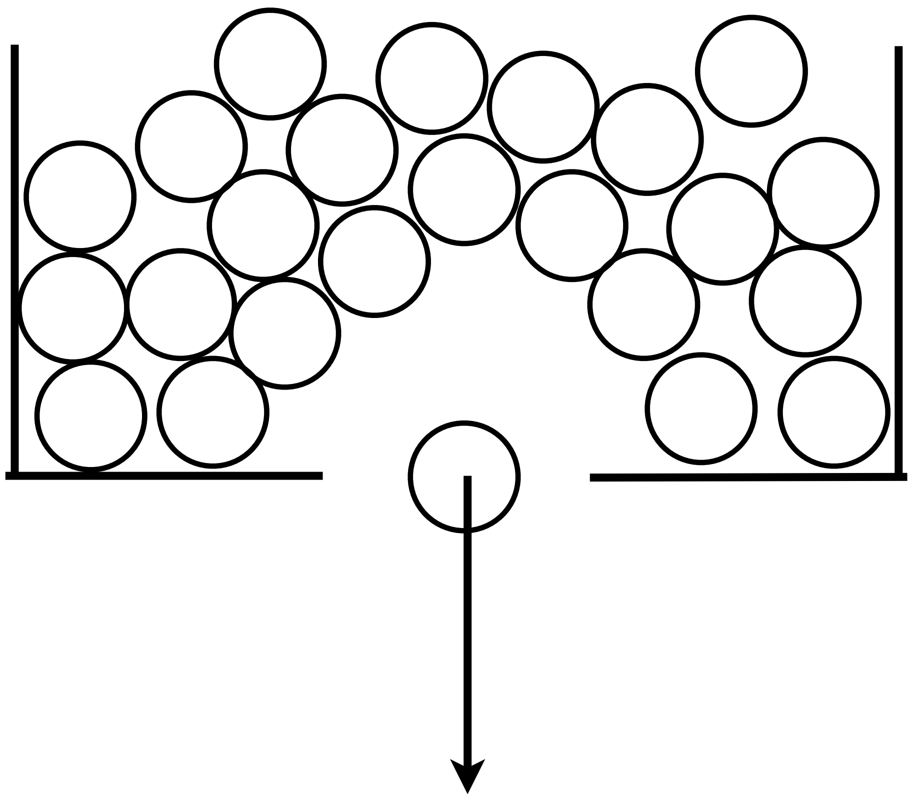

Nedderman

10.3 The free-fall arch and the minimum energy theory

All the early theoretical predictions of the mass flow rate from hoppers were based on the concept of the 'free-fall arch'. This is a surface spanning the orifice and represents the lower surface of the packed material. Above the free-fall arch the particles are assumed to be in contact with each other and inter-particle stresses occur. Below the free-fall arch, the particles lose contact and accelerate freely under gravity.

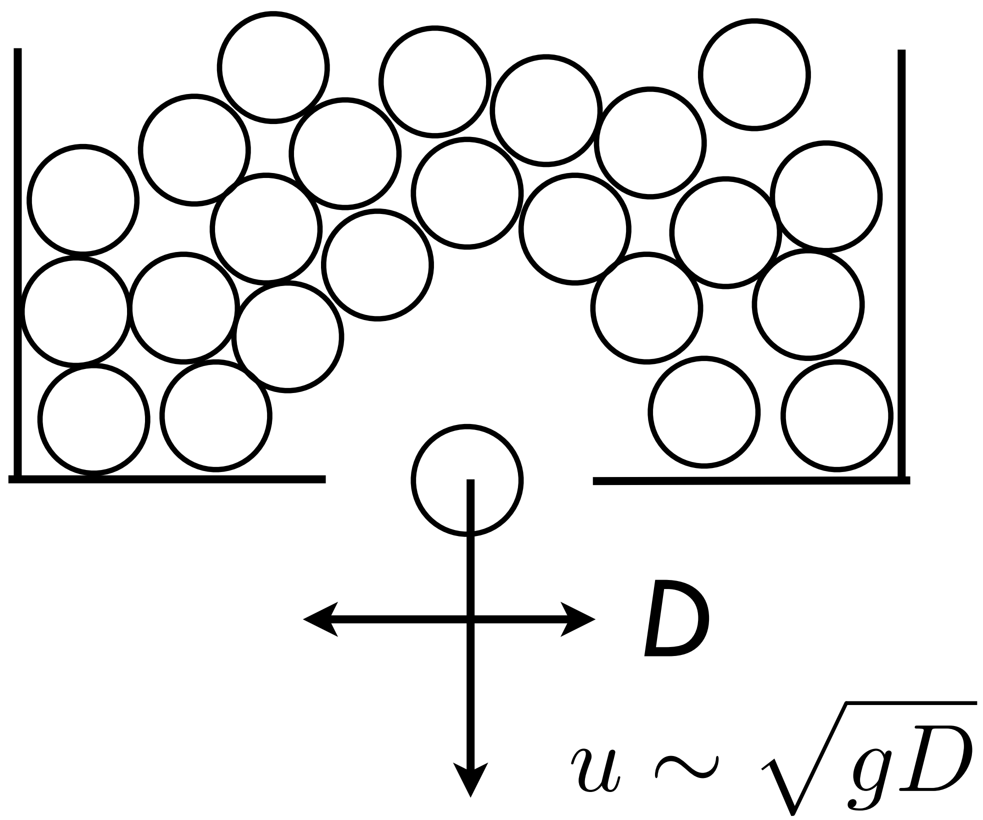

Nedderman

10.3 The free-fall arch and the minimum energy theory

All the early theoretical predictions of the mass flow rate from hoppers were based on the concept of the 'free-fall arch'. This is a surface spanning the orifice and represents the lower surface of the packed material. Above the free-fall arch the particles are assumed to be in contact with each other and inter-particle stresses occur. Below the free-fall arch, the particles lose contact and accelerate freely under gravity.

Gotthilf Hagen 1797-1884

- Hagen 1852 Beverloo 1961 constant discharge law

mass flow rate

$$W = C\rho\sqrt{g(D-kd)^5}$$ in 3D

$$C \simeq 0.6 \qquad k \simeq 1.5$$

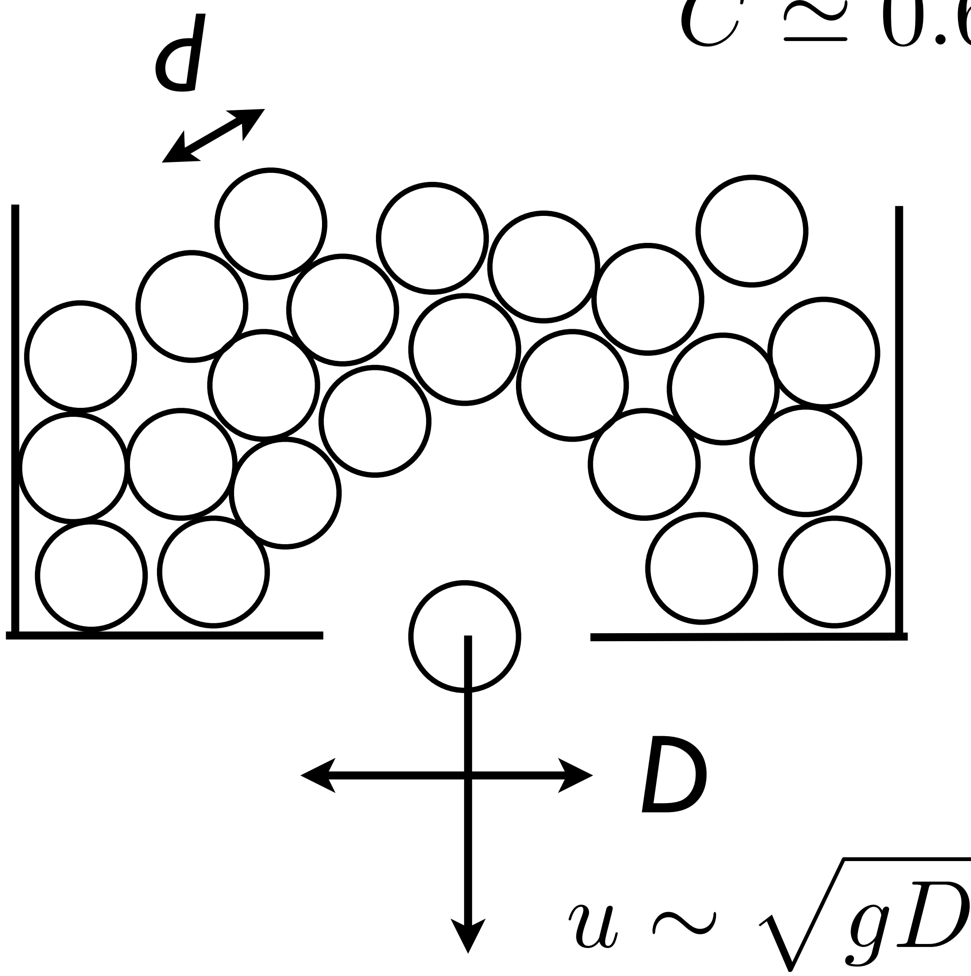

no influence of the hight
nor the width
influence of *D*, *d* and ρ,
so by dimensional analysis:

$$W = C\rho\sqrt{g(D-kd)^3}$$ in 2D

- A well know experimental result:
  Hagen Beverloo constant discharge law

- Problem:

  Simulate the hour glass with discrete and continuum theories

- try to recover the Beverloo 1961 Hagen 1852 law from <u>discrete</u> and <u>continuum</u> simulations

- Flow in a Hourglass Discharge from Hoppers

simulation DCM

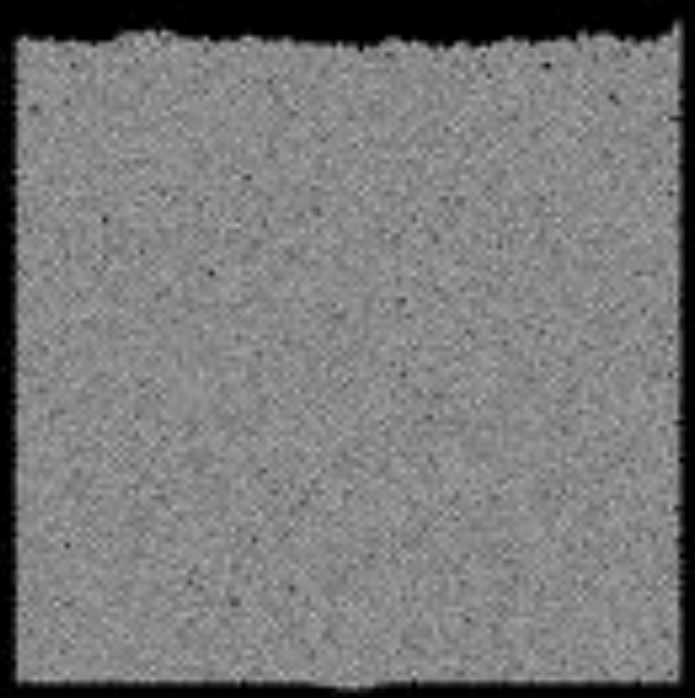

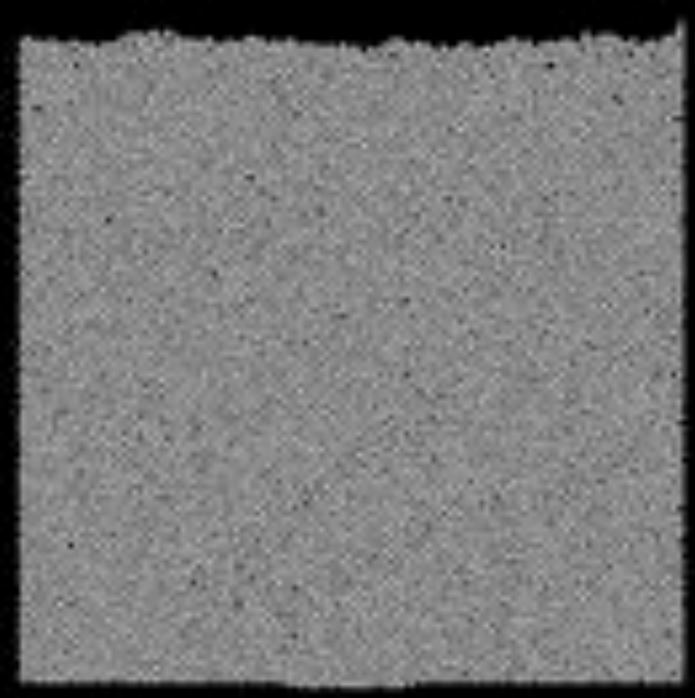

- Flow in a Hourglass Discharge from Hoppers simulation Navier Stokes *μ(I)*

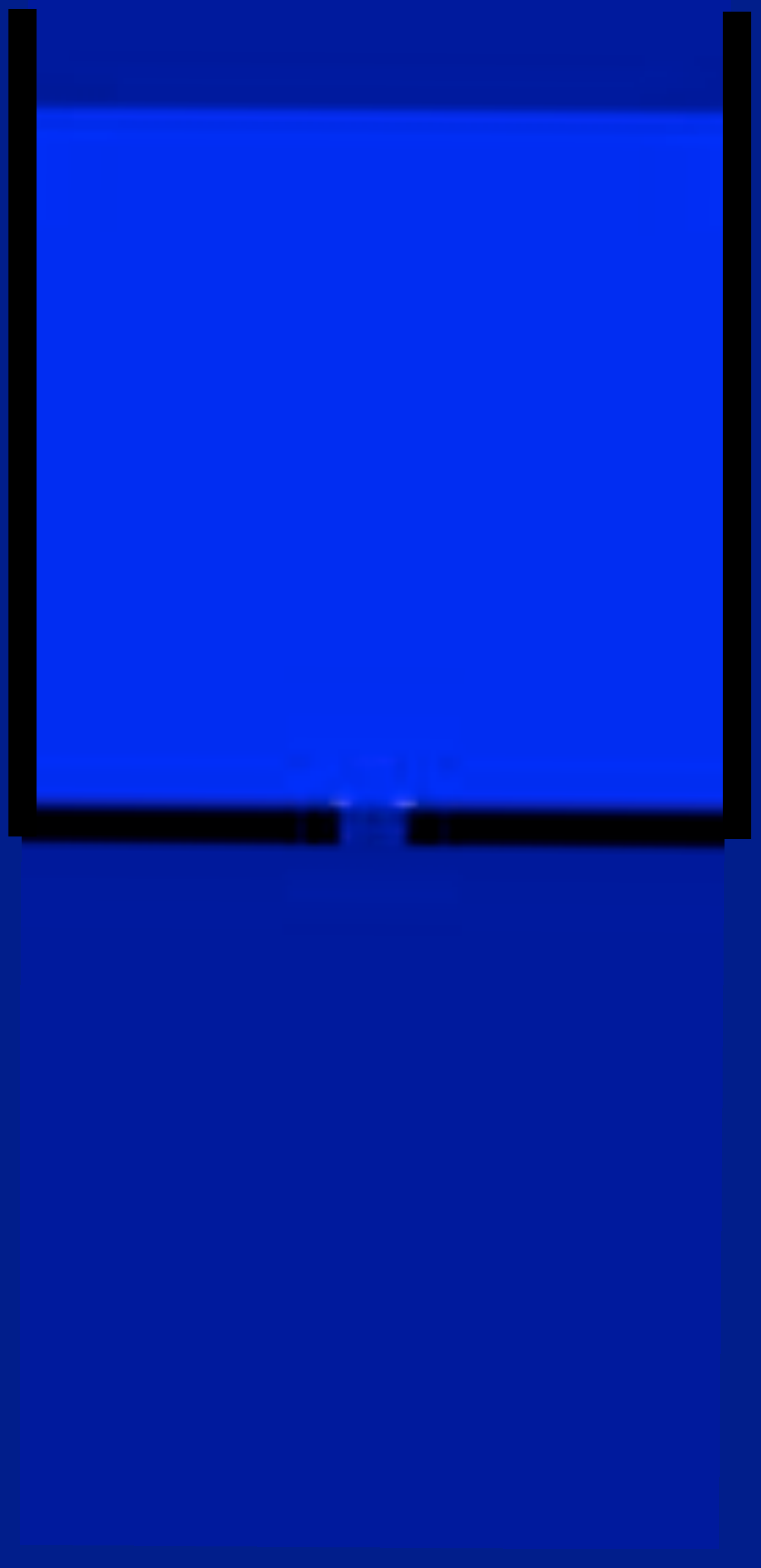

- Flow in a Hourglass Discharge from Hoppers

simulation discrete *vs* continuum

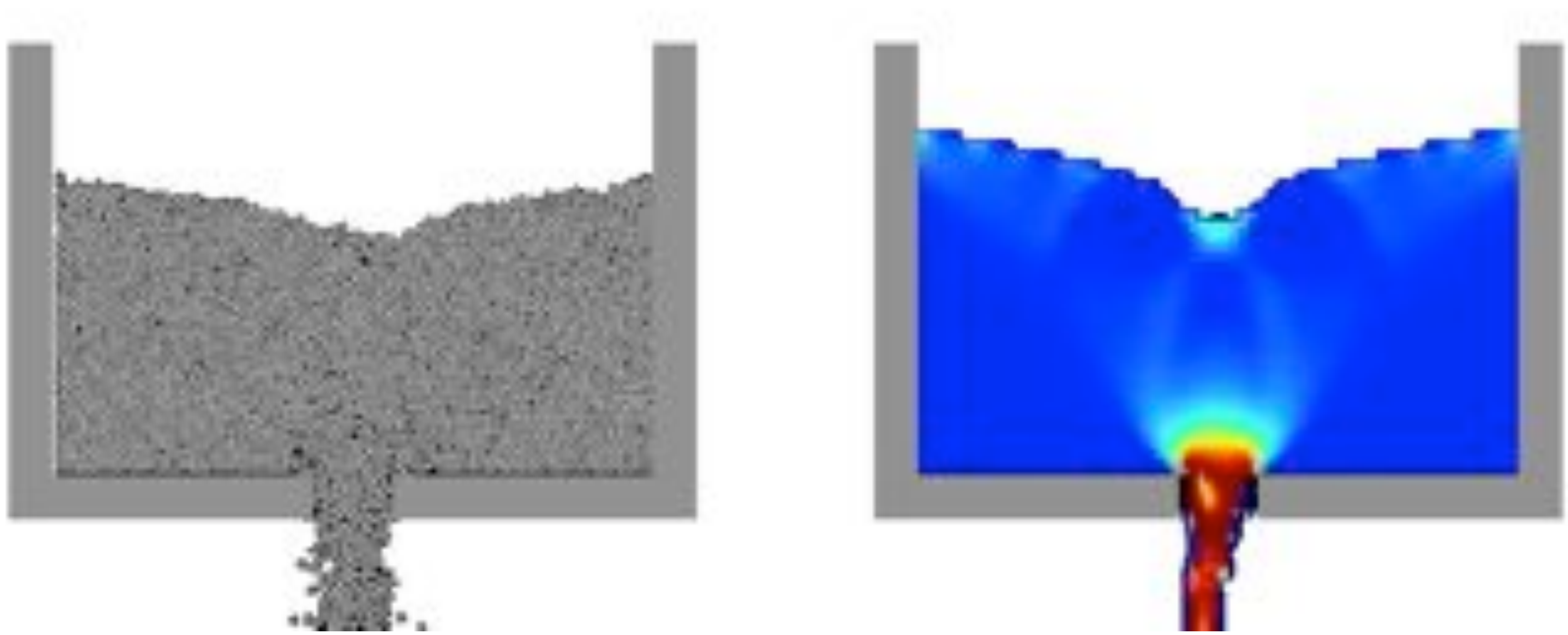

- comparing Torricelli

Evangelista Torricelli 1608 1647

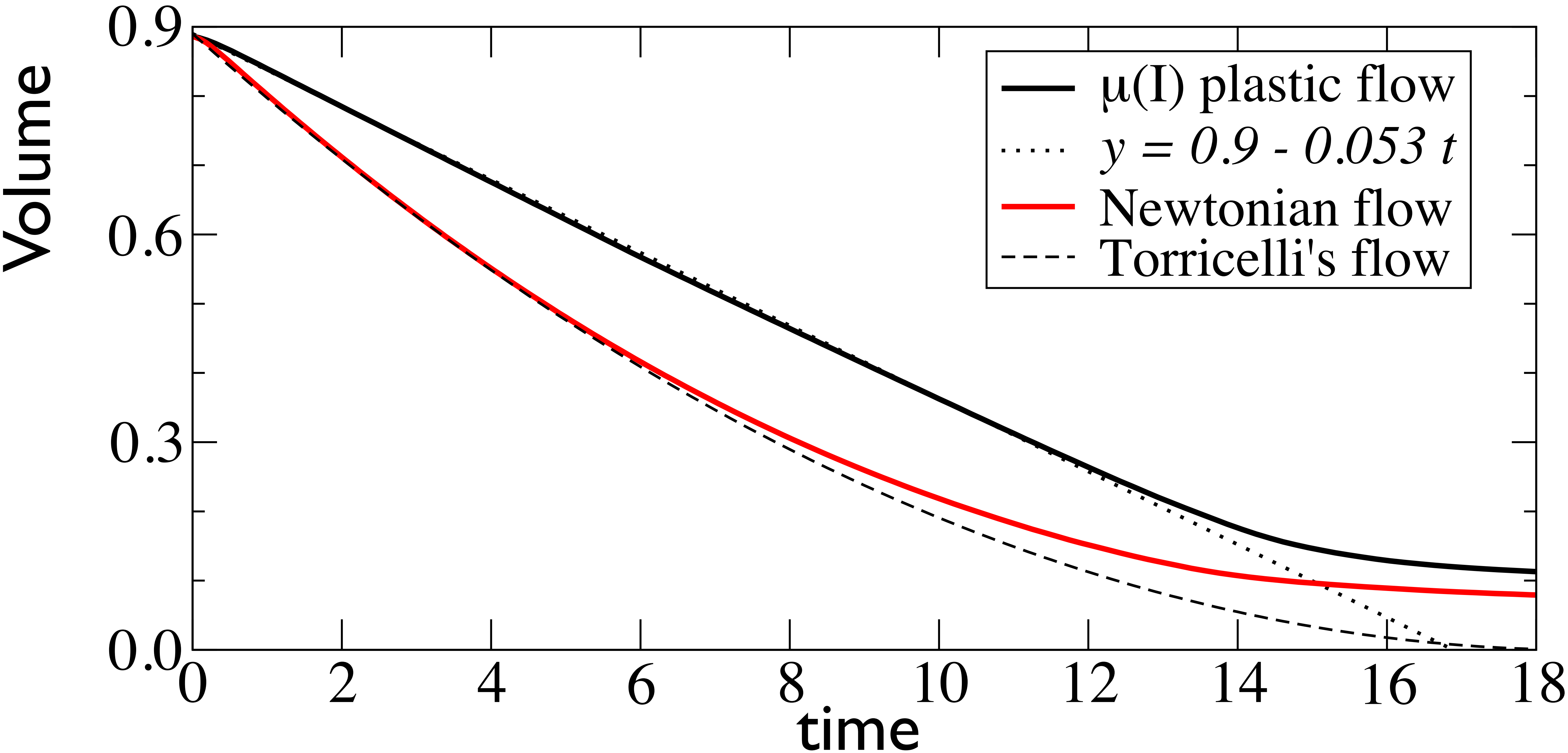

viscosity of the Newtonian flow extrapolated from the μ(I) near the orifice

- Flow in a Hourglass Discharge from Hoppers

discrete *vs* continuum (a shift)

Beverloo (1961)
Hagen (1852)

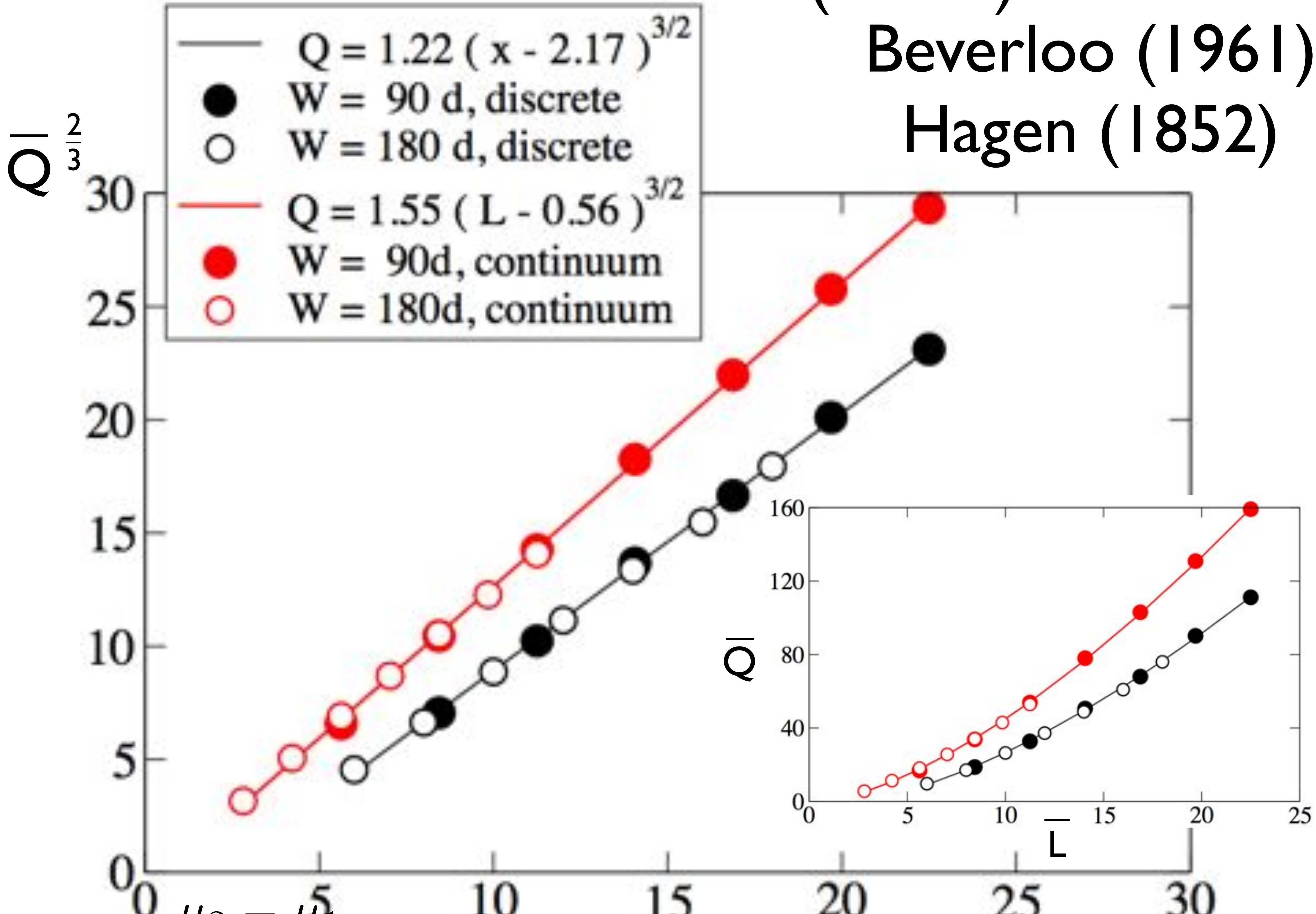

$$\mu(I) = \mu_1 + \frac{\mu_2 - \mu_1}{I_0/I + 1}$$

Width of the aperture

NO influence of initial filling height

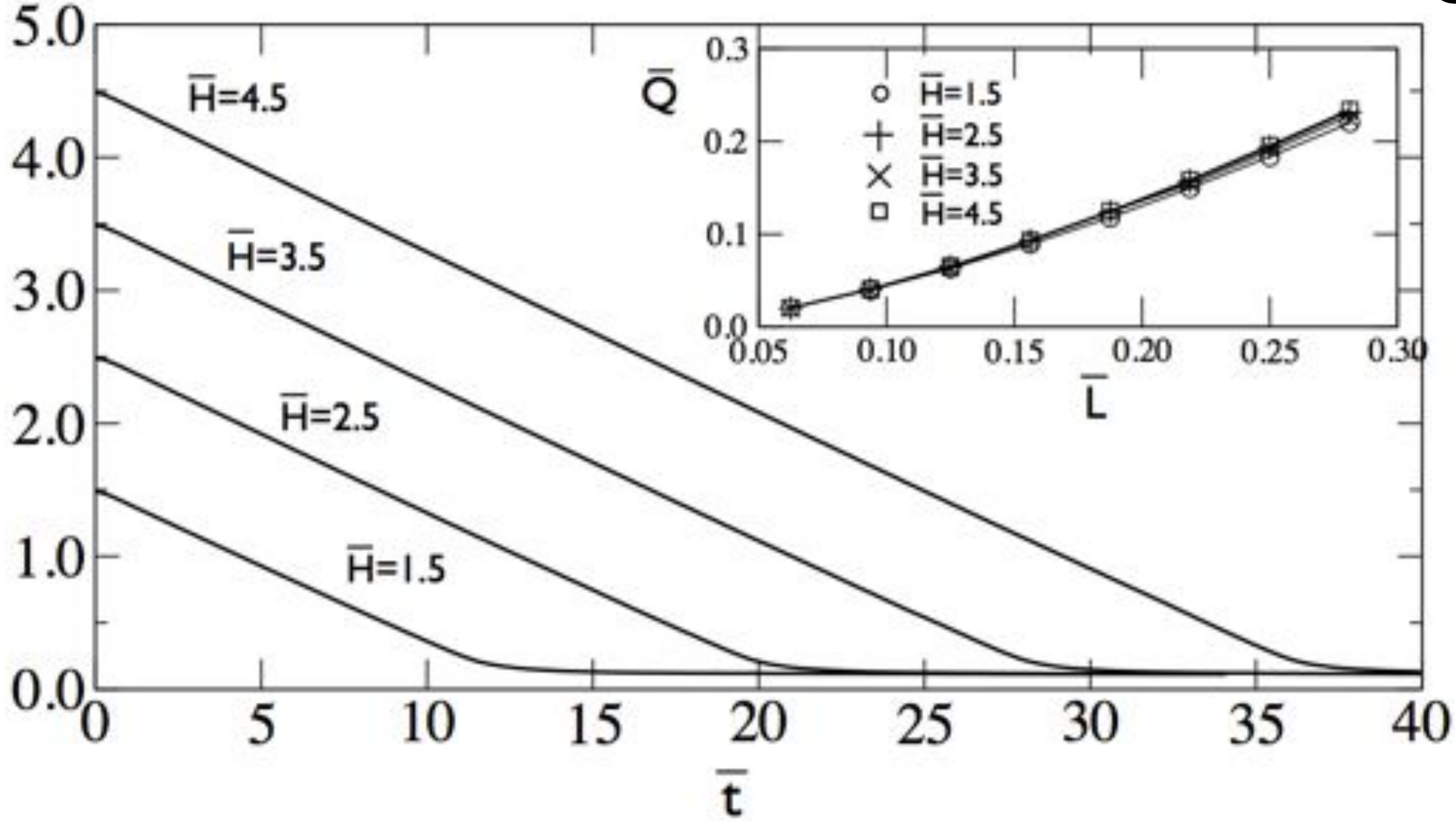

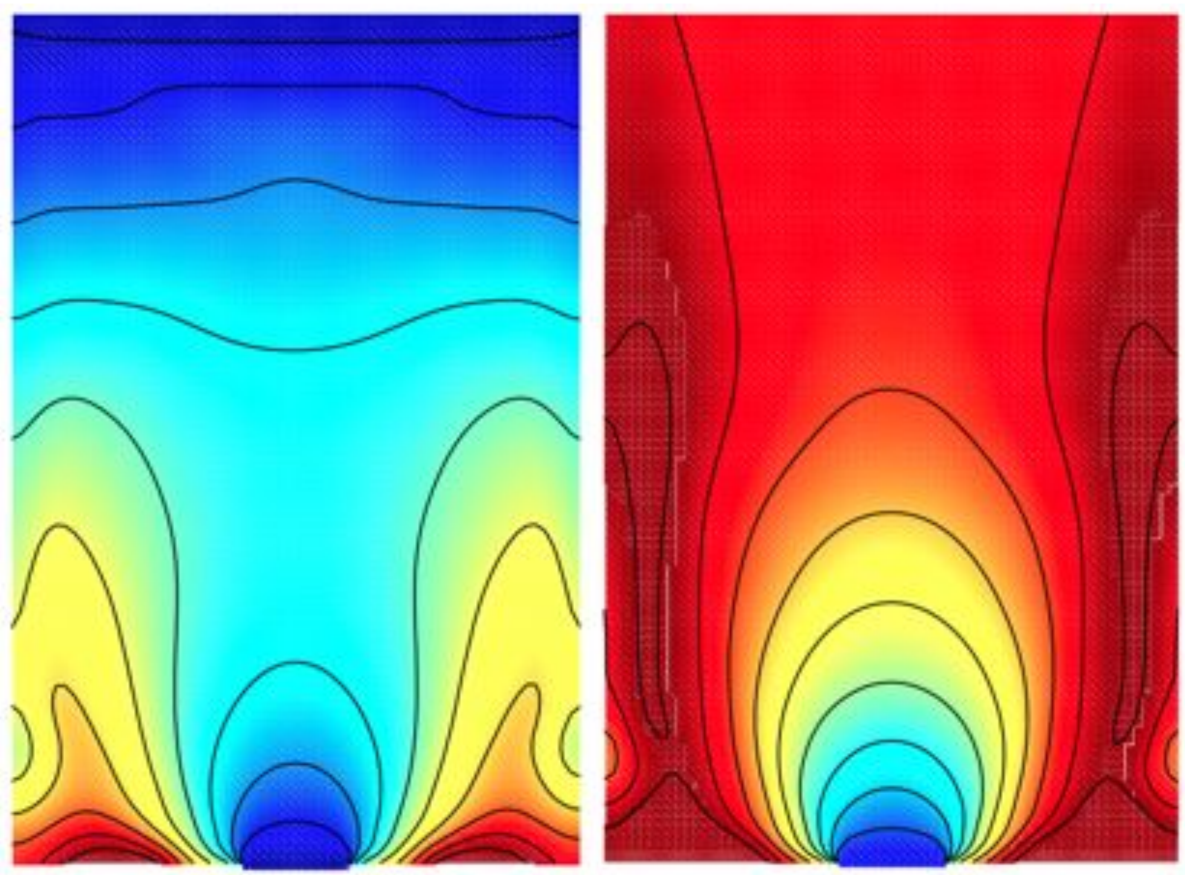

$\bar{H}$ = 1.5 $\bar{H}$ = 4.5

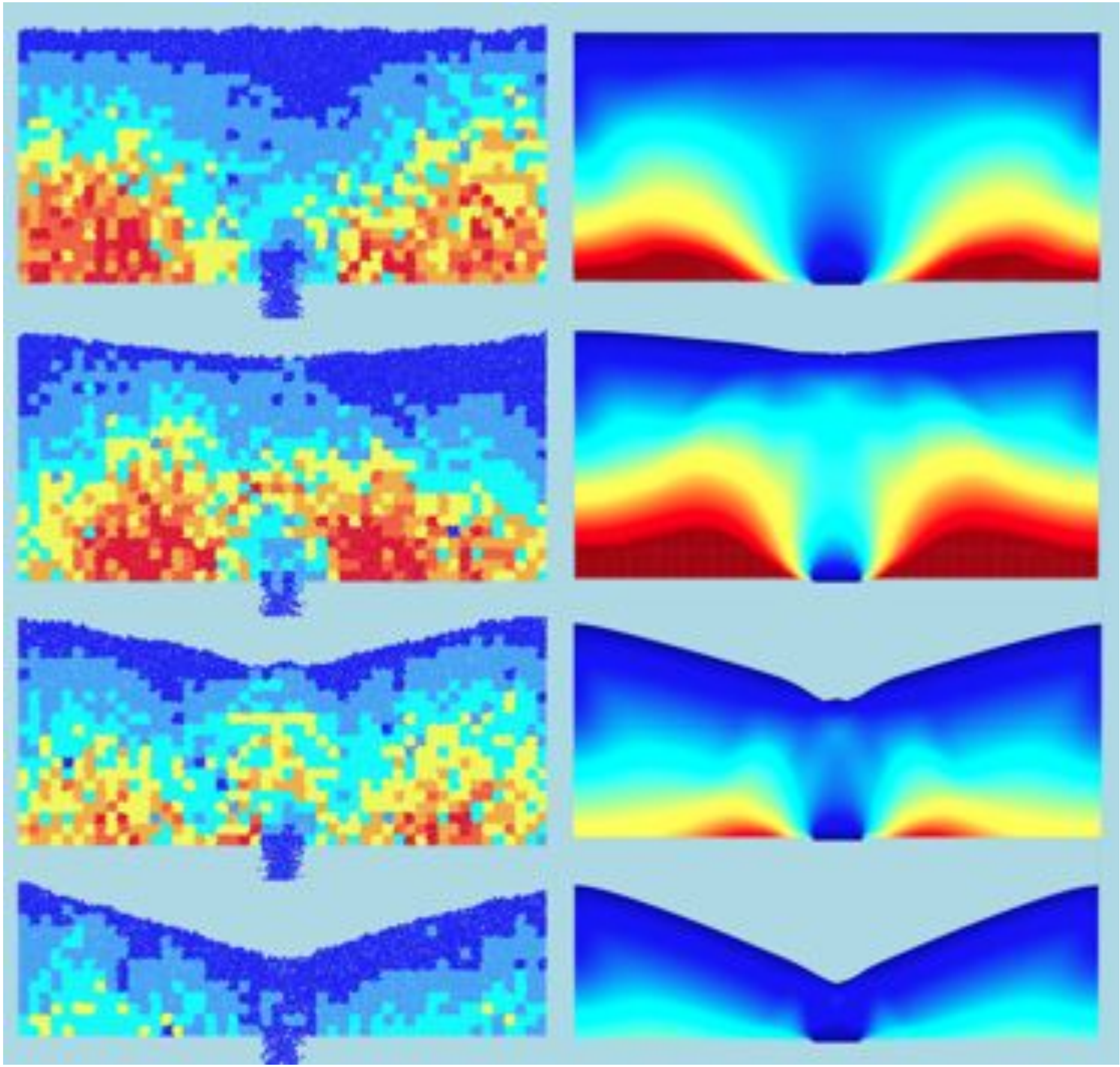

discrete *vs* continuum (at same rate)

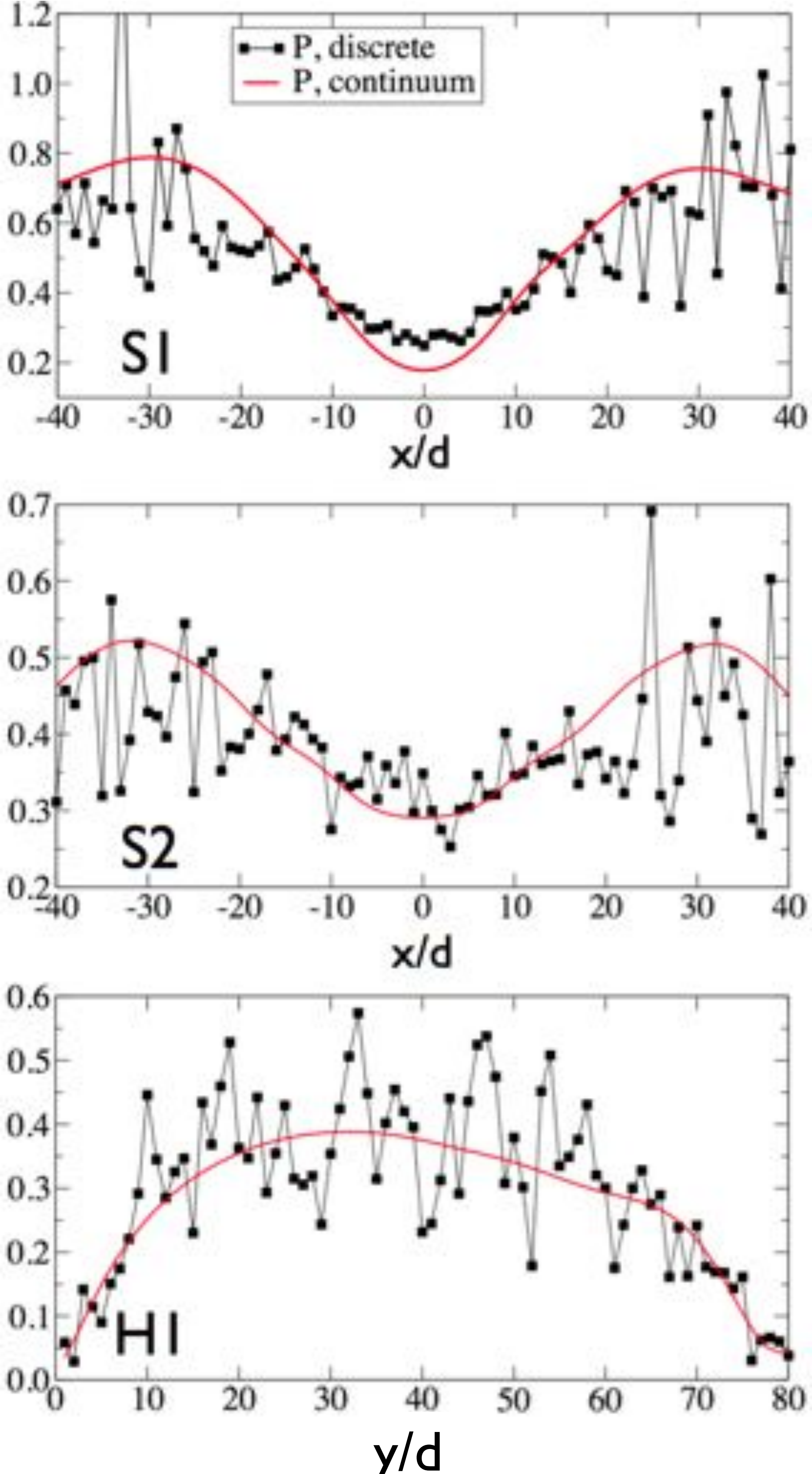

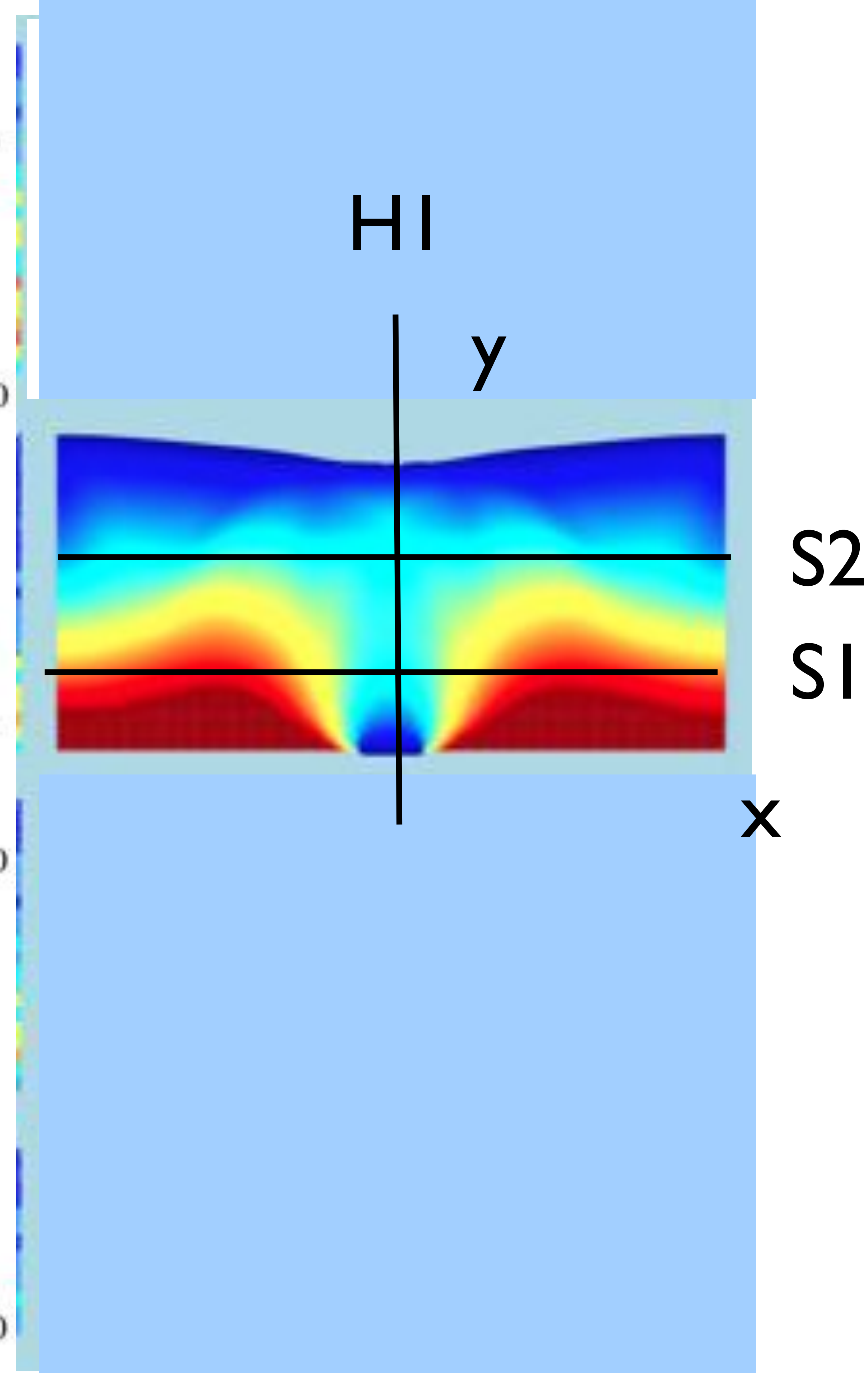

discrete *vs* continuum (at same rate)

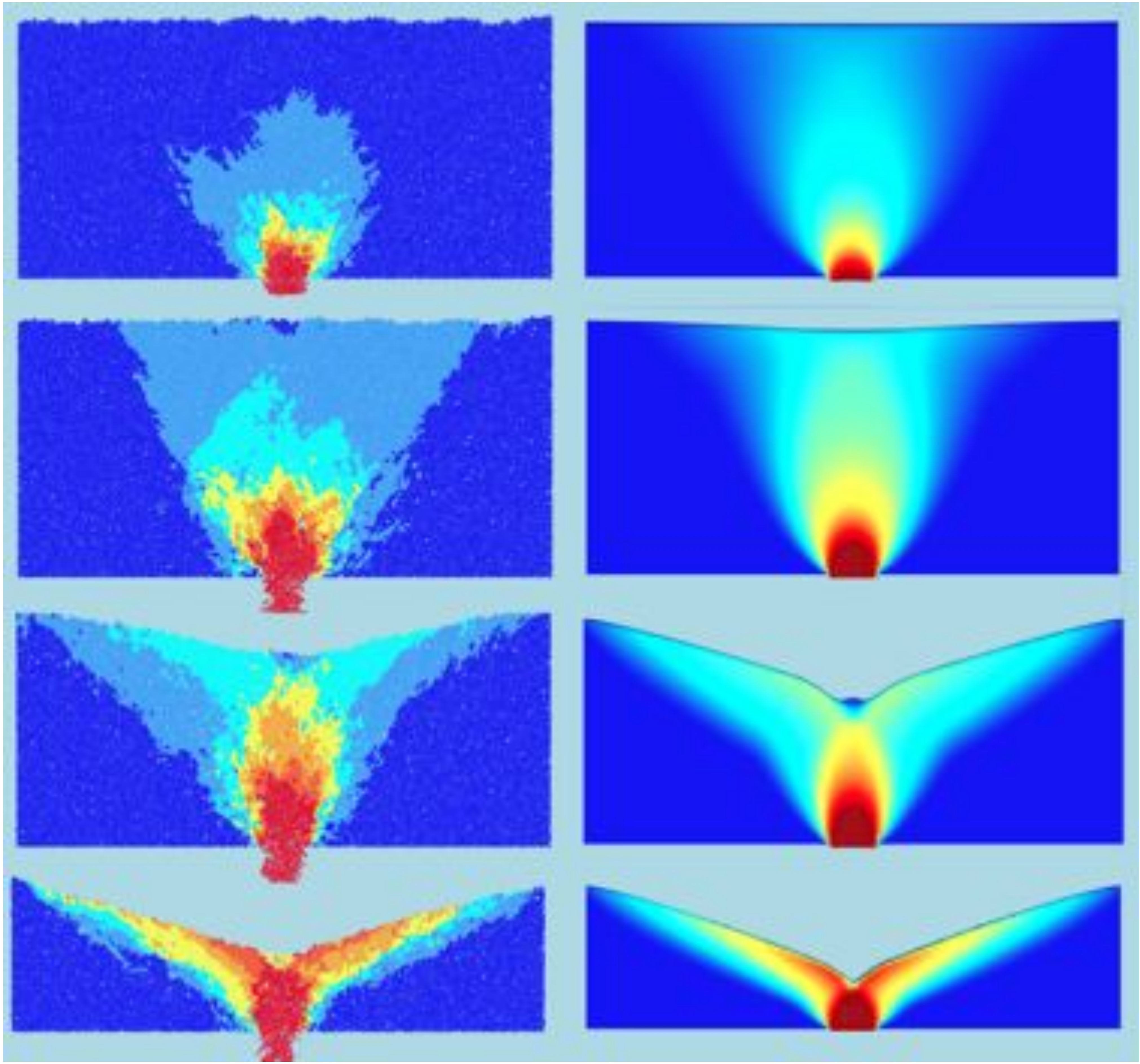

discrete *vs* continuum (at same rate)

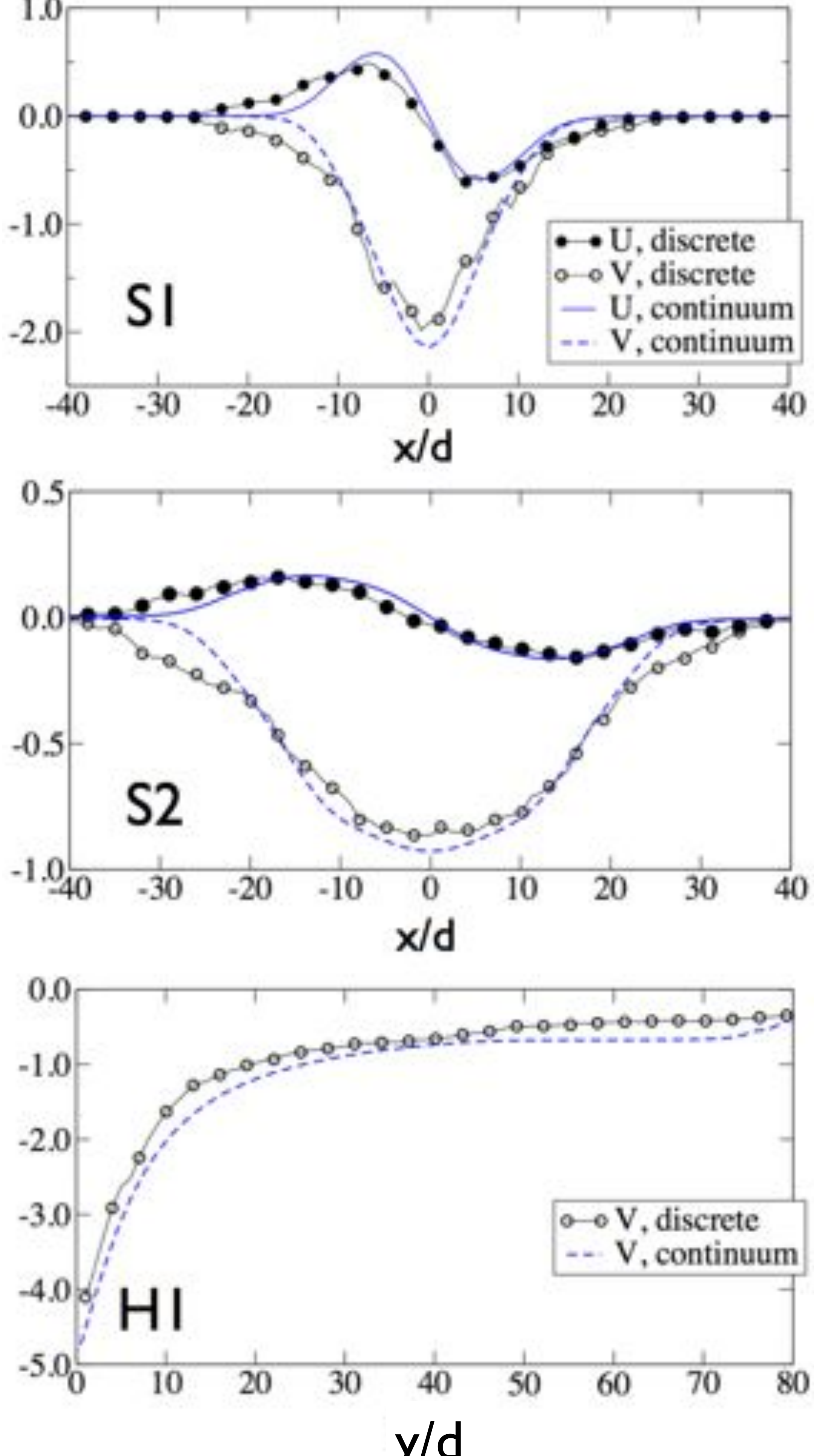

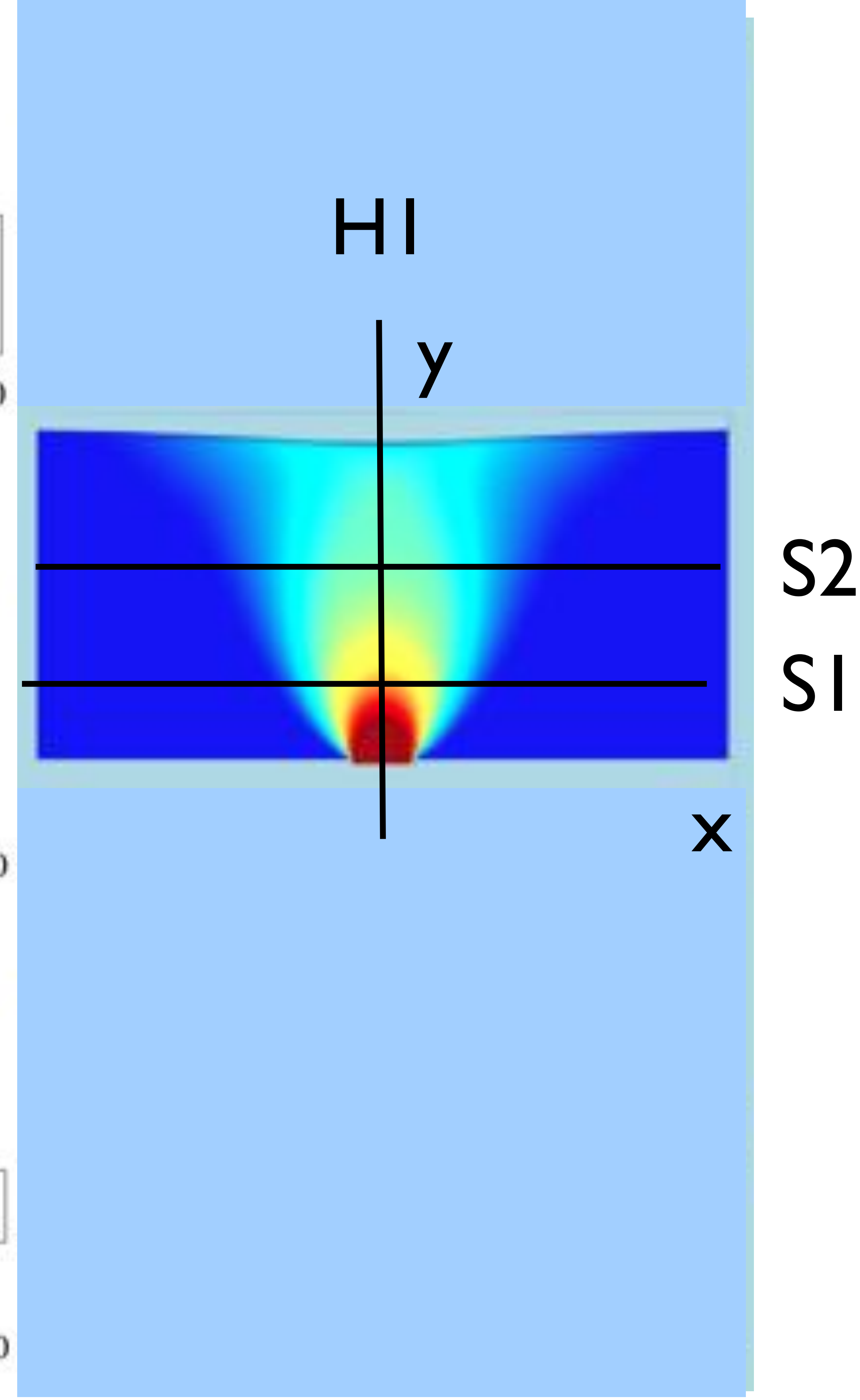

discrete *vs* continuum (at same rate)

Rotating Drum

Vidange de Benne

Vidange de Benne

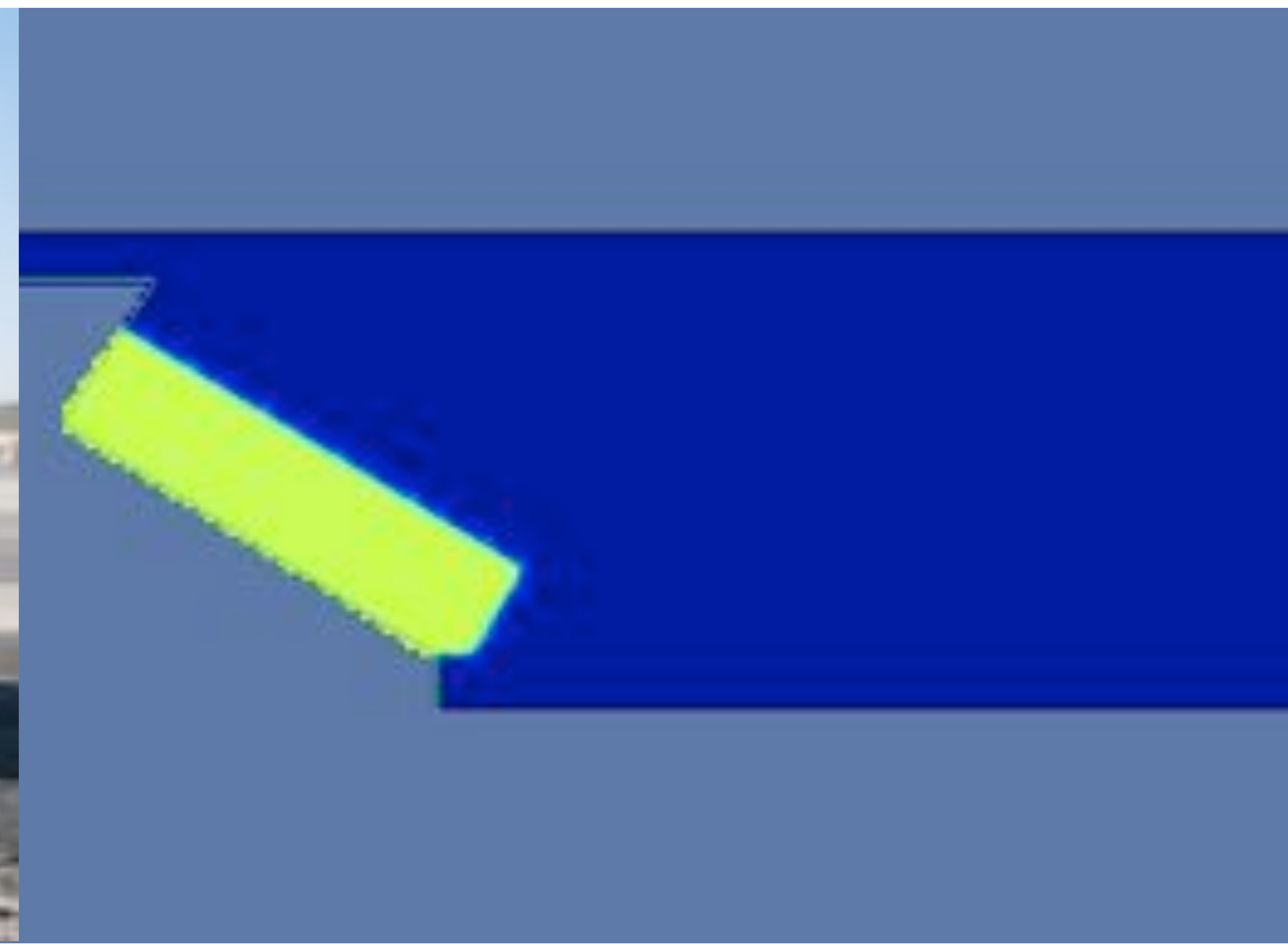

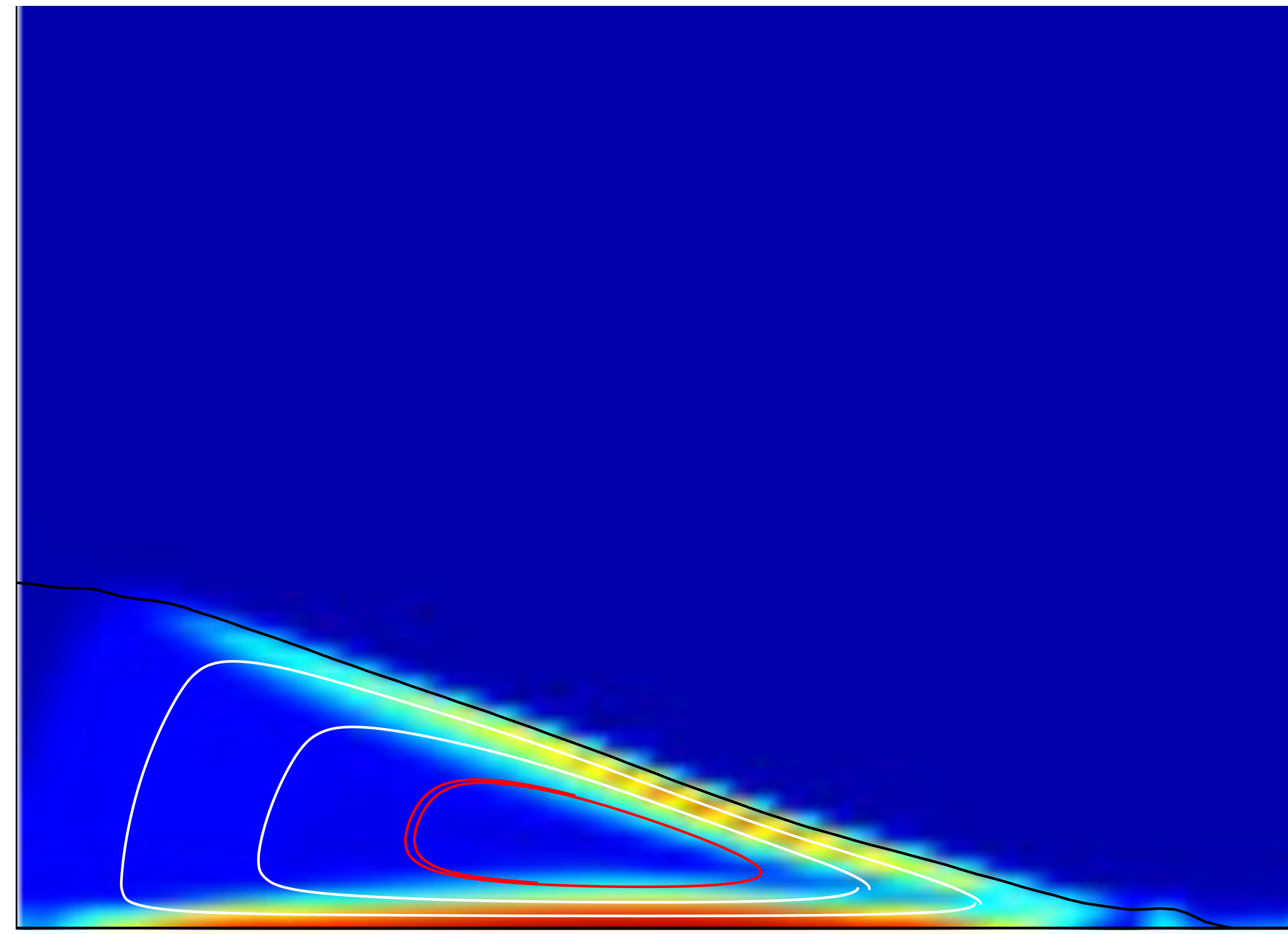

Conclusion

- µ(I) Rheology for granular flows?
- granular: ubiquitous
- Shallow Water: good tool for avalanches (geophysics)
- good qualitative behaviour (discr. / cont.)
- Collapse scaling - Beverloo scaling: µ(I)
- Beverloo at same rate: velocity pressure superposed
- but: coef. µ(I) depend on the geometry?

Conclusion

- discrete continus (like air water..)

grains discretes ⟷ Continus fluid , Navier Stokes

simplified system : Saint Venant

- lot of applications

Conclusion

- non local effects? Kamrin Boquet
- instabilities?
- μ(I) ill posed: Barker, Schaeffer, Bohorquez, Gray…
- Shallow Water: extra term Edwards, Baker, Gray…
- Segregation: Gajjar, Gray…

Thanks for attention

Time for questions ?